E.O. Paton Electric Welding Institute of the National Academy of Sciences of Ukraine

International Scientific-Technical and Production Journal

The Paton WELDING JOURNAL

Issue 08 2020

Published Monthly Since 2000

English Translation of the Monthly «Avtomatychne Zvaryuvannya»
(Avtomaticheskaya Svarka/Automatic Welding) Journal Published in Ukrainian and Russian Since 1948

Founders
E.O. Paton Electric Welding Institute
International Association «Welding»

Publisher
International Association «Welding»

Translators
A.O. Fomin, I.M. Kutianova
Editor
N.G. Khomenko
Electron galley
D.I. Sereda, T.Yu. Snegiryova

Address
E.O. Paton Electric Welding Institute,
International Association «Welding»
11 Kazym yr Malevych Str. (former Bozh enko),
03150, Kyiv, Ukraine
Tel.:/Fax: (38044) 200 82 77
E-mail: journal@paton.kiev.ua
www://patonpublishinghouse.com/eng/journals/tpwj

State Registration Certificate
KV 4790 of 09.01.2001
ISSN 0957-798X
DOI: http://dx.doi.org/10.37434/tpwj

Subscriptions
12 issues per year, back issues available.
$384, subscriptions for the printed (hard copy) v rsion, air postage and packaging included.
$312, subscriptions for the electronic version (sending issues of Journal in pdf format or prov ding access to IP addresses).
Institutions with current subscriptions on printed v rsion can purchase online access to the electronic v rsions of any back issues that they hav not subscribed to.
Issues of the Journal (more than two years old) are available at a substantially reduced price.

CONTENTS

E.O. PATON INSTITUTE OF MATERIALS SCIENCE AND WELDING WAS FOUNDED AT THE IGOR SIKORSKY KPI

I.V. Krivtsun, P.I. Loboda, S.K. Fomichov and **V.V. Kvasnytskyi**

According to the order of the rector, Professor Zgurovskyi M.Z, Academician of the NAS of Ukraine, in accordance with the Decision of the Academic Council at the National Technical University of Ukraine «Igor Sikorsky Kyiv Polytechnic Institute» on the basis of Engineering Physics (EPF) and Welding (WF) faculties and departments of Laser Engineering and Physics and Technical Technologies of the Institute of Mechanical Engineering (IME) on July 1, 2020, the newly founded E.O. Paton Institute of Materials Science and Welding, the abbreviated name — E.O. Paton IMSW, started its work. The acting Director of the E.O. Paton Institute of Materials Science and Welding, Dr. of Techn. Sci., Professor Loboda P.I., the Corresponding Member of the NAS of Ukraine was appointed. The founded Institute is not an ordinary association of materials science faculties and departments. In essence, it is a new modern form of educational, research and production organization — a cluster, whose activities involve close cooperation with the institutes of the National Academy of Sciences of Ukraine and industrial enterprises. The main idea of creating a new institute is not a usual integration of these three, undoubtedly the most important areas of activity, but the achievement of a certain synergetic effect, when as a result of interaction of particular components, a new quality is formed. The partners of the E.O. Paton IMSW are the institutes of the Department of Physical and Technical Problems of Materials Science of the NAS of Ukraine, first of all, E.O. Paton Electric Welding Institute, I.M.Frantsevich Institute for Problems of Materials Science, V.M. Bakul Institute for Superhard Materials and Physico-Technological Institute of Metals and Alloys. Among the industrial business partners there are strategic enterprises of Ukraine, in particular, the group of Companies «PlasmaTech», one of the leading manufacturers of consumables for welding, mining and metallurgy Company «Metinvest», one of the world's leading manufacturers of basic structural material — steel. The main task of the E.O. Paton IMSW is to accelerate the formation of a scientific worldview of engineering and scientific personnel through a close integration of educational, scientific and practical industrial training. The basis of the scientific worldview is mastering the principles of creating new, or choosing from existing ones, materials with the necessary set of physical, chemical and technological properties that provide a reliable operation of products under certain conditions. Namely the complex of properties depends on the nature, atomic-crystalline structure, microstructure, phase composition of material and directly affects parameters of the processes of materials treatment or manufacture of parts and components of modern engineering. The choice of parameters for the technological process primarily depends on the physical, chemical and technological properties of materials. Therefore, the choice of the most productive, resource- and energy-saving process, the safest for the environment and nature in general for high-tech production, requires knowledge of the relationship between the chemical composition — parameters of technological processes of treatment or manufacturing — microstructure and properties of material or product that provide the performance of the functions specified by the operating conditions. This approach will allow combining knowledge of creation, production, operation and disposal of materials with the longest reliable service life. In other words, combining the efforts of scientific and pedagogical teams of departments will form a modern scientific worldview on the choice of materials and technologies, the most effective power, technical, economic and environmental support of materials at all stages of creating new materials of long-term operation. The main competitive advantage of the E.O. Paton IMSW is that the scientific activities of the departments cover all stages of the product life cycle based on the advanced technologies, starting from the devel-

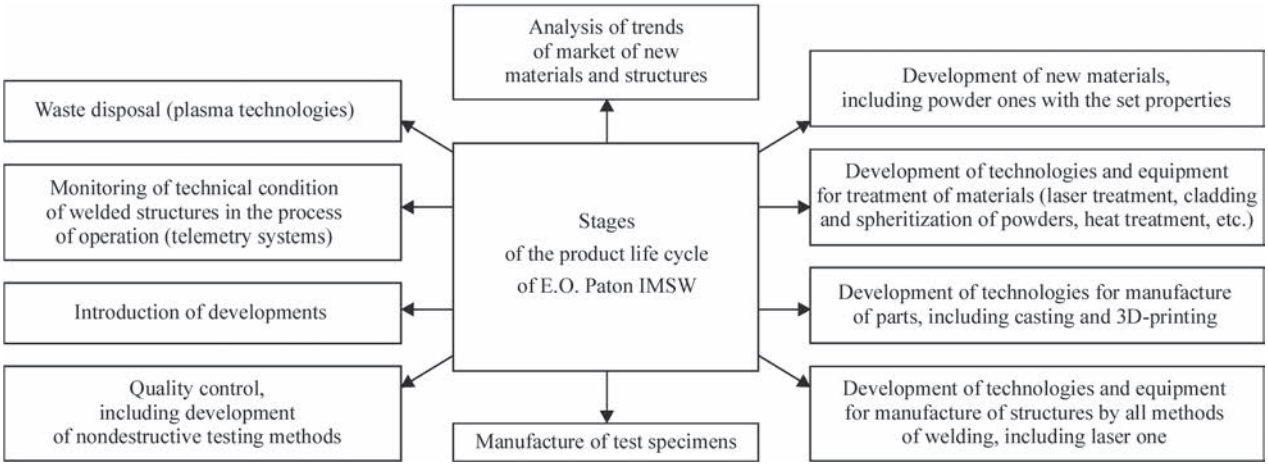

Figure 1. Stages of the product life cycle, which are covered by the activities of the E.O. Paton IMSW

opment of new materials with specified characteristics and the creation of parts and structures and ending in solving recycling problems (Figure 1).

The main purpose of combining scientific and pedagogical potential, methodological and laboratory base of the departments of the Institute is to create conditions for generating scientific knowledge with the direct participation of students (bachelors, masters), graduate students and employers. The main topics for research works are expected to be found on the basis of specific technological problems of industrial products manufacturers. To strengthen both the scientific and pedagogical potential and the laboratory base, close cooperation with the institutes of the National Academy of Sciences of Ukraine is envisaged. Starting from the 2nd year, scientists of the institutes of the National Academy of Sciences of Ukraine will be able to select and manage qualification scientific works of bachelors, masters and doctors of philosophy. Thus, in the field of education, a new quality of training is provided in accordance with a three-level system in keeping with the scheme «Bachelor – Master – PhD». Such training will take place in close cooperation with academic institutes, which, in turn, require the involvement of young researchers, as well as with industrial and partner companies that are in dire need of young, well-trained and highly qualified engineers. At the same time, such training will be carried out within the framework of large scientific and technical and research-production projects, which will be realized by the E.O. Paton IMSW together with academic institutes and business partners. In other words, training will actually take place under conditions as close as possible to real production. This will significantly improve the level and quality of training of graduates — professionals who will be more adapted for further work in science and industry. In the field of science, the main problem of today's Ukraine is the lack of able-minded and talented young scientists — specialists who are able to solve complex problems put forward by modern science, especially materials science. Creation of new laboratories within the E.O. Paton IMSW, their equipping with state-of-the-art research equipment at the financial support of business partners will allow realizing joint large-scale scientific and technical projects with the partner institutes of the NAS of Ukraine and, in particular, international ones with the involvement of young people — students, which are able to solve complex problems of modern materials science. Regarding the field of production, within the newly established laboratories of the E.O. Paton IMSW not only fundamental research works will be carried out, the results of which will provide a significant contribution to modern materials science, but also applied, technological investigations aimed at improving existing and creating new production technologies for producing, treatment and joining of materials. At the same time, the problematic of basic investigations should be formed on the basis of inquiries and unresolved issues of production in order to solve existing problems and increase the efficiency of production processes, provide resource conservation and extend the service life of products and structures, which will create new breakthrough technologies and effective use of energy and labor resources, creation of new materials. The results of such investigations should be used in the creation of technological processes and equipment for their

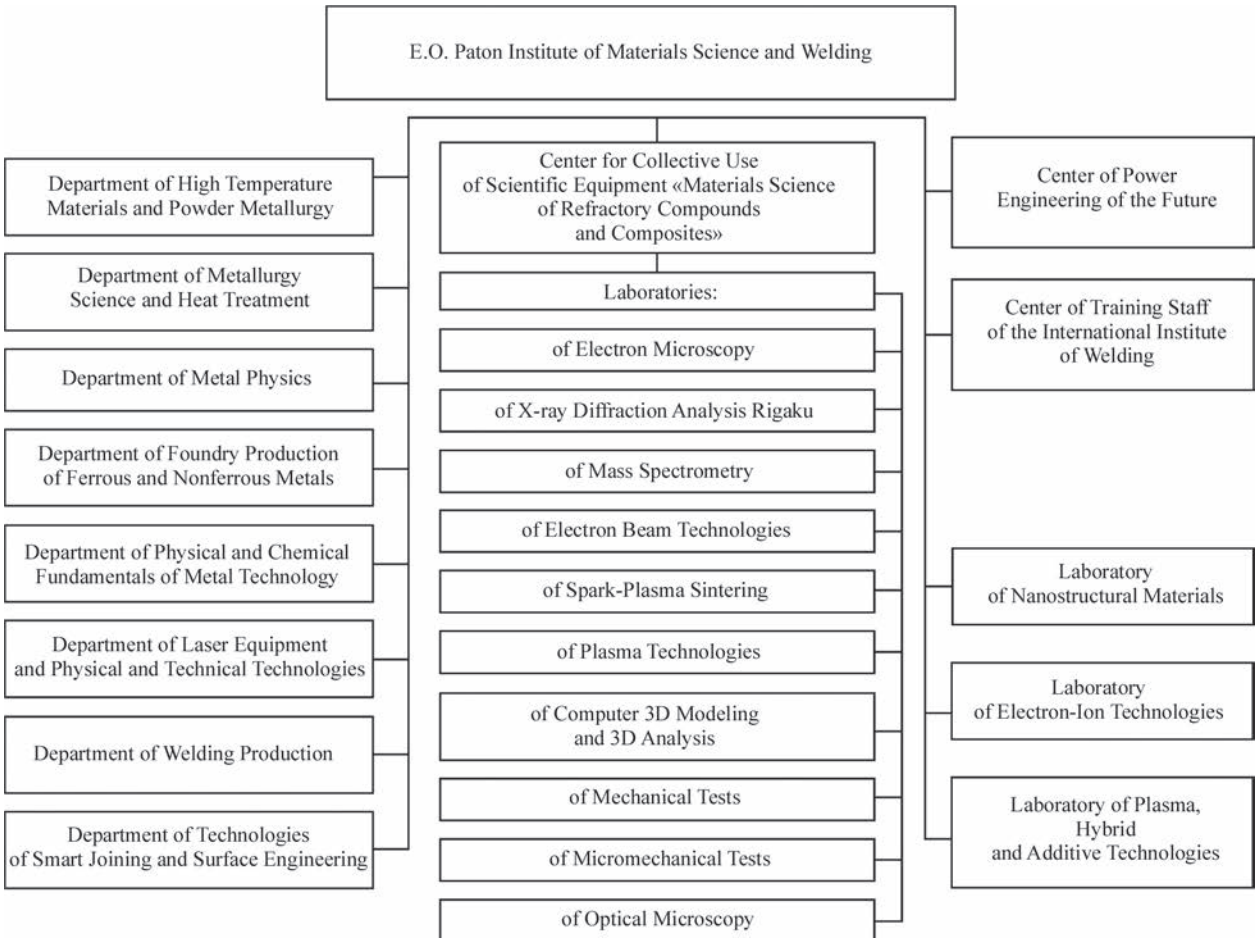

Figure 2. Organiа tional structure of the E.O. Paton Institute of Materials Science and Welding

realization not only at industrial partner enterprises, but also at other industrial enterprises of Ukraine and in the world. According to the proposed concept, approved at the meeting of the Academic Council of the Igor Sikorsky KPI on June 30, 2020, the structure of the E.O. Paton IMSW was organized (Figure 2).

The E.O. Paton IMSW was founded on the base of 9 departments of three faculties of the Igor Sikorsky KPI, in particular:

- Faculty of Laser Equipment and Physical and Technical Technologies — IME;
- Faculty of High-Temperature Materials and Powder Metallurgy — EPF;
- Faculty of Foundry Production of Ferrous and Nonferrous Metals — EPF;
- Faculty of Metallurgical Science and Heat Treatment — EPF;
- Faculty of Physical and Chemical Fundamentals of Technology of Metals — EPF;
- Faculty of Physics of Metals — EPF;
- Faculty of Welding Production — WF;
- Faculty of Electric Welding Machines — WF;
- Faculty of Surface Engineering — WF.

By merging the departments of Electric Welding Machines and Surface Engineering (WF) within the framework of the E.O. Paton IMSW, a new powerful Department of Smart Technologies of Joining and Surface Engineering was founded. The prospects of founding the E.O. Paton IMSW are associated with the expansion of capabilities of individual structural units, being a part of the Institute. In particular, such a merging creates preconditions for strengthening the scientific-innovative and educational potential of structural units, provides an opportunity for lecturers and research associates of large departments to carry out major complex strategic scientific and educational projects of the state-civilization level, including quality of life. In addition, it reduces the process of creating a new innovative competitive product with a simultaneous synergetic increase in the leading scientific schools as well as strengthening and improving the professionalism of scientific and pedagogical potential of departments. This is extremely important, because according to the data of QS World University Rankings

2020, Igor Sikorsky KPI occupies a fourth place among Ukrainian higher educational institutions (HEI), which were included in the ranking of the best universities in the world. When compiling the ranking, the authors are guided by a number of criteria, such as academic reputation of the institution, citation index of articles by its lecturers and associates, percentage of foreign students, reputation of a HEI among employers, etc. However, according to the analysis, the existing domestic network of HEI does not seem to be resulting and efficient as far as it is «closed in itself», and being a modern world-class university implies a tangible participation of the corresponding scientific-production and educational institution in the global space. According to the Regulation on accreditation of educational programs, applied to train applicants for higher education, which is approved by the Order of the Ministry of Education and Science of Ukraine, dated July 11, 2019 No. 977, the self-analysis of departments for compliance with the requirements of the National Agency for Quality Assurance in Higher Education (NAQAHE) was carried out, the results of which indicate an incomplete compliance of particular departments with the current requirements. Therefore, the foundation of E.O. Paton IMSW is one of the ways to overcome the lag of Igor Sikorsky KPI from the world's leading universities and provide a full compliance of the quality of student training by the departments of the Institute and current educational programs at all levels to the Criteria for assessment of the quality of educational programs accepted by NAQAHE. An extensive integration and involvement of institutes of the NAS of Ukraine and employers' enterprises in the implementation of the educational process at the E.O. Paton IMSW creates preconditions for improving the results of its activity according to the criteria for access to educational programs and recognition of learning outcomes, human resources, educational environment and material resources, internal assurance of quality of educational programs, transparency and publicity, learning through investigations. This will promote deepening of the internationalization of the University, strengthening of the international component in all aspects of its activities and, in particular, attract more foreign students and invite well-known foreign scientists and lecturers to participate in the educational process with a simultaneous expansion in the participation of associates of the Institute in the international projects. The world trends in higher education indicate the need in creating favorable conditions within the framework of the University for self-realization of students, young lecturers and scientists, providing a continuous improvement of knowledge of specialists throughout the life, which is one of the most important tasks of founding the E.O. Paton IMSW. A rapid orientation of structural units of the Institute in the training of highly-qualified specialists to the challenges of the world market, taking into account the requirements of employers and industry of Ukraine is provided through the implementation of modern management methods within the framework of the E.O. Paton IMSW, including also the project management. Such approach provides a significant improvement in the quality of scientific and educational projects of a newly founded Institute both at the stage of their preparation for submission and at the stage of realization. On the other hand, the integration provides new enhanced opportunities for students and associates of departments to improve the efficiency of the educational process and investigations through the joint use of modern laboratory facilities of departments of the Institute and the centers and educational and scientific laboratories equipped with the modern equipment, created within the E.O. Paton IMSW jointly with organizations and enterprises. This provides not only the improvement in the quality of training specialists by the departments of the Institute, but also helps to expand the competitiveness of graduates in solving the threefold problem material–treatment–joining. With this aim, the structure of the E.O. Paton IMSW includes research centers and laboratories. In particular, the Center for Collective Use of Scientific Equipment «Materials Science of Refractory Compounds and Composites» includes the following laboratories: Laboratory of Electron Microscopy; Laboratory of X-ray Diffraction Analysis Rigaku; Laboratory of Mass Spectrometry; Laboratory of Electron Beam Technologies; Laboratory of Spark Plasma Sintering; Laboratory of Plasma Technologies; Laboratory of Computer 3D Modeling and 3D Analysis; Laboratory of Mechanical Tests; Laboratory of Micromechanical

Tests; Laboratory of Optical Microscopy. Within the framework of the Institute, the following centers act: the Center of Power Engineering of the Future, the Center of Staff Training in accordance with the requirements of the International Institute of Welding and the following joint educational and scientific laboratories: Laboratory of Nanostructural Materials; Laboratory of Electron-Ion Technologies; Laboratory of Plasma, Hybrid and Additive Technologies (Figure 3).

The founded research centers and laboratories contribute to the solution of both scientific and educational tasks of the E.O. Paton IMSW. They allow strengthening the scientific component by involving not only lecturers of departments to the research team, but also research associates of leading research institutes, enterprises and organizations of Ukraine, provide the creation of a scientific experimental base of collective use with the involvement of modern equipment for research works, strengthen the competitiveness of the E.O. Paton IMSW in the preparation of joint projects within the framework of national and international research programs. In the field of education, the functioning of such structures contributes to the improvement of existing and creation of new programs of training courses for students, which take into account the modern experience and needs of institutions being a part of the National Academy of Sciences of Ukraine, leading companies and enterprises, facilitates the introduction of modern educational technologies, creates a basis for attracting well-known Ukrainian and international scientists to teach series of lectures for students of the Institute (Figure 4), conducting specialized laboratory works in unique equipment.

In addition, the presence of a close cooperation of the team of the E.O. Paton IMSW with scientists from the institutes of the NAS of Ukraine and leading enterprises promotes an increase in the quality of educational and methodical materials of departments, facilitates the organization of a three-level system for preparation of experts according to the scheme bachelor–master–PhD, gives an opportunity to carry out training of experts of all levels under the common scientific management. The innovative component is also of great importance in the work of the Institute. Such a broad integration allows intensifying the process of publishing the results of scientific investigations, promotes concentration of joint efforts in the organization of conferences, seminars, publication of results in well-known scientific journals, which provides an effective information to enterprises and manufacturers about the created new materials and technologies, promotes an exchange of experience with leading experts in Ukraine and in the world. Such work contributes to the development of human resources of the University and relevant scientific schools. In general, the presence of such scientific centers and laboratories in the structure of the Institute contributes to the involvement of enterprises and employers' organizations in the realization of the educational process and scientific work of students and graduate students, facilitates an increase in the quality of performing qualification works by students at all levels and an improvement of teaching disciplines, taking into account modern requirements of science, industry and employers. E.O. Paton IMSW is a part of the joint German-Ukrainian faculty (Otto von Guericke University). It participates in a dual degree program with the Federal University of Uberland (Brazil). An extremely important task is assigned to the Center of Staff Training of the International Institute of Welding (IIW), which is accredited by the Education Center of IIW for training of the following international certified welding specialists according to the training programs: International Welding Engineer, International Welding Technologist, International Welding Inspector. It provides an increase in the level of training not only of bachelors, masters and graduate students of the E.O. Paton IMSW and other engineering faculties of the Igor Sikorsky KPI, as well as certified specialists of enterprises and organizations working in the field of welding. The development of this area of activity is facilitated by the involvement of leading specialists of Ukraine in the creation of the latest methodical base that meets international requirements, including textbooks for training international engineers, technologists and welding inspectors in accordance with the International Institute of Welding, taking into account the trends of development of welding science, equipment and technologies. Thus, the foundation of the E.O. Paton IMSW will provide the existence of the modern educational and scientific center of the international level at the Igor Sikorsky KPI, which

Figure 3. Students work in the Laboratory of Optical Microscopy (*a*); Laboratory of Electron Microscopy (*b*); conducting research in the Laboratory of X-ray Diffraction Analysis Rigaku (*c*); computerized installation PM-300 for plasma-powder surfacing in the Laboratory of Electron-Ion Technologies (*d*)

is aimed at the development of new materials and smart technologies for their joining on the basis of combining the potential of the leading scientific schools of the Igor Sikorsky KPI in the field of materials science, metallurgy, welding, surface engineering and laser technologies, as well as quality assurance of materials, products and structures. And the main advantage of the newly founded structure is the ability to provide the full life cycle of materials, which combines their creation, production, joining, application and disposal. Such an approach allows E.O. Paton IMSW to carry out an expanded range of scientific and innovative projects and increase the contribution of Ukrainian science to modern world materials science.

Figure 4. Yuryi Gogotsi, world famous graduate of EPF of KPI. Dr. of Techn. Sci., Prof., founder of the Institute of Nanotechnology of Drexel University (Philadelphia, USA), nominee for the Nobel Prize in Physics in 2019, delivers an open lecture at the Igor Sikorsky KPI (2020)

https://doi.org/10.37434/tpwj2020.08.01

INFLUENCE OF INTRODUCTION OF REFRACTORY PARTICLES INTO WELDING POOL ON STRUCTURE AND PROPERTIES OF WELD METAL

V.V. Holovko, D.Yu. Yermolenko, S.M. Stepanyuk, V.V. Zhukov and **V.A. Kostin**
E.O. Paton Electric Welding Institute of the NAS of Ukraine
11 Kazymyr Malevych Str., 03150, Kyiv, Ukraine. E-mail: office@paton.kiev.ua

The investigations of influence of change of sizes of primary dfinishrites in the structure of weld metal on their secondary microstructure and mechanical properties were carried out. It is shown that an increase in the width of dfinishrites is accompanied by a rise in the temperature of start of bainite transformation, but the content of low-temperature bainite in the microstructure of weld grows. The possibility of effect of inoculation by dispersed particles of refractory compounds into welding pool on relationship between the content in the microstructure of weld of components with a coarse-acicular and fine-acicular morphology and, accordingly, on mechanical properties of weld was established. 9 Ref., 4 Tables, 10 Figures.

Keywords: weld, microstructure, dfinishrites, bainite transformation, inoculation, refractory compounds, mechanical properties

The weld metal can start its crystallization during welding in the form of δ-ferrite or austenite of low-alloy steels. From the results presented in [1], it is seen that at the cooling rates of steel melts typical to the weld metal, crystallization begins from the structure of δ-ferrite, with which during further cooling solid transformations take place. From the phase diagram of Fe–C it follows that at the temperatures around 1400 °C the formation of austenite begins. The centers of austenite initiation, as a rule, are the boundaries of dfinishrites [2]. The authors of [3] expressed the assumption on the formation of austenite as a result of peritectic reaction between the melt and δ-ferrite at the high-energy boundaries of dfinishrites (Figure 1). An important result of this transformation depends on the size of the primary structure, because namely this index is one of the key factors influencing the nature of formation of the secondary structure.

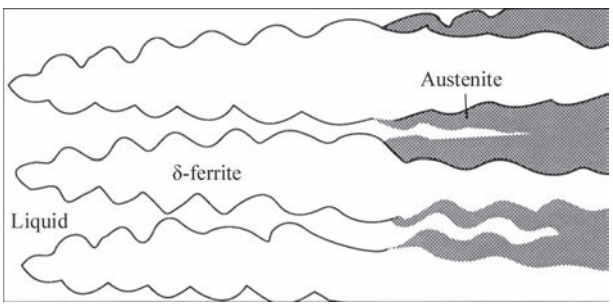

Figure 1. Scheme of austenite grain formation on dfinishrites boundaries as a result of peritectic reaction [3]

In the section 1 of [4], it was shown that δ-ferrite grains have a columnar morphology and the size of austenitic grains depfinishs on the width of dfinishrites. In order to expand understanding of the peculiarities of forming the secondary structure in the weld metal of low-alloy steels, special investigations were conducted, the results of which are presented in the section 2.

2. Influence of inoculants on the secondary structure of weld metal. *2.1. Procedure of experiments.* To study the decay kinetics of supercooled austenite in the metal of the investigated weld, dilatometric tests were performed. During these tests, the metal specimens were subjected to heating and cooling at specified thermal cycles. In the process of thermal effect, dilatometric data were recorded. The specimens of each weld metal were subjected to heating to 1170 °C and cooling. Five thermal cycles were selected, which differed in the cooling rate within the temperature range of 600−500 °C ($w_{6/5}$ = 45; 30; 17; 10; 5 °C/s). The tests were performed in the installation Gleeble 3800.

In the work the procedure of analysis of dilatometric data developed by the authors was applied. To determine critical temperatures of structural-phase transformations, dilatometric data are presented in the form of a diagram of depfinishence of a changed linear size (diameter) of metal specimen during cooling (Figure 2, *a*). To the linear areas of the obtained dilatogram, which correspond to the law of thermal expansion of ferrite or austenite, the tangents are laid

V.A. Kostin — https://orcid.org/0000-0002-2677-4667

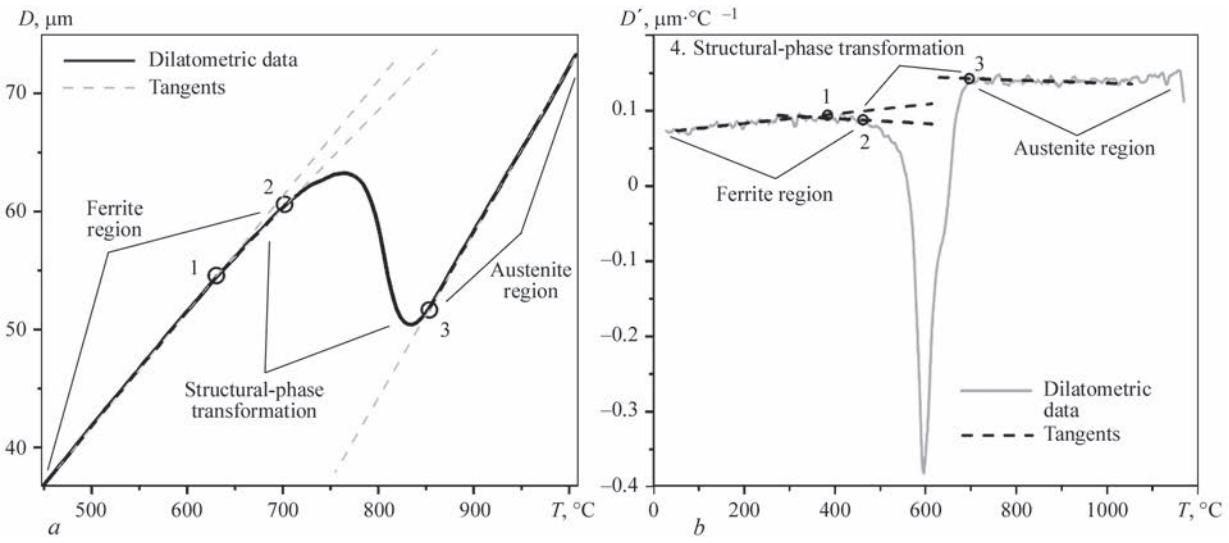

Figure 2. Methods for determining critical temperatures of structural-phase transformation by the method of tangents: *a* — on the diagram of depfinishence of dilatometric data on temperature; *b* — on the diagram of depfinishence of the first derivative of dilatometric data on temperature (points *1*–*3* – critical transformation temperatures, which can be obtained by the method of tangents)

down [5]. The temperature points, at which the tangents begin to deviate from the experimental dilatometric curve, are denoted as the critical temperatures (T_n and T_c) of structural-phase transformations.

However, the accuracy of this method is not high enough [6] and depfinishs entirely on the choice of temperature range for drawing tangential. The more sensitive method is the method, in which the curves of depfinishence of the first derivative of dilatometric data on temperature are used to draw tangents [7]. It should be noted that, as is seen in Figure 2, *b*, this method is also sensitive to the selection of a linear area on the curve of dilatometric data.

Thermal expansion of solid bodies is not a linear depfinishence on temperature and the formation of a final depfinishence is influenced by many factors [8]. Therefore, to determine the critical temperatures, at which the inverse change of the linear size is observed against the background of thermal expansion, which is predetermined by the rearrangement of a crystal lattice during structural-phase transformation, we used approximations for the areas corresponding to the temperature depfinishence of linear thermal expansion.

The most accurate results showed empirical depfinishences in the form of polynomials of odd degrees of the following form (Figure 3):

$$F(T) = a_1T + a_2T^3 + a_3T^5 + a_4, \quad (1)$$

where $F(T)$ is the function of depfinishence of thermal expansion of ferrite or austenite; T is the temperature; a_{1-4} are the approximation constants.

Based on the proposed procedure, it was proposed to use the index T_V to determine the characteristics of transformation. T_V is the temperature of the maximum intensity of transformation (see Figure 3, *b*). This characteristic has a correlation with the start and fin-

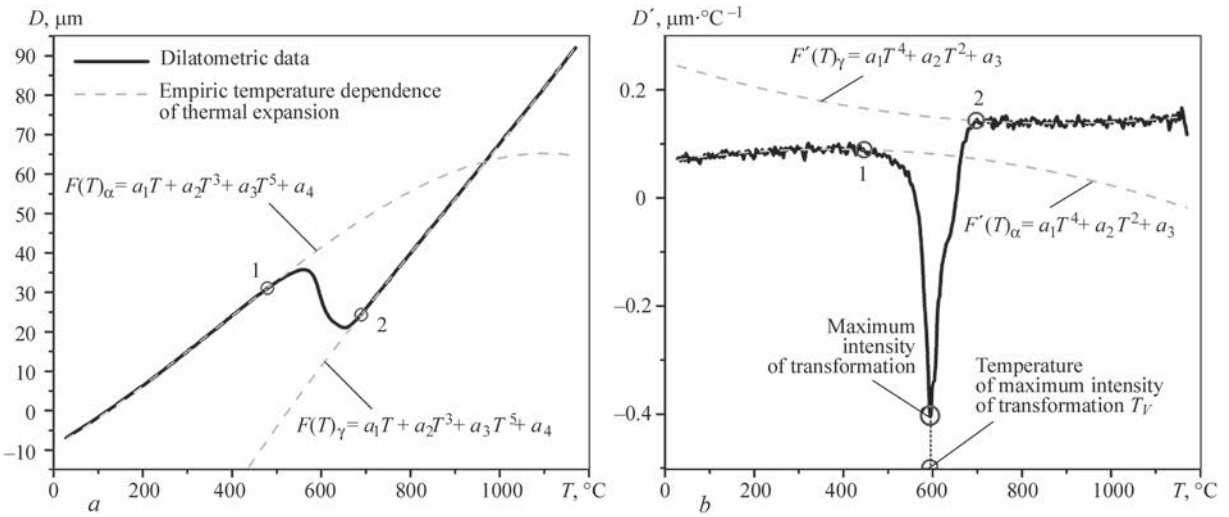

Figure 3. Approximation method of analysis of dilatometric data: *a* — approximation of dilatometric data; *b* — approximation of the first derivative (1, 2 — critical transformation temperatures)

Table 1. Results of determination of temperatures of phase transformations in weld metal

Weld	A_{c3}, °C	B_s, °C	B_f, °C	ΔB, °C	Δ*A*, °C	T_V, °C
BA	870	603.07	443.07	160.00	266.93	567
FeTi	869	583.90	423.10	160.80	285.10	493
TiN	853	589.88	403.04	186.84	263.12	487
VC	863	603.03	412.07	190.96	259.97	549
NbC	893	582.01	431.07	150.94	310.99	534
SiC	851	644.17	435.06	209.11	206.83	540
TiC	870	648.27	435.18	213.09	221.73	562
TiO_2	885	666.42	431.22	235.2	218.58	559
Al_2O_3	890	656.52	437.26	219.26	233.48	559
MgO	873	680.36	457.18	223.18	192.64	574
ZrO_2	867	687.36	458.07	229.29	179.64	570

Notes. A_{c3} is the temperature of start of δ-γ-transformation; B_S is the temperature of start of bainite transformation; B_f is the temperature of finish of bainite transformation; Δ*B* is the temperature range of bainite transformation; Δ*A* is the temperature range of δ-γ-transformation.

ish temperatures of transformation and can be used as a separate additional index of transformation.

For each weld metal, the values of phase transformation temperatures determined from the diagrams were compared with the results of metallographic analysis of the microstructure. The scheme of sampling for investigations and methods of their etching for metallographic analysis are given in the section 1 [4].

2.2. Influence on temperature of structural transformations. To the influence of nonmetallic inclusions on the formation of the microstructure of weld a large number of works is devoted. These works present the results of thermodynamic modeling and data of experimental works on this problem. However, today there is no generalized idea about the mechanisms of influence of dispersed inclusions on the formation of weld metal structure. In connection with the uncertainty of the conditions that determine the content, composition and morphology of nonmetallic inclusions in liquid metal, it is advisable to conduct experiments in which a certain number of chemically pure compounds of a determined size with the known physicochemical indices are artificially introduced into the welding pool. The inoculation of dispersed particles of certain refractory compounds into the welding pool made it possible to investigate the peculiarities of their influence on the size of the structural components of weld metal.

Table 1 shows the results of the analysis of the results of dilatometric investigations, as well as determination of the temperature of the maximum intensity of transformation (T_V), performed according to the abovementioned procedures.

2.3. Secondary structure of weld metal. Metallographic examinations were performed in a light microscope Neophot-30 with image registration on a computer screen.

The results of metallographic analysis showed that the main structural components of the metal of all investigated joints are upper and lower bainite, differ-

Table 2 Content of basic structural components in weld metal

Weld	Ferrite					Bainite		Other
	Acicular	Polygonal	Intragranular	Globular	Widmanstatten	Upper	Lower	
BA	10	12	8	16	4	15	26	9
FeTi	6	7	9	17	8	18	30	5
TiC	14	9	9	9	3	19	30	7
TiN	12	10	20	19	16	6	13	4
SiC	5	8	12	16	5	18	33	3
VC	6	9	14	14	14	19	21	3
NbC	7	12	10	6	18	21	15	11
TiO_2	15	7	15	17	6	17	18	5
Al_2O_3	4	19	18	7	15	15	15	7
MgO	18	10	11	10	3	10	33	5
ZrO_2	20	15	8	6	3	13	30	5

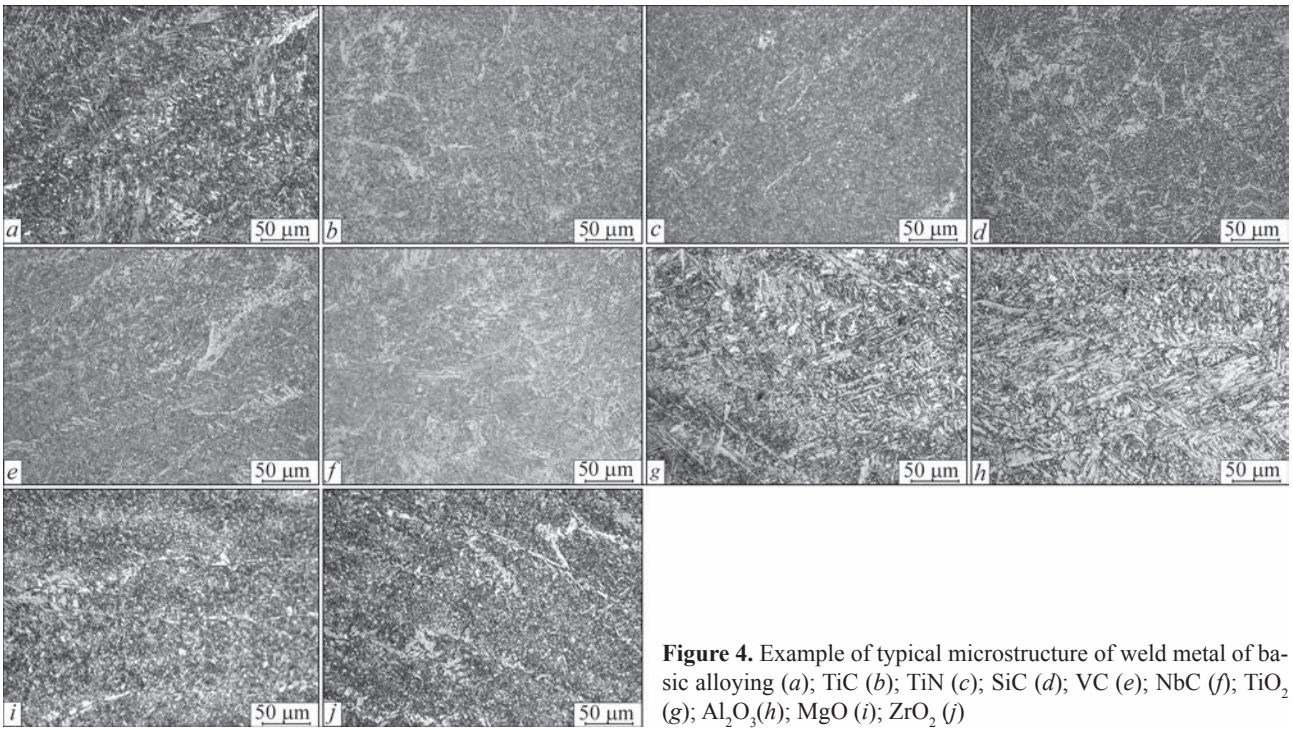

Figure 4. Example of typical microstructure of weld metal of basic alloying (*a*); TiC (*b*); TiN (*c*); SiC (*d*); VC (*e*); NbC (*f*); TiO_2 (*g*); Al_2O_3(*h*); MgO (*i*); ZrO_2 (*j*)

ent morphologies of ferrite (acicular, polygonal, intragranular, globular, Widmanstatten) and martensite. The composition of structural components are given in Table 2. Figure 4 shows typical examples of the secondary structure of the weld metal.

Regarding the peculiarities of the structure of particular weld, it should be noted that the weld metal of basic alloying (BA) is characterized by a fine-grained structure with some fragmentation and formation of intravolume dispersed phases.

In the weld metal of FeTi, a nonuniform structure (fine-grained lower bainite and coarse-laminar upper bainite) is formed at its slight fragmentation with the formation of both intravolume dispersed phases and their clusters along the boundaries.

The structure of TiC weld metal consists mainly of bainitic-ferritic components at a slight fragmentation. The structure of SiC weld metal contains mainly bainitic-ferritic component at a slight fragmentation with an extfinished spectrum of intravolume dispersed phases and the presence of phase precipitations along the boundaries of a lath structure.

Microstructure of Al_2O_3 weld metal consists mainly of bainitic-ferritic structure at a slight fragmentation and an extfinished spectrum of intravolume dispersed phases and the presence of phase precipitations along the boundaries of a lath structure.

In the weld metal of ZrO_2 mainly homogeneous bainitic-ferritic structure is formed at the presence of dispersed phase precipitations in the inner volumes of bainitic structure, as well as along the boundaries of fragmented structures.

2.4. Influence on mechanical properties. The chemical composition of the weld metal is given in Table 3

Table 3. Chemical composition of metal of investigated weld, wt.%

Weld	C	Si	Mn	S	P	Ni	Mo	Al	Ti	Zr	CE_w
BA	0.034	0.340	1.21	0.021	0.020	2.13	0.28	0.028	0.013	N/D	0.356
FeTi	0.036	0.335	1.22	0.022	0.021	2.14	0.26	0.038	0.029	Same	0.390
TiN	0.035	0.317	1.24	0.019	0.009	2.15	0.26	0.036	0.021	–	0.357
VC	0.052	0.227	1.21	0.022	0.021	2.13	0.25	0.027	0.004	–	0.384
NbC	0.049	0.253	1.19	0.021	0.020	2.15	0.27	0.029	0.003	–	0.387
SiC	0.053	0.351	1.20	0.020	0.025	2.12	0.26	0.025	0.004	–	0.365
TiC	0.046	0.340	1.25	0.021	0.019	2.15	0.24	0.023	0.021	–	0.370
TiO_2	0.035	0.405	1.24	0.018	0.021	2.17	0.27	0.031	0.027	–	0.332
Al_2O_3	0.034	0.424	1.26	0.019	0.023	2.15	0.29	0.042	0.015	–	0.315
MgO	0.031	0.227	1.21	0.025	0.024	2.15	0.29	0.023	0 ″.013		0.297
ZrO_2	0.033	0.223	1.25	0.024	0.024	2.14	0.30	0.024	0.013	0.06	0.303

Table 4. Mechanical properties of metal of investigated weld

Weld	σ_y	$\sigma_{0.2}$	δ	ψ	*KCV*, J/cm² at T, °C			
	MPa		%		20	0	–20	–40
BA	685	610	15	54	97	87	75	53
FeTi	747	690	19	60	74	69	63	61
TiC	716	644	19	63	110	97	85	73
TiN	712	580	5.3	14.7	55	47	40	–
SiC	726	650	21	62	85	72	65	61
VC	780	706	14	56	57	55	52	–
NbC	820	757	18	57	45	39	31	–
TiO_2	709	636	19	57	85	72	60	50
Al_2O_3	728	621	17	54	82	58	50	36
MgO	644	586	19	60	103	85	69	60
ZrO_2	649	592	21	64	97	91	84	76

together with the indices of carbon equivalent, which was calculated according to the standard EN1011-2 [9]. The results of determined mechanical properties of the weld metal are shown in Table 4. From the abovementioned results it is seen that chemical composition of the metal in the investigated weld corresponds to low-alloy steels. The introduction of certain inoculants into the welding pool affected only the content of aluminium and titanium in the weld metal, which can be explained by the peculiarities of deoxidation processes under the influence of introduced joints.

The results given in Table 4, show that introduction of particles of refractory compounds into the welding pool has a noticeable effect on mechanical properties of the weld metal. Such an influence is connected with the changes in the structure of metal, to which this work is devoted.

2.5. Analysis of investigation results. In [4], it was shown that introduction of dispersed particles of refractory compounds into the welding pool affects the size of both dfinishrites and grains of a primary austenite. As is seen from Table 2, a significant share of the microstructure components in the investigated weld is represented by morphological forms of bainite. Figure 4 shows the results of comparing the sizes of dendrites formed in the first stages of the welding pool crystallization process [4] with the temperature of start of bainite transformation.

As is seen from the abovementioned data, with an increase in the width of dfinishrites, the temperature of the start of bainite transformation rises. According to the modern notions about the formation of bainite structure, the origination of this phase can be initiated either from the boundaries of austenitic grains or from the middle. If in the first case the initiation of a new phase is controlled by the dislocations density at the grain boundaries, then in the second case it is controlled by the presence of centers of initiation of a new phase in the body of grains of the primary structure. Such centers can be represented by such refractory inclusions as oxides of magnesium, titanium, aluminium, as well as silicon and titanium carbides (Figure 6), which were captured by the crystallization front.

The rate of diffusion of carbon to the interphase boundary in the process of δ-γ-transformation affects the formation of a lower bainite in the microstructure of the weld metal. As is seen from the abovementioned data, the microstructure of weld, to the compo-

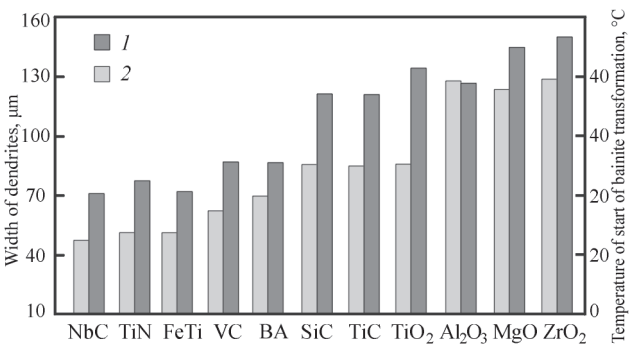

Figure 5. Change in temperature of start of bainite transformation (*1*) depfinishing on width of dfinishrites (*2*) in the primary structure of weld metal

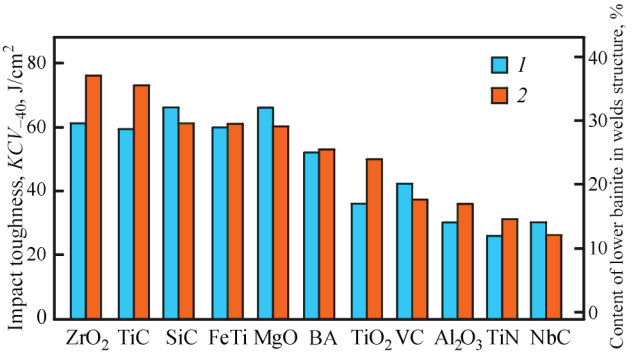

Figure 6. Content of lower bainite in the structure (*1*) and impact toughness (*2*) of weld metal depfinishing on composition of inoculants

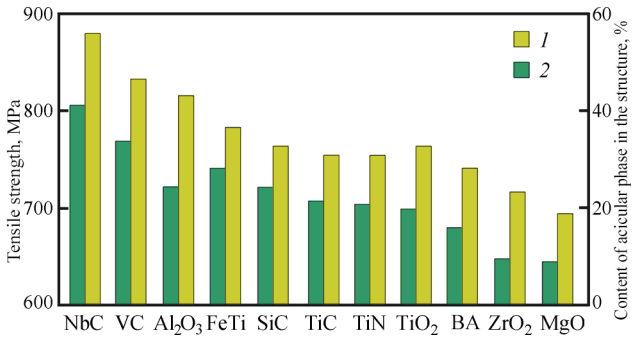

Figure 7. Nature of influence of content of coarse-acicular phases between weld metal

sition of which magnesium and zirconium oxides, vanadium and silicon carbides were inoculated, contains an increased amount of a lower bainite. In low-alloy steels, the lower bainite is characterized as a structural component that allows providing the formation of a metal with a high level of toughness while maintaining the appropriate strength.

Two forms of bainite in the metal of low-alloy steels differ both in the nature of a carbide phase formation as well as in their morphology. If during the formation of the upper bainite a significant part of carbon diffuses at the boundary of ferritic grains, where it is precipitated in the form of cementite, then the lower bainite is characterized by precipitation of small carbides in the body of ferritic grains. The lower bainite is formed in the form of a fine-grained structure with small-angle grain boundaries. Such a structure has an increased resistance to the propagation of brittle cracks. The structure of the upper bainite consists of coarser needles with an increased grain disorientation. An increase of the upper bainite together with the second coarse-acicular structural component — Widmanstatten ferrite in the weld of the structure — helps to increase the strength of the metal, but reduces its toughness. The nature of the influence of the total content in the structure of the upper bainite and Widmanstatten ferrite on the yield strength of the weld metal is shown in Figure 7.

The results obtained after the carried out experiments showed that the change in the morphology of dfinishrites at the initial stages of crystallization during inoculation to the welding pool of dispersed particles of refractory compounds, which was reported in [4], affects the peculiarities of formation of secondary microstructure and complex mechanical properties of weld metal.

Based on the application of the proposed parameter of T_V transformation, the effect of alloying was established (carbon equivalent CE_W) on the transformation temperature T_V) (Figure 8).

It was found that with a decrease in a carbon equivalent CE_W, the transformation temperature T_V

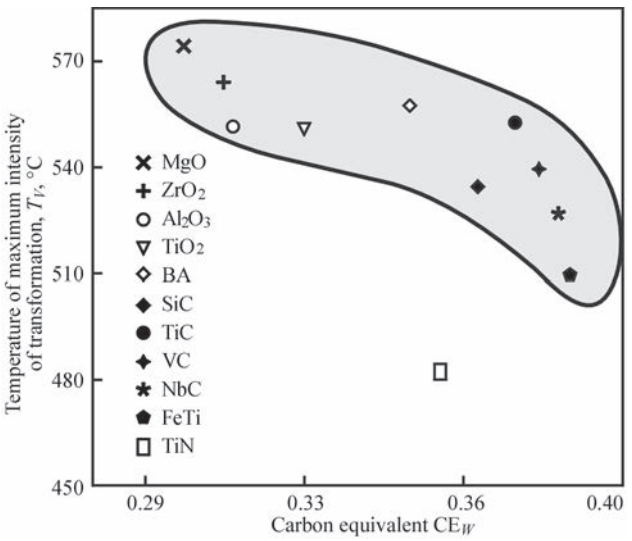

Figure 8. Influence of chemical composition of weld metal CE_W on transformation temperature T_V

increases nonlinearly. It is shown that inoculation of oxides MgO, ZrO_2, TiO_2 into the weld metal increases the temperature T_V, while the introduction of carbides TiC, SiC and NbC, on the contrary, reduces it. The difference in the transformation temperatures ranges from 20 to 50 °C.

It is shown that the index of temperature T_V can be used to analyze the ratio of structural components in the metal of the weld of high-strength low-alloyed steels, as is shown in Figure 9.

It was found that a decrease in the temperature T_V increases the share of bainitic acicular structures. To the greatest extent, an increase in the share of acicular bainitic structures is influenced by SiC and NbC carbides, which is accompanied by a corresponding increase in strength of weld metal (Table 4, Figure 6) and decrease in the level of impact toughness of weld metal (Table 4, Figures 7 and 10)

The analysis of the obtained results showed that the modification of the weld metal with oxide parti-

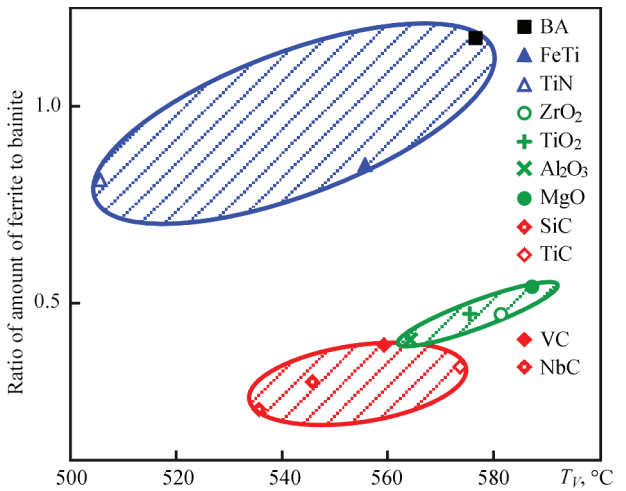

Figure 9. Influence of transformation temperature T_V on ratio of structural (F/B) components

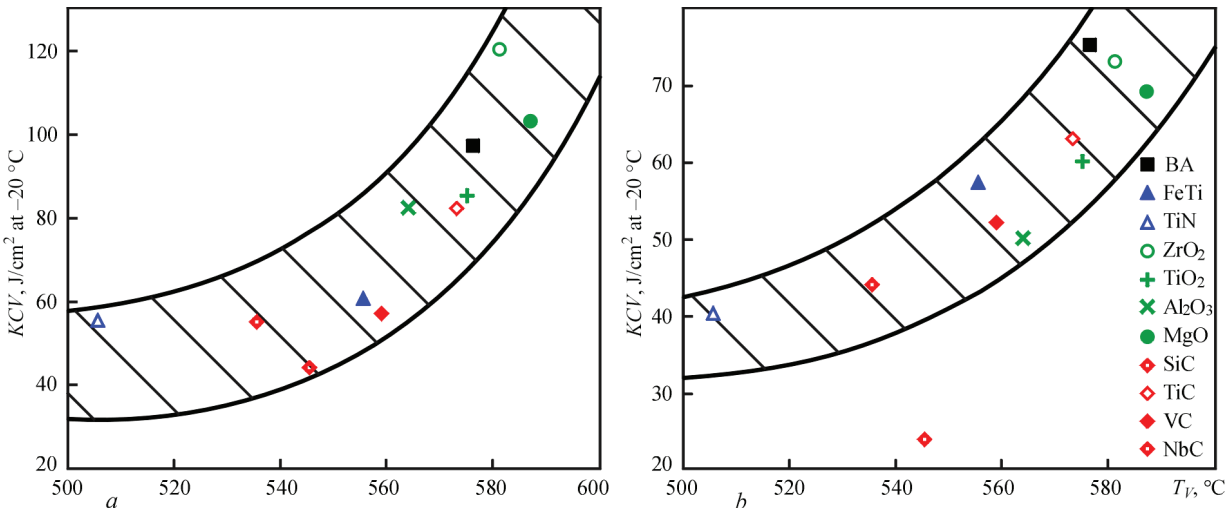

Figure 10. Influence of transformation temperature T_V on toughness of weld metal at different test temperatures: *a* — 20; *b* — −20 °C

cles (ZrO_2, TiO_2) is optimal from the point of view of forming the fine-acicular structure of the lower bainite, which provides a high complex of mechanical properties — a combination of high strength, ductility and toughness at low climatic test temperatures.

Conclusions

The influence of change in the size of dfinishrites, which occurs during inoculation of dispersed particles of refractory compounds into the welding pool, on the formation of the secondary microstructure and mechanical properties of weld metal of low-alloy steels was investigated, as a result of which it was established that:

1. An increase in the width of dfinishrites is accompanied by a rise in the temperature of start of the bainite transformation.

2. Despite an increase in the temperature of start of bainite transformation in the weld metal with an increased width of dfinishrites in the process of cooling, the microstructure with a high content of the lower bainite is formed. This may indicate the inhibition of the diffusion of carbon from austenitic grains during the δ-γ-transformation in the weld metal inoculated with oxides of magnesium and zirconium, as well as silicon and titanium carbides.

3. A decrease in the width of dfinishrites as compared to the variant of basic alloying is accompanied by a rise in the content of structural components of a coarse-acicular morphology in the metal of weld.

4. Depfinishing on the ratio of the components of a fine-acicular and a coarse-acicular morphology in the microstructure of the weld, the level of strength and toughness of the metal changes.

5. The use of the index of transformation temperature T_V to describe the influence of thermokinetic parameters on the formation of metal structure of weld was proposed.

6. Inoculation of dispersed particles of refractory compounds into the welding pool affects the change in the size of dfinishrites of the primary structure and, accordingly, the formation of the secondary microstructure of the weld metal and their mechanical properties.

1. Hideyuki, Y., Takahiro, H., Naoki, S. et al. (2019) Investigation using 4D-CT of massive-like transformation from the δ to γ phase during and after δ-solidification in carbon steels. *IOP Conf. Series: Mater. Sci. & Engin*. doi:10.1088/1757-899X/529/1/012013, 1–8.
2. Phelan, D., Dippenaar, R. (2004) Instability of the delta-ferrite/austenite interface in low carbon steels: The influence of delta-ferrite recovery sub-structures. *ISIJ Int*., 44(**2**), 414–421.
3. Svensson, L.-E. (2000) *Control of microstructures and properties in steel arc weld*. CRC Press, Inc. Corporate Blvd.
4. Holovko, V.V., Yermolenko, D.Yu., Stepanyuk, S.M. (2020) The influence of introducing refractory compounds into the weld pool on the weld metal dfinishritic structure. *The Paton Welding J*., **6**, 2–8.
5. Selivanova, O.V., Polukhina, O.N., Khotinov, V.A., Farber, V.M. (2017) *Modern methods of investigation of polymorphous transformations in steels*: Manual. Ekaterinburg, Uralsky Un-t [in Russian].
6. Teplukhina, I.V., Golod, V.M., Tsvetkov, A.S. (2018) Plotting of overcooled austenite decomposition diagrams in steel on the base of numerical analysis of dilatometric testing results. *Pisma o Materialakh*, 8(**1**), 37–41 [in Russian].
7. Motycka, P., Kover, M. (2012) Evaluation methods of dilatometer curves of phase transformations. In: *Proc. of 2nd Int. Conf. on Recent Trfinishs in Structural Materials, COMAT 2012 (21–22.11.2012, Plzen, Czech Republic)*, EU.
8. Novikova, S.I. (1976) *Heat expansion of solids*. Moscow, Nauka [in Russian].
9. *EN 1011-2:* Welding — Recommfinishations for welding of metallic materials. Pt 2: Arc welding of ferritic steels. British Standards Institution, March 2001 AMD A1 Dec. 2003.

Received 30.04.2020

https://doi.org/10.37434/tpwj2020.08.02

INVESTIGATION OF THE METHODS OF MODIFYING THE STRUCTURE OF AUSTENITIC WELDS AND THE ZONE OF THEIR FUSION WITH PEARLITIC BASE METAL

K.A. Yushchenko, O.V. Bulat, G.V. Svyagintseva, V.I. Samoilenko and **Yu.M. Kakhovskyi**
E.O. Paton Electric Welding Institute of the NAS of Ukraine
11 Kazymyr Malevych Str., 03150, Kyiv, Ukraine. E-mail: office@paton.kiev.ua

Investigation of the effect of nitrogen alloying and yttrium and zirconium oxide additives to the weld pool on the structure of an austenitic weld and its microhardness in the zone of its fusion with pearlitic base metal was studied for the case of joints of dissimilar steels (austenitic with pearlitic), made by coated-electrode arc welding. It is shown that nitrogen alloying of weld metal of Kh20N9G6 type through the electrode coating practically does not affect the dendrite dimensions, but lower the microhardness (risk of martensite formation) in the zone of fusion with pearlitic base metal. In the case of yttrium or zirconium oxide additives to the austenitic metal of Kh15N25M6AG2 type through the coating, its dendrite structure is refined significantly, and metal microhardness in the fusion zone drops to the level that is indicative of martensite absence. 8 Ref., 2 Tables, 4 Figures.

Keywords: arc welding, coated electrodes, austenitic deposited metal, transition zone with pearlitic metal, structure, microhardness

Structure refinement and prevention of transcrystallinity in multipass welded joints of high-alloyed austenitic steels enable improving their technological strength and service properties [1, 2]. Known are the techniques of structure refinement due to electromagnetic impact on the molten metal, pulsed melting or welding wire feeding, adding metal powders or master alloys to the weld pool can be implemented at automatic welding. Under the conditions of coated electrode arc welding (MMA), a positive effect can be obtained by modifying the weld metal through the electrode coating by refractory metals (Zr, Ti, Nb, Mo) [3], as well as oxides (Cr, Zr, REM) [2].

In welding dissimilar steel joints by austenitic electrodes, in addition to structure refinement, it is also necessary to minimize or exclude the formation of martensite in the zone of fusion with pearlitic base metal. This is due to the fact that the low-ductility martensite is the source of stress concentration and premature failure of the joint. Martensite formation can be prevented by increasing the nickel content in the austenitic weld and lowering the energy input in welding [4, 5].

More over, use of nickel-based electrodes can not only prevent formation of martensite in the fusion zone, but also prevent development of stresses and strains as a result of a considerable difference in TEC between the austenitic and pearlitic metal [4, 5]. In a number of cases, particularly, during performance of repair operations, use of nickel-base electrodes allows welding equipment from heat-resistant pearlitic steels without preheating or final heat treatment. At the same time, it is not rational to use such electrodes for joints exposed to temperatures of up to 450 °C in service.

Under these conditions electrodes of Kh20N9G6S or Kh15N25M6AG2 types are used [4]. Meanwhile, as was shown in [6], only in the case of electrodes of Kh15N25M6AG2 type at welding current limitation below 80 A, it is possible to avoid martensite formation in the zone of fusion of austenitic weld metal with pearlitic base metal. For the conditions of automatic welding of such joints by Sv08Kh20N9G6S wire the authors of [7] determined that martensite formation can be essentially limited due to weld metal alloying by nitrogen through the gas phase.

The objective of this work consists in studying the techniques of improvement of the quality of welded joints of dissimilar steels (austenitic with pearlitic) due to application of nitrided manganese (nitrogen alloying), as well as yttrium and zirconium oxides (modifying by refractory particles) in the welding electrode coating.

The influence of nitrogen alloying was studied using 3 mm test electrodes of Kh20N9G6 type, in the

K.A. Yushchenko — https://orcid.org/0000-0002-6276-7843, O.V. Bulat — https://orcid.org/0000-0003-2237-5260,
G.V. Svyagintseva — https://orcid.org/0000-0002-6450-4887, V.I. Samoilenko — https://orcid.org/0000-0001-6370-277X,
Yu.M. Kakhovskyi — https://orcid.org/0000-0002-9520-2996

Table 1. Chemical composition of deposited metal of test electrodes of 10Kh20N9G6S type

Electrode designations	Weight fraction, % in the deposited metal*							Ferrite phase content, %
	N	Cr	Ni	Mn	Si	S	P	
C1	0.07	21.3	9.1	7.1	0.70	0.015	0.025	4–5
C2	0.32	20.0	10.0	6.6	0.65	0.016	0.024	1–1.5
C3	0.44	20.4	9.8	6.2	0.62	0.015	0.022	0.8
*Content of other elements in the deposited metal: 0.09 % C; 0.40 % Mo; 0.30 % Cn.								

coating of which the content of nitrided manganese was varied instead of that of metal manganese (C1–C3 electrodes in Table 1).

Before that these electrodes were used to make eight-layer deposits to determine the chemical composition of the deposited metal by the methods of X-Ray microprobe, chemical and gas analysis. The results are given in Table 1.

Then, 3 mm test electrodes C1–C3 were used to make single-layer deposits on a plate from 10 mm steel St3sp(killed) at I_w = 90–100, U_a = 26–28 V; v_w = = 9 m/h; from which sections were cut out for metallographic studies. The structure of the transition zone and deposited metal was revealed by combined chemical and electrochemical etching. Martensite formation was recorded by measuring the microhardness of the transition zone, using microhardness meter PMT-3. Here, it was assumed that microhardness values above 3000 MPa correspond to martensite formation. Obtained results are given in Figure 1, from which one can see that increase of nitrogen content in the deposited metal from 0.07 up to 0.32 % leads to microhardness lowering in the fusion zone from 3380 to 3000 MPa. Further increase of nitrogen content up to 0.44 % increases the microhardness in this area up to 3320 MPa. Average microhardness in the deposited metal rises from 1814 up to 2732 MPa, that is indicative of increase of strength and is in agreement with the data of [2, 8].

Nitrogen effect at its concentration of 0.32 % is attributable to the fact that it is an interstitial impurity, similar to carbon, and blocks carbon diffusion from pearlitic metal into the austenitic deposit. Due to that in the transition zone austenite decomposes at cooling by γ→γ + α reaction instead of γ→γ + M + α. Microhardness increase at additional alloying of the

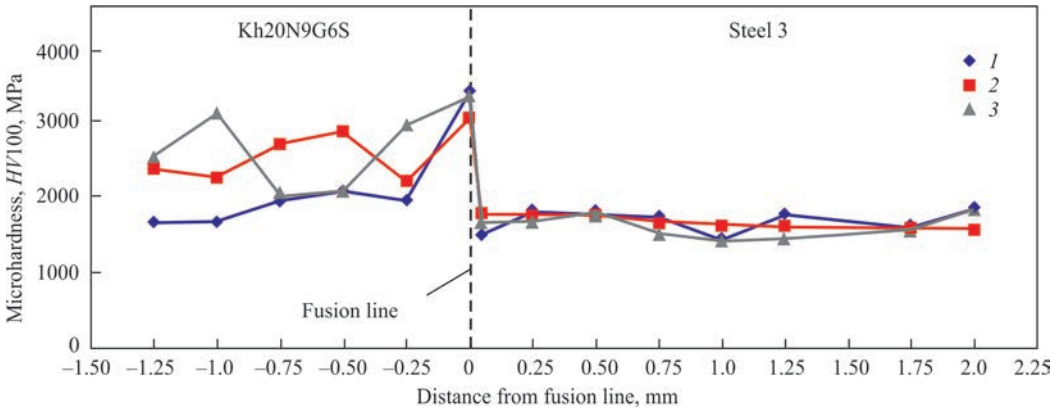

Figure 1. Effect of nitrogen alloying on microhardness in the joint of austenitic deposited metal of 10Kh20N9G6S type with pearlitic base metal: *1* — [N] = 0.7; *2* — 0.32; *3* — 0.44 %

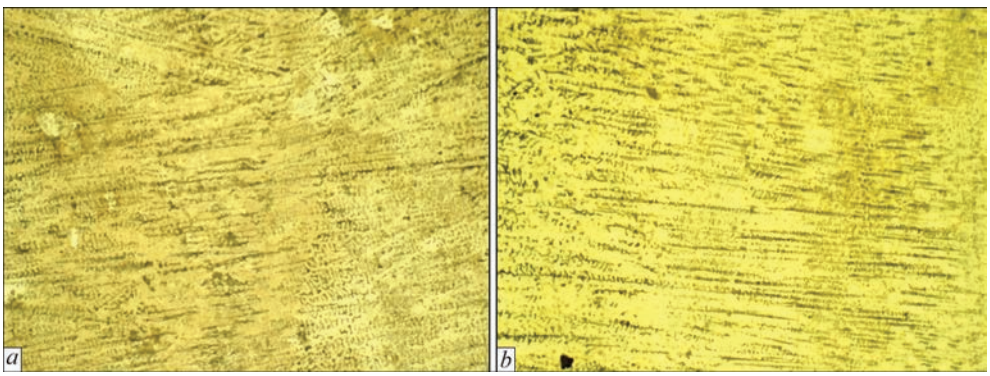

Figure 2. Dendritic structure (×200) of deposited metal of 10Kh20N9G6S type: *a* — unalloyed by nitrogen; *b* — alloyed by 0.32 % of nitrogen

Table 2 Chemical composition of the deposited metal of test electrodes of 10Kh15N25M6AG2 type

Electrode designations	Description and number of modifiers in the coating	Weight fraction of test electrodes								
		Cr	Ni	Mo	Mn	Si	N	C	S	P
C4	–	15.3	24.8	6.2	2.1	0.35	0.18	0.10	0.017	0.024
C5	Y_2O_3, 1%	15.1	24.2	6.0	2.0	0.34	0.18	0.09	0.019	0.025
C6	ZrO_2, 1 %	15.4	25.0	6.2	1.8	0.36	0.17	0.11	0.017	0.026
C7	ZrO_2, 2 %	15.4	24.5	6.4	1.9	0.39	0.17	0.10	0.018	0.026

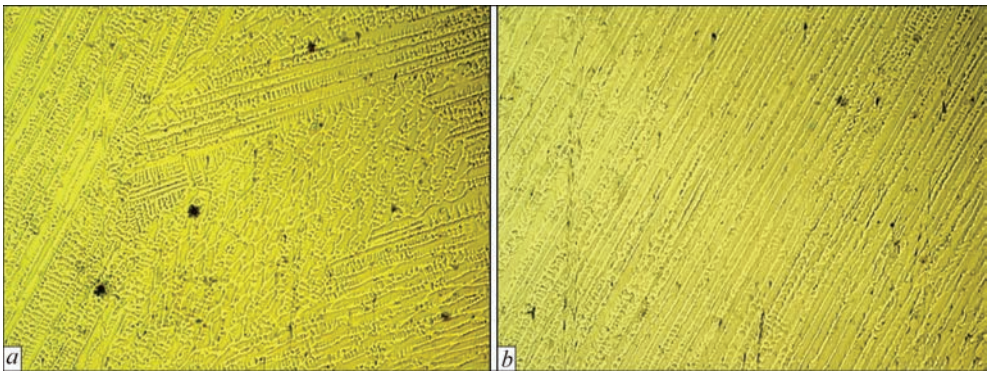

Figure 3. Dendritic structure (×200) of deposited metal of 11Kh15N25M6AG2 type: *a* — without ZrO_2 in the coating; *b* — with 2 % ZrO_2 in the coating

deposited metal by nitrogen (up to 0.44 %) is attributable to formation of chromium, manganese and silicon nitrides during solidification, which strengthen the austenitic matrix. Studying the structure of the deposited metal of C1–C3 electrodes using Neophot-32 microscope showed that irrespective of nitrogen content, the dendrite dimensions remain practically unchanged (Figure 2) and are equal to 7–8 in the lower and 13–14 μm in the upper part of the deposit.

The next stage was to study the possibility of refining the structure of austenitic weld of Kh15N25M6AG2 type and lowering the microhardness in the zone of its fusion with pearlitic base metal due to application of electrodes with yttrium or zirconium oxides in the coating. The powders of these materials with particle dimensions less than 100 μm were added to the coating of 3 mm test electrodes C4–C7 through the rutile concentrate.

Results of determination of the chemical composition of the deposited metal of these electrodes are given in Table 2.

C4–C7 electrodes of 3 mm diameter were used to perform single-layer deposition on the surface of plates from St3sp steel 10 mm thick. Here, the deposition mode remained the same as in the previous test series. Metal structure in the respective sections was revealed by a similar procedure. Metallography of the produced sections using Neophot-32 microscope was used to determine (Figure 3) that the maximum reduction of the average width of dendrites from 20.97 to 11.39 μm is achieved in the deposited metal of C7 electrodes which contain 2 % ZrO_2 in the coating. Refinement of the austenitic structure of the deposited metal of Kh15N25M6AG2 type at its modification by zirconium oxide can be explained by that the surface dissolution of these particles in the molten met-

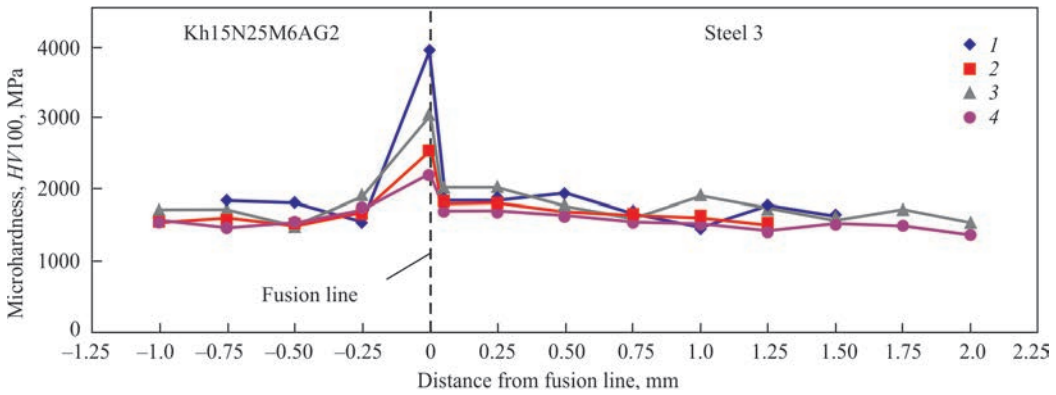

Figure 4. Effect of yttrium and zirconium oxides on microhardness in the joint of austenitic deposited metal of 11Kh15N25M6AG2 type with pearlitic base metal: *1* — without modifiers; *2* — 1 % Y_2O_3; *3* — 2 % ZrO_2; *4* – 2 % ZrO_2

al volume proceeds with heat absorption. Due to that the weld pool temperature decreases, and it solidifies faster. Investigations of microhardness of the transition zone between the pearlitic base and the deposited metal of C4–C7 electrodes, made using PMT-3 microhardness meter (Figure 4), revealed that the minimum microhardness is ensured in the transition zone of the metal deposited with C7 electrodes. This effect is somewhat lower in the case of C5 electrodes which contain 1 % Y_2O_3 in the coating. Unlike the previous test series, addition of refractory oxides to the deposited metal did not lead to increase of its average microhardness (strength).

Conclusions

1. Alloying of the deposited weld metal of Kh20N9G6S type by nitrogen up to 0.32 % due to nitrided manganese in the electrode coating composition, lowers the microhardness in the zone of fusion with the pearlitic base metal from 3250 to 3000 MPa and practically does not affect the dimensions of dendrites in the weld metal structure.

2. Modification of weld metal of Kh15N25M6AG2 type by yttrium or zirconium oxides through the electrode coating leads to microhardness lowering in the zone of fusion with the pearlitic base metal from 3950 to 2500 and 2200 MPa, respectively, as well as a considerable reduction of the dimensions of dendrites in the weld metal structure.

3. Nitrogen alloying and modifying of high-alloyed austenitic weld metal by particles of refractory oxides allows reducing the risk, or preventing martensite formation in the joined dissimilar steels (austenitic and pearlitic).

1. Shorshorov, M.Kh., Erokhin, A.A., Chernyshova, T.A. et al. (1973) *Hot cracks in welding of heat-resistant alloys*. Moscow, Mashinostroenie [in Russian].
2. Kakhovsky, N.I. (1975) *Welding of high-alloyed steels.* Kiev, Tekhnika [in Russian].
3. Braun, M.P. (1982) *Microalloying of steel*. Kiev, Naukova Dumka [in Russian].
4. Zemzin, V.N. (1966) *Welded joints of dissimilar steels*. Moscow, Leningrad, Mashinostroenie [in Russian].
5. Gotalsky, Yu.N. (1981) *Welding of dissimilar steels*. Kiev, Tekhnika [in Russian].
6. Yushchenko, K.A., Kakhovsky, Yu.N., Bulat, A.V. et al. (2014) Investigation of transition zone of low-carbon steel joint with high-alloyed Cr–Ni deposited metal. *The Paton Welding J.*, **6–7**, 143–146.
7. Elagin, V.P., Lipodaev, V.N., Gordan, G.N. (2016) Peculiarities of development of structural heterogeneity in the fusion zone of pearlitic steel with nitrogen-containing weld metal. In: *Proc. of 9th Int. Conf. on Arc Welding, Materials and Quality (31 May–3 June 2016, Volgograd, Russia)*, 116–126.
8. Pickering F.B. (1982) *Physical metallurgy and development of steel.* Moscow, Metallurgiya [in Russian].

Received 16.01.2020

https://doi.org/10.37434/tpwj2020.08.03

APPLICATION OF PLASMA-POWDER AND ELECTRIC ARC COATINGS TO INCREASE TRIBOCORROSION RESISTANCE OF STEELS IN CHLORIDE-CONTAINING MEDIA WITH HYDROGEN SULFIDE AND AMMONIA

V.I. Pokhmurskyi[1], **M.S. Khoma**[1], **I.O. Ryabtsev**[2], **Ye.F. Pereplyotchikov**[1], **V.A. Vynar**[1], **V.M. Gvozdetskyi**[1], **Kh.B. Vasyliv**[1], **N.B. Ratska**[1], **V.R. Ivashkiv**[1] and **Ye.M. Rudkovskyi**[1]

[1]G.V. Karpenko Physical-Mechanical Institute of the NAS of Ukraine
5 Naukova Str., 79060, Lviv, Ukraine. E-mail: khomams@gmail.com
[2]E.O. Paton Electric Welding Institute of the NAS of Ukraine
11 Kazymyr Malevych Str., 03150, Kyiv, Ukraine. E-mail: office@paton.kiev.ua

The work was performed within the framework of the complex program of the NAS of Ukraine «Problems of life and safe operation of structures, constructions and machines», 2011–2020. The corrosion and tribocorrosion characteristics of plasma-powder and electric arc coatings on pipe steels in chloride-containing media with hydrogen sulfide and ammonia were studied. It was established that the corrosion resistance of the coatings applied by plasma-powder surfacing and electric arc spraying is improved with an increase in pH of the solution. It was shown that the coatings deposited by the plasma method with the powder of 08Kh17N35S3R alloy were the most resistant to corrosion and mechanical fracture in these media. It was established that electric arc coatings sprayed from the flux-cored wire 75Kh19R3S2 reduce the corrosion current density of carbon steels in a hydrogen sulfide solution by 40 %. In the same medium on the surface of the coatings sulfide compounds are formed, which act as a solid lubricant during friction, facilitating a reduction in wear of the material by 40–42 %. The electric arc coatings produced by the flux-cored wire 75Kh19R3S2 were proposed to be used to restore damaged surfaces of parts and protect them from corrosion and abrasive wear in the hydrogen sulfide media. 14 Ref., 5 Tables, 4 Figures.

Keywords: plasma-powder surfacing, electric arc coatings, corrosion, tribocorrosion, chlorides, hydrogen sulfide, ammonia

Corrosion and mechanical wear occurs during friction of parts in aggressive media and is often the reason for reducing the life of many parts of equipment and structures in the oil, gas, petrochemical and municipal industries, as for example, stop valves, end seals, rolling bearings, etc. [1–3].

The main methods for restoration and improvement of serviceability of surfaces of parts operated under the conditions of corrosion and mechanical wear include plasma-powder surfacing [4, 5] and electric arc spraying of protective coatings from flux-cored wires [3, 6–8].

Plasma-powder surfacing is used to improve the physical and mechanical characteristics of working surfaces and restoration of worn parts. In particular, using this method the surfaces of parts of stop valves are deposited: gate valves, seats, rods and other parts of oil and gas equipment [4–10]. The use of powders based on Ni, Fe, Cr, B, Si, etc. allows regulating the chemical composition of deposited layers and expands the range of their functional properties [6–8].

Electric arc metallization (EAM) using flux-cored wires is one of the widespread methods of deposition wear-resistant coatings, the cost of which is 2–3 times lower than that of plasma-powder surfacing [6]. During melting of flux-cored wires in the electric arc a melt is formed, which during dispersion into droplets, forms an electric arc coating with a high structural heterogeneity. The combination of hard and soft components provides their high wear resistance. To improve the corrosion and tribocorrosion resistance of coatings, to the charge of flux-cored wires chromium compounds are added and to reduce the porosity of the sprayed layer, FeMn and FeSi are introduced, which form a low-melting eutectic. Comprehensive investigations of corrosion and tribocorrosion properties of coatings with different chemical composition, produced by plasma-powder surfacing

V.I. Pokhmurskyi — http://orcid.org/0000-0003-1042-829X, M.S. Khoma — https://orcid.org/0000-0002-0951-3975, I.O. Ryabtsev — https://orcid.org/0000-0001-7180-7782, V.A. Vynar — http://orcid.org/0000-0002-5314-7052

Table 1. Chemical composition of powders for plasma-powder surfacing, wt.%

Powder grade	C	Cr	Si	Mn	Ni	Fe	B
PR-06Kh17N80S3R3	0.6–0.9	15–17	2.7–3.7	–	Base	≤5.0	2.3–3.0
PR-01Kh17N8S6G	0.05–0.12	15–18	4.8–6.4	1–2	7–9	Base	–
PR-08Kh17N35S3R3	0.8	18	3.5	≤ 1.0	35	35	2.5

and electric arc spraying of powder materials have a significant importance for restoration of serviceability and increasing the life of equipment operated in corrosive-active media at the presence of hydrogen sulfide, chlorides and ammonia.

The aim of this work is to investigate the possibility of using plasma-powder and electric arc coatings to restore serviceability and increase the service life of friction units in the equipment of oil and gas, refining and municipal industries, which are operated in corrosive media.

Investigation procedure. Plasma-powder surfacing, the technology of which is developed by the PWI, was performed in the universal installation OB2184 on the basis of the device A1756 [4, 5]. The chemical composition of powders for surfacing is given in Table 1. Surfacing mode: current is 250–300 A, powder feed is 3 kg/h, deposition rate is 6 m/h, amplitude of oscillations of the plasmatron is 10 mm, their frequency is 45 min^{-1}. The consumption of carrier, plasma-forming and shielding gases (argon) is 3 l/h, 2 and 12 l/min, respectively. The beads deposited under these conditions, had a width of 25–35 mm and a height of 6.0–6.6 mm during two-beads surfacing.

Electric arc metallization was performed according to the technology developed by the G.V. Karpenko PMI [3, 6–9]. The coatings were produced by spraying electrode flux-cored wires PD-60Kh15R2GS and PD-75Kh19R3S2 with the use of the electric arc metallizer EM-17 with a modified spraying system, where an electric arc burns in the channel of the spraying head, which allows producing fine-dispersed coatings. Surfaing conditions: current is 150 A, operating voltage is 32 V, distance from the nozzle to the spraying surface is 150 mm, compressed air pressure is 0.65 MPa. Sheath of flux-cored wires is made of steel 08kp (rimmed) (0.05–0.11 % C; ≤ 0.02 % S; 0.025–0.5 % Mn; 0.04 % P), chemical composition of the charge is given in Table 2.

Corrosion-mechanical wear of materials was studied in the installation of friction with a reciprocating motion of the indenter according to the scheme ball-plane [2]. The counterbody is a corundum ball with a diameter of 9 mm. The applied normal load is 10 N, the length of the friction track is 16 mm, the speed of the indenter movement is 0.003 m/s. The specimens for investigations were polished to a roughness R_z = = 2.5 μm. The nature of the change in the investigated parameters during tribocorrosion tests was recorded by an analog-digital device using a personal computer with a measurement step of 0.25 s. The degree of wear of the specimens after friction was determined by the width of the track formed as a result of interaction of the ball with the surface of the coating, the hardness of which is significantly lower than that of corundum.

Table 2 Chemical composition of charge of flux-cored wires, wt.%

Powder wire grade	Composition of charge
PD-60Kh15R2GS	FeCr 72 %; B_4C 13 %; FeSi 10 %; FeMn 5 %
PD-75Kh19R3S2	Cr 72 %; FeSi 13 %; B_4C 10 %

To determine the elastic-plastic properties of structural components of the produced coatings, in particular Meyer microhardness, the method of dynamic indentation was used. For this purpose the device Micron-gamma was applied [11].

Electrochemical investigations under static conditions and during friction were performed using the potentiostat IPC-ProM. The electrode potentials of the specimens in corrosive media were measured relative to the saturated chloride-silver reference electrode. The auxiliary electrode is platinum. The media for corrosion and tribocorrosion tests are: free-aerated 3% solution of NaCl, pH 7; 3 % solution of NaCl + 0.025 % of NH_4OH, pH 9–10; 3% solution of NaCl + H_2S (saturated), pH 4.

The microstructure of the surfaces was studied by metallographic method in a scanning electron microscope EVO 40XVR with a system of micro-X-ray spectral analysis using an energy-dispersion spectrometer INCA ENERGY 350.

Results of investigations and their discussion. *Plasma-powder surfacing*. Deposited layers (Figure 1) from the powders PR-01Kh17N8S6G (base Fe), PR-06Kh17N80S3R3 (base Ni) and PR-08Kh17N35S3R3 (base Ni–Fe) having different composition and structure were investigated. It was found that they have a heterogeneous structure, which determines their micromechanical, corrosion-electrochemical and tribocorrosion properties. The deposited iron-based layer has two structural components with a microhardness of 6.0–6.5 and 7.5–8.0 GPa. In the nickel-based layer after surfacing, three components with a microhardness of 6.0–7.0, 7.0–8.5 and 15 GPa are formed. The highest microhardness (~ 15 GPa) is predetermined by the presence of borides of type FeCrB. The coating with

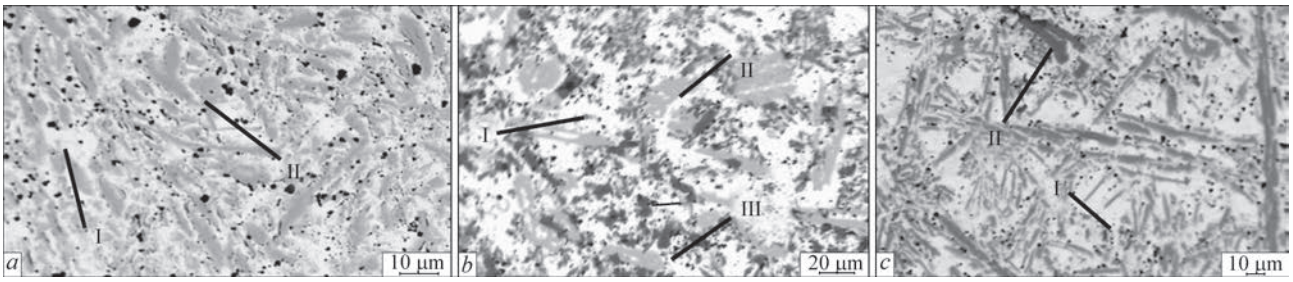

Figure 1. Microstructure of layers deposited by the method of plasma-powder surfacing: *a* — 01Kh17N8S6G (Fe base); *b* — 06Kh17N80S3R3 (Ni base); *c* — 08Kh17N35S3R3 (Ni–Fe base)

an iron-nickel base contains two components with a microhardness of 7.0–7.5 and 10.1–12.2 GPa. Nickel and nickel-iron based coatings, as compared to iron-based coatings, are characterized by a higher microhardness of structural components, which is associated with the presence of boron and a higher concentration of carbon in the powders (0.6–0.9 % against 0.12 %, respectively).

The electrochemical behavior of deposited layers in corrosion-active chloride-containing media with the addition of hydrogen sulfide and ammonia was studied (Table 3). It was found that application of plasma-powder layers makes it possible to reduce the corrosion current density of steel 17G1SU, which was chosen for comparison by about 2 orders. With an increase in the hydrogen index of the medium from pH4 to pH9, it is observed that the corrosion current density of alloys 01Kh17N8S6G and 06Kh17N80S3R3 is decreased by 7–15 %, and that of 08Kh17N35S3R3 is decreased by three times. The corrosion rate is determined by anodic processes in a solution of 3 % of NaCl + NH_4OH and cathodic processes in 3 % of NaCl and 3 % of NaCl + H_2S. In terms of corrosion resistance in the investigated media, the layer deposited by the powder on Ni–Fe base is inferior to two other, its corrosion current density is $(0.47–1.60)\cdot10^{-3}$ against $(0.56–0.80)\cdot10^{-3}$ mA/cm^2. However, under conditions of tribocorrosion in pair with a ceramic corundum ball coating based on Ni–Fe has the lowest values of the coefficient of friction and material loss in all the investigated media (Table 4), which indicates its higher resistance to fracture. In a hydrogen sulfide medium, the width of the wear track of this coating and the friction coefficients are 3–4 times lower than the original steel, and in neutral and alkaline solutions — by 30–50 %, which indicates a significant effect of corrosion products on friction and wear. In particular, during friction sulfide films formed on the friction surface in a solution of 3 % of NaCl + H_2S, perform the function of lubricant, which reduces the coefficient of friction and the width of the wear track.

A clear relationship between tribotechnical characteristics and the rate of corrosion of deposited layers is observed. As pH of the medium grows, the density of corrosion currents for layers with different base decreases, and the coefficient of friction and material losses increase (Table 3). The mechanisms of contact interaction of layers are determined by structural heterogeneity and tribological characteristics of separate structural components. Thus, during contact interaction of surface layers of 06Kh17N80S3R3 with a ceramic

Table 3. Density of corrosion currents, coefficient of friction and width of friction tracks of the layers deposited by the method of plasma-powder surfacing in different media

Medium	01Kh17N8S6G (base Fe)			06Kh17N80S3R3 (base Ni)			08Kh17N35S3R3 (base Ni–Fe)		
	i_{cor}, mA/cm^2	B, μm	μ	i_{cor}, mA/cm^2	B, μm	μ	i_{cor}, mA/cm^2	B, μm	μ
3 % of NaCl+H_2S (pH 4)	0.00075	180	0.10	0.0006	210	0.13	0.0016	140	0.09
3 % of NaCl (pH 7)	0.00065	190	0.21	0.0008	230	0.16	0.0019	160	0.10
3 % of NaCl+0.025 % NH_4OH (pH 9)	0.00065	260	0.41	0.00056	300	0.35	0.00047	190	0.31

Table 4. Coefficients of friction and width of wear track of electric arc coatings in different media

Medium	60Kh15R2GS				75Kh19R3S2			
	E, mV	i, mA/cm^2	μ	B, μm	E, mV	i, mA/cm^2	μ	B, μm
3 % of NaCl + H_2S (pH 4)	–586	0.053	0.30	350	–626	0.052	0.25	240
3 % of NaCl (pH 7)	–525	0.034	0.38	510	–525	0.024	0.30	480
3 % of NaCl + 0.025 % NH_4OH (pH 9)	–468	0.024	0.50	490	–468	0.022	0.55	400

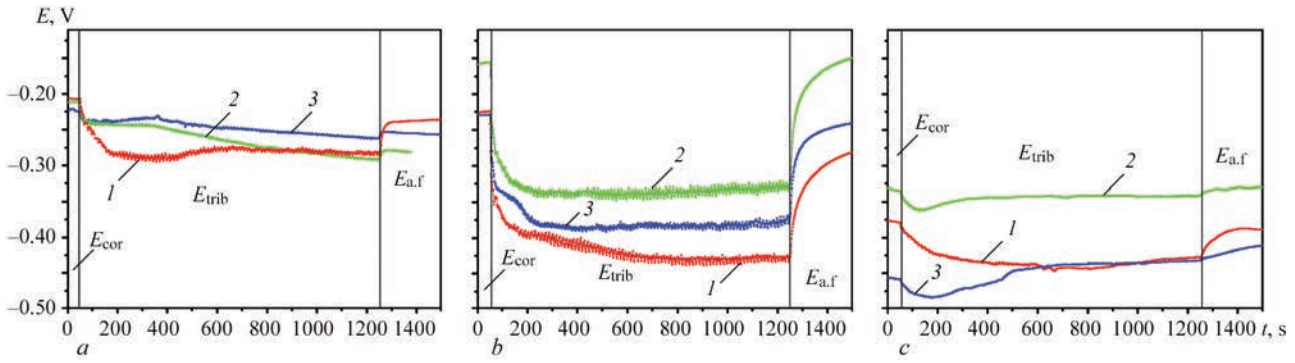

Figure 2. Change of electrode potentials of the surface of alloys during friction in 3 % of NaCl (*a*), 3 % of NaCl + NH_4OH (*b*), 3% of NaCl + H_2S (*c*): coatings based on Fe (*1*), Ni (*2*) and Ni–Fe (*3*)

ball, brittle components with a high microhardness (15 GPa) enter the friction zone. This is manifested in low values of the friction coefficient, but more intensive wear according to the mechanism of microcutting, the losses of material are approximately 45% higher than in the coating on iron-nickel base. In the matrix of layers of 01Kh17N8S6G and 08Kh17N35S3R3, the brittle component is absent and solid phases are uniformly distributed in the plastic matrix, which corresponds to the Charpy–Bochvar rule [12], and the contact interaction takes place in the absence of abrasive wear element, which explains a high resistance of tribocorrosion.

By changing the electrode potentials during corrosion-mechanical wear, it is possible to qualitatively evaluate the fracture and formation of secondary structures in the zone of frictional interaction [13]. It is shown (Figure 2) that the largest difference between the corrosion potentials in the initial state (E_{cor}), tribocorrosion during friction (E_{trib}) and surface potentials after friction ($E_{a.f}$) for all deposited layers is characteristic for the medium of 3 % of NaCl + NH_4OH. This indicates the formation of dense secondary structures on the surface of the contact zone, which are destroyed with the beginning of a frictional interaction. During steady friction, the secondary structures are intensively destroyed and restored, which is manifested in the tribopotential oscillations, which indicate a high rate of surface repassivation and fracture of the material according to the mechanism of oxidative wear. As pH index of the medium decreases, the rate of repassivation processes is reduced, which are minimal in the hydrogen sulfide medium. The difference between these potentials is insignificant and local oscillations of the tribopotential are almost absent, which indicates the incompatibility of the initial surface films of corrosion products. The coefficient of friction under such conditions is the lowest as compared to other media. The frictional interaction of layers with the counter-body occurs from the formation of secondary structures that reduce the adhesion between the surfaces.

It was found that the difference between the potentials of corrosion, tribocorrosion and passivation correlates with the hardness of the coatings. In particular, this is clearly observed when comparing the material 01Kh17N8S6G (Ni–Fe base) and 08Kh17N35S3R3 (Ni–Fe base) in the investigated media. The biggest difference between the potentials as well as local oscillations of the tribopotential are typical to the deposited layer of complex carbides, which is associated with a greater surface damage because of a lower hardness in the surface layers of the coating.

Plasma surfacing from the powder PR-08Kh17N35S3R was proposed for depositing protective layers on a surface of parts of stop valves (Figure 3) with the aim of improving their corrosion and tribocorrosion resistance in aggressive media and it was used at the PJSC «Konotop armature plant».

Electric arc spraying. To restore worn or damaged surfaces and improve the service characteristics of parts, thermal spraying is widely used [3, 6–9]. This method makes it possible to significantly extend the life cycle of parts by creating a layer of coatings with the specified properties on their surface. During spraying, thermal buckling of a part does not occur and physicochemical properties of the base material are not changed. The ability to repair parts instead of replacing them helps to reduce costs and increase the efficiency of production.

The coatings produced by electric arc spraying from the flux-cored wires PD-60Kh15R2GS and PD-75Kh19R3S2 were investigated. They have a heterogeneous structure consisting of a martensitic

Figure 3. Parts of stop valves deposited by the plasma method using the powder PR-08Kh17N35S3R

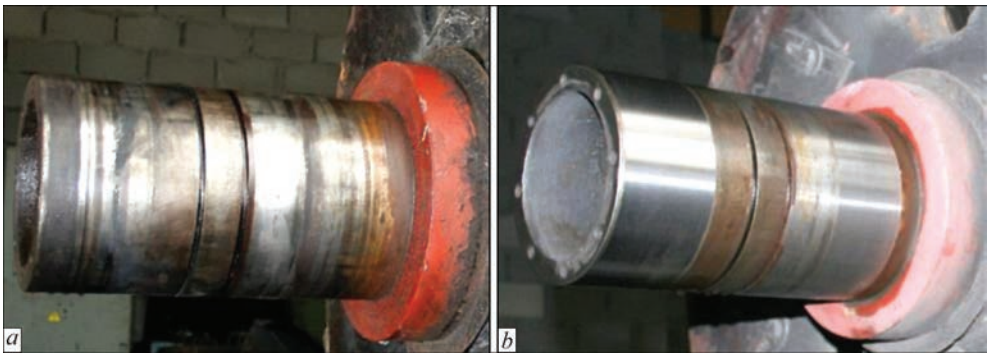

Figure 4. General appearance of damaged shaft of centrifuge of wastewater treatment plants in the initial state (*a*) and after electric arc spraying and grinding (*b*)

matrix strengthened by fine-dispersed inclusions of FeCrB and $FeCr_2B$ borides. The hardness of the coatings is *HV* 545−545, cohesive strength is 140−150 MPa [3]. The presence of ferrochrome-boron and chromium in the charge provides a high content of chromium in the coating.

The electrochemical characteristics of sprayed coatings in the media containing ammonia, hydrogen sulfide and chlorides were investigated. On the obtained polarization curves passivation regions are absent, which indicates electrochemically active dissolution of materials. After electric arc spraying, the values of the electrode potentials in all corrosive media are shifted to the region of positive values by 60−70 mV. The corrosion currents density of sprayed coatings in hydrogen sulfide and chloride solution is reduced by 40 % as compared to the initial material (Tables 4, 5). In ammonia solution, the corrosion currents of the base material and coatings have the lowest values. The corrosion rate of electric arc coatings is controlled by cathode processes. It was established that the corrosion rate of coatings from PD-75Kh19R3S2 is lower than from PD-60Kh15R5GS, which is associated with a higher concentration of chromium (Tables 4, 5).

The width of the friction track and the values of the friction coefficients of both electric arc coatings are the lowest in 3 % of NaCl + H_2S, and the highest are in 3 % solution of NaCl. The tribological characteristics of coatings from PD-75Kh19R3S2 are better than those from PD-60Kh15R2GS, in particular, in 3 % of NaCl + H_2S its wear is lower by a third (Table 4). The parameters of friction and wear of coatings are determined by their chemical composition, heterogeneity of the structure, ratio of strength characteristics of its components, relief, etc. The most effective electric arc coatings were revealed in the solution of 3 % of NaCl + H_2S, where the width of the wear track after spraying decreased by 40−42 % (Tables 4, 5).

The highest values of friction coefficients were revealed during friction of coatings in a medium containing ammonia. Probably, in the solution on the surface secondary structures are formed, which are destroyed during friction and play the role of abrasive. This facilitates an increase in the coefficient of friction and wear of the material. Depassivating chlorine ions in the medium initiate corrosion of coatings and the combined action of corrosion and mechanical factors during friction leads to a decrease in wear resistance. In the hydrogen sulfide medium, the wear and friction coefficients of electric arc coatings are the lowest, which is associated with the formation of sulfide-containing films on the surface, which act as a solid lubricant during friction, reducing the adhesive component of contact interaction, which reduces friction and wear coefficients [2, 13, 14]. In addition, during friction, sulfides can fill the pores in the coating, improving its homogeneity, which facilitates an increase in the corrosion resistance of the material.

Electric arc coatings produced from the flux-cored wire PD-75Kh19R3S2 were proposed to be used to restore damaged surfaces of parts and protect them from corrosion and abrasive wear in hydrogen sulfide media. The coatings were deposited to the surface of the shafts in the centrifuges of the wastewater treatment facilities of LMKP Lvivvodokanal and passed the test and industrial inspection.

Table 5. Electrode potentials, corrosion current density, friction coefficient and width of friction tracks of steel 17G1SU (base) in different media

Medium	*E*, mV	*i*, mA/cm^2	*B*, μm	μ
3 % of NaCl + H_2S (pH 4)	–660	0.08	580	0.28
3 % of NaCl (pH 7)	–580	0.04	310	0.25
3 % of NaCl + 0.025 % NH_4OH (pH 9)	–530	0.025	360	0.41

Conclusions

1. Corrosion and tribocorrosion characteristics of plasma deposits from the powders based on iron (PR-01Kh17N8S6G), nickel (PR-06Kh17N80S3R3) and Fe–Ni system (PR-08Kh17N35S3R3) and coatings produced by electric arc spraying using the wires PD-60Kh15R2GS and PD-75Kh19R3S2 in the media containing chlorides, hydrogen sulfide and ammonia were investigated.

2. In the deposits produced from the powders 01Kh17N8S6G and 08Kh17N35S3R3, two structural components with a microhardness of 6.0−6.5 and 7.5−8.0 GPa and 7.0−7.5 and 10.1−12.2 GPa were revealed. The deposited layer from the nickel-based powder PR-06Kh17N80S3R3 has three components with a microhardness of 6.0−7.0, 7.0−8.5 and 15 GPa. An increased microhardness of structural components is associated with the presence of boron and a higher concentration of carbon in the powder. The highest microhardness (~ 15 GPa) is predetermined by the presence of borides of FeCrB type.

3. The coatings produced by electric arc spraying from the flux-cored wires PD-60Kh15R2GS and PD-75Kh19R3S2 have a structure consisting of a martensitic matrix strengthened by fine-dispersed inclusions of borides FeCrB and $FeCr_2B$. The hardness of coatings is *HV* 545−545, cohesive strength is 140−150 MPa.

4. As a result of tests it was shown that deposits from the powder based on Fe−Ni and electric arc coatings from the wire PD-75Kh19R3S2 have the highest resistance to corrosion-mechanical wear in corrosive-active media.

5. It was found that depositing layers by the plasma method from the powder PR-08Kh17N35S3R allows reducing the corrosion rate by approximately 2 orders in the media containing chlorides, ammonia and hydrogen sulfide. During friction in a hydrogen sulfide medium, the width of the wear track and the friction coefficients are 3−4 times smaller than that of the initial steel, and in neutral and alkaline solutions — by 30−50 %.

6. Plasma-powder surfacing by the powder PR-08Kh17N35S3R was proposed for depositing protective coatings on the surface of gate and stop valves in order to improve their corrosion-mechanical properties and it was used at the PJSC «Konotop Armature Plant».

7. It was established that the corrosion rate of electric arc coatings sprayed from the flux-cored wire PD-75Kh19R3S2 in ammonia solution is commensurated with the corrosion rate of carbon steel. In chloride and chloride-hydrogen sulfide solutions, deposition of coatings reduces the corrosion rate of steel by almost 40 %. In the presence of hydrogen sulfide in the medium, on the surface of the coatings sulfide compounds are formed, which act as a solid lubricant during friction, reducing the adhesive component of the contact interaction, which facilitates the reduction in wear of the material by 40−42 %.

8. Electric arc coatings produced from the flux-cored wire PD-75Kh19R3S2 were proposed to be used to restore damaged surfaces of parts and protect them from corrosion and abrasive wear in hydrogen sulfide media. The coatings were deposited on the surface of the shafts in the centrifuges of the wastewater treatment plants of LMKP Lvivvodokanal and successfully passed the test and industrial inspection.

1. Landolt, D., Mischler, S. (2011) *Tribocorrosion of passive metals and coatings*. Woodhead Publishing Ltd.
2. Khoma, M.S. et al. (2019) Corrosion and tribocorrosion properties of plasma sprayed coatings based on iron, nickel and chrome in environment containing hydrogen sulfide, chlorides and ammonia. *Naukovi Notatky*, **66**, 356−361 [in Ukrainian].
3. Student, M., Veselivska, H., Gvozdecki, V. et al. (2008) Corrosion-mechanical resistance of arc-sprayed coatings made from cored powders. *Ukrainian J. of Mechanical Engineering and Materials Sci.*, 4, **1**, 12–20.
4. Gladky, P.V., Pereplyotchikov, E.F., Ryabtsev, I.A. (2007) *Plasma-powder surfacing*. Kiev, Ekotekhnologiya [in Russian].
5. Pereplyotchikov, E.F., Vasyliv, Kh., Vynar, V. et al. Plasma-powder surfacing of high-alloyed alloys based on iron, chrome and nickel on low-alloyed structural steels to improve their wear resistance. *Fiz.-Khimich. Mekhanika Materialiv*, **3**, 81–88 [in Ukrainian].
6. Pokhmurska, G.V., Student, M.M., Pokhmurskyi, V.I. (2017) *Thermal sprayed coatings*: Manual. Lviv, Prostir-M [in Ukrainian].
7. Pokhmurskyi, V., Student, M., Gvozdeckii, V. et al. (2013) Arc-sprayed iron-based coatings for erosion-corrosion protection of boiler tubes at elevated temperatures. *J. Thermal Spray Technol.*, 22, **5**, 808–819.
8. Wielage, B., Pokhmurska, H., Student, M. et al. (2013) Ironbased coatings arc-sprayed with cored wires for applications at elevated temperatures. *Surface and CoatingTechnol.*, 220, 27–35.
9. Bolelli, G., Milanti, A., Lusvarghi, L. et al. (2016) Wear and impact behaviour of high velocity air-fuel sprayed Fe–Cr–Ni–B–C alloy coatings. *Tribology Int.*, **95**, 372–390.
10. Bobzin, K., Zhao, L., Öte, M., Königstein, T. (2017) Novel Fe-based wear and corrosion resistant coatings by three-cathode. Plasma Technology. *Ibid*., 318, 288–292.
11. Ignatovich, S.R., Zakiev, I.M. (2011) Universal micro/nanoindentor «Micron-gamma». *Zavodskaya Laboratoriya*, 77(**1**), 61−67 [in Russian].
12. Zakalov, O.V., Zakalov, I.O. (2011) *Fundamentals of friction and wear in machines*: Manual. Ternopil, TNTU [in Ukrainian].
13. Khoma, M.S., Ivashkiv, V.R., Chuchman, M.R. et al. (2018) Corrosion cracking of ferrite-pearlitic steels of different structure in the hydrogen sulfide environment under static load. *Procedia Structural Integrity*, **13**, 2184–2189.
14. Khoma, M.S., Ivashkiv, V.R., Galaichak, S.A. (2019) Influence of structure of steels on corrosion, hydrogenation and corrosion cracking in hydrogen sulfide environment. *Fiz.-Khimich. Mekhanika Materialiv*, **2**, 121−125 [in Ukrainian].

Received 07.05.2020

https://doi.org/10.37434/tpwj2020.08.04

PECULIARITIES OF PRODUCING Al–Ti BIMETAL SHEET JOINTS BY THE METHOD OF VACUUM DIFFUSION WELDING

Iu.V. Falchenko, L.V. Petrushynets and **Ye.V. Polovetskyi**
E.O. Paton Electric Welding Institute of the NAS of Ukraine
11 Kazymyr Malevych Str., 03150, Kyiv, Ukraine. E-mail: office@paton.kiev.ua

Given are the results of investigation of the effectiveness of application of vacuum diffusion welding technology to obtain aluminium-titanium bimetal sheets of 120×120 mm size. The effect of welding parameters on the joint microstructure and mechanical properties was studied. It is established that welding of foil materials is complicated, because of its low deformability. Application of thermally stable SiC and WC powders as «activators» in welding does not allow producing sound joints, because of hard particles embedding into the material being welded, and formation of defects in the form of through-thickness holes. It is shown that application of steel net for activation of plastic deformation on the foil contact surfaces, allows a significant lowering of welding pressure and producing defect-free joints between titanium and aluminium, with 1.7 times higher strength values, compared to layered Al+Ti joints, produced without using the net. 12 Ref., 1 Table, 6 Figures.

Keywords: aluminium, titanium, foil, bimetal joints, diffusion welding

Owing to low specific weight and corrosion resistance under atmospheric conditions, panels from aluminium alloys have become widely accepted in aerospace and mechanical engineering sectors. Prior research by the authors of work [1] showed that strength of three-layer aluminium panel is limited by that of the honeycomb core. In order to widen the possibilities for application of such structures, there is the need to replace the core material by the one more resistant to compression. So, in [2], it was proposed to replace the core from ATs5K5 aluminium alloy by VT6S titanium alloy 3–4 mm thick. However, considering the fact that the specific weight of titanium is two times greater than that of aluminium, its application as the core will lead to an essential reduction of overall weight of the structure that is undesirable when used in the aerospace sector.

Development of new materials, having higher mechanical properties, for working under the specific loading conditions in aircraft, and rocket construction, chemical industry, etc., is urgent. Over the recent years, layered composite materials (LCM) have attracted a lot of attention of scientists, due to the ability to combine the properties of the metals present in their composition [3–5]. Owing to its low density, high heat conductivity and corrosion resistance, aluminium is widely used in different sectors. Titanium at relatively low density has anticorrosion properties and high strength. Light layered Al–Ti composite materials that combine the properties of both the metals, have high values of strength, rigidity and impact toughness [6, 7]. Hence, the need to develop the technology of producing such LCM for further use in manufacture of the honeycomb core.

In the previous work by the authors [8], it was shown that joining foil with Al and Ti in the welding modes lower than the aluminium melting temperature (660 °C) prevents formation of a continuous intermetallic interlayer between these metal layers. From this viewpoint, it is rational to apply the methods of solid-phase joining, in particular, vacuum diffusion welding (VDW) is promising. It is known that in order to improve the welding quality, it is necessary to create in the butt joint the conditions for increase of shear deformations that can be achieved due to application of plastic deformation activators in the form of perforated interlayers, net or powder mixture. Authors of work [9] in welding thin bimetal foil propose applying mobile backing from powdered material.

In view of the above-said, the objective of this work was studying the features of vacuum diffusion welding of sheet materials from aluminium and titanium, using plastic deformation activators in the form of powder or steel net.

Foil from aluminium alloy AD1 and titanium alloy BT1-0 of 150 and 60 μm thickness, respectively, was used as material for investigations. The sheet size was 120×120 mm. Chemical composition of the materials is given in the Table. Before welding, samples were cleaned using a scraper and were degreased with alcohol.

Iu.V. Falchenko — https://orcid.org/0000-0002-3028-2964, L.V. Petrushynets — https://orcid.org/0000-0001-7946-3056,
Ye.V. Polovetskyi — https://orcid.org/0000-0002-8113-0434

Chemical composition of AD1 and VT1-0 alloys [10]

Alloy	Element content, wt.%								
	Al	Ti	Fe	Si	Mn	Cu	Mg	Zn	Sum of impurities
AD1	Base	0.15	0.3	0.3	0.025	0.02	0.05	0.1	–
VT1-0	–	Base	0.025	0.10	–	–	–	–	0.30

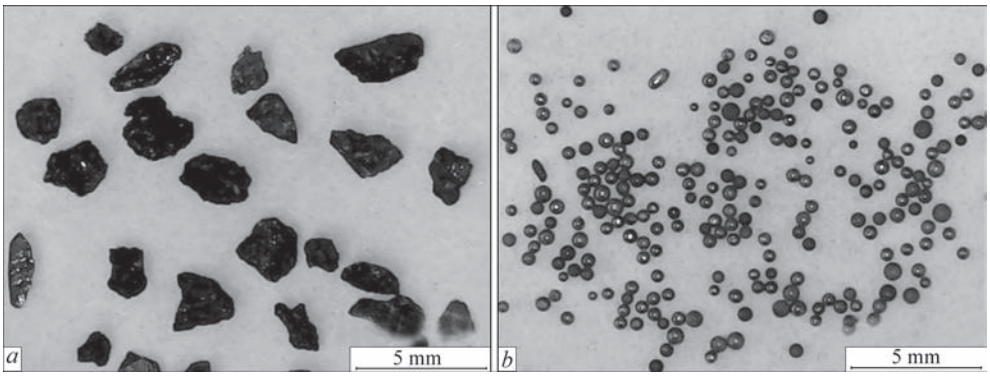

Figure 1. Appearance of SiC (*a*) and WC (*b*) powder, which was used in the investigations in welding aluminium foil to titanium

Welding was performed in a free state in the vacuum chamber of P115 unit, which is fitted with radiation heating system. The assembly with the samples was mounted between the massive steel rods with ground surfaces.

Heating was performed by molybdenum heaters, located around the samples. Heating temperature was controlled by chromel-alumel thermocouple, fastened to the fixture. Pressure was applied to the samples from the press through the lower rod. A dynamometer was used to control the pressure.

Backing from SiC or WC powder, or metal net from 12Kh18N9T stainless steel 1 mm thick with 4×4 mm cell size was used to localize the deformation on the foil surface in welding.

Powder was selected proceeding from the fact that it should be thermally stable at the welding temperature. SiC powder of irregular shape with particle size of 2–3 mm, and WC spherical powder with particle size of 0.5–1.0 mm, respectively, were used (Figure 1).

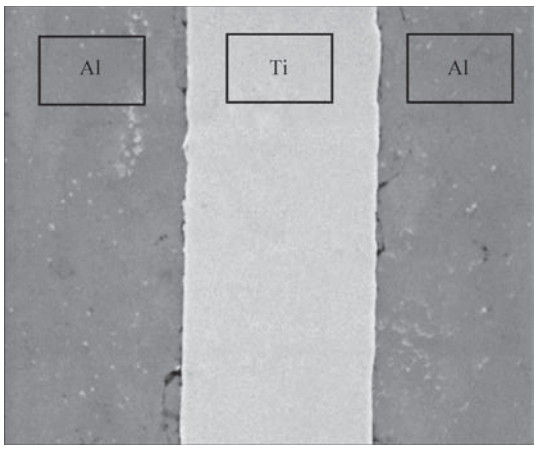

Figure 2. Microstructure of Al+Ti joint produced in the free state in the following mode: T_w = 580 °C, P_w = 20 MPa, t = 20 min

Welding was performed in the following mode: temperature T_w = 580 °C, pressure P_w = 5–20 MPa, welding time t_w = 20 min.

Analysis of structural characteristics of the foil and welded joints was conducted using scanning electron microscope CAMSCAN 4, fitted with a system of energy-dispersive analysis EDX INCA 200 for local chemical composition on flat samples, as well as optical microscope Biwyily USB 500. Transverse sections of welded joints were prepared by the standard procedure, using grinding-polishing equipment of Struers Company.

Digital pressure controller of KOLI Company of XK3118T1 grade and pressure sensor of CAS Company of MNC-1 grade with working interval from 0 to 1000 kg was used, when studying the mechanical properties in compression.

Our literature review [8] showed that it is rational to apply vacuum diffusion welding, in order to obtain the layered material from Al and Ti foil without formation of a continuous intermetallic layer in the butt joint.

In welding thin foil from aluminium alloys it was necessary to take the following factors into account:

- aluminium has a dense, thermally stable oxide film on the surface;
- the foil proper as a material has a work-hardened surface due to manufacturing by rolling methods;
- with reduction of foil thickness its welding becomes more complicated, as a result of reduction of the volume of metal, capable of plastic deformation.

Our investigations in welding thin materials in the form of aluminium foil (Al+Al) 50–200 μm thick in the modes recommended in reference books [11] showed that defects in the form of pores are observed in the butt joint. In order to eliminate the defects, in

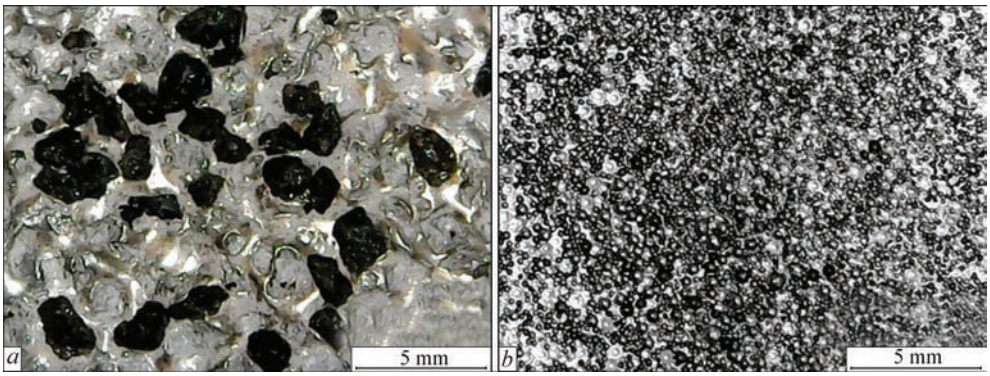

Figure 3. Appearance of the surface of Al+Ti joint after welding using SiC (*a*) and WC (*b*) particles produced in the following mode: T_w = 580 °C, P_w = 5 MPa, t = 20 min

foil welding it is necessary to increase the values of process parameters, namely temperature from 500 to 600 °C and welding pressure from 10–15 up to 40 MPa [1]. However, in welding aluminium and titanium foil this technological measure does not yield any results, although massive materials from these alloys have satisfactory weldability even at lower welding parameters T_w = 560 °C, P_w = 20 MPa [12].

As shown by our investigations, welding of sheet Al+Ti bimetal materials (up to 200 μm thickness) at higher pressure values up to 20 MPa is difficult, because of the low deformability of the foil. A dense contact between titanium and aluminium with individual pores and cracks is observed in the joint zone (Figure 2). Taking into account the sample dimensions, application of such forces leads to deformation of the welding fixture and its quick failure.

According to the technique, described in [9], an interlayer from SiC or WC powder was additionally placed between the foil and fixture for welding that created shear deformations in individual points, and enabled increasing the foil deformability on the whole. Powder application allowed lowering the welding pressure from 20 to 5 MPa.

As shown by the conducted studies, when using SiC powder, its particles are embedded into the bimetal material being welded, with formation of through-thickness irregular holes of considerable dimensions (Figure 3, *a*). Moreover, under the impact of thermodeformational welding cycle, individual SiC granules are partially enveloped by aluminium that makes impossible their further removal without damaging the bimetal material.

Replacement of SiC powder by WC with particles of spherical shape, allows lowering the defect level of the joint surface: the hole dimensions are reduced, and sharp corners disappear in them (Figure 3, *b*). However, reduction of particle dimensions and their regular shape promote a more intensive «absorption» of the powder by aluminium foil surface.

General disadvantages at application of both the «powder–activators» are as follows:

- high values of surface roughness;
- nonuniform distribution of particles over the foil surface;
- embedding of hard particles in the material being welded;
- formation of defects in the form of through-thickness holes;
- increase of bimetal sample weight.

The above-said may lead to the conclusion that application of powder to produce sheet bimetal material does not allow producing the joints suitable for further application.

In order to improve the deformability of foil with simultaneous lowering of pressure value in welding, steel net was furtheron used as plastic deformation activator. This technique allows uniformly localizing plastic deformation over the entire foil surface. No defects were found between aluminium and titanium in the microstructure of the joints produced using the net (Figure 4).

Mechanical compressive testing was conducted for evaluation of strength of the produced bimetal material. For this purpose, 70×12 mm strips were cut out of the bimetal plates and they were rolled into cylinders with 5 mm overlapping of the edges. In order to prevent cylinders unrolling during testing, two tacks were placed

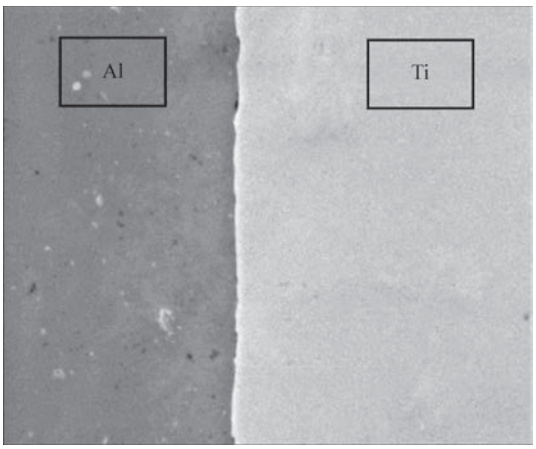

Figure 4. Microstructure of Al+Ti joint produced using the net in the following mode: T_w = 580 °C, P_w = 5 MPa, t = 20 min

Figure 5. General view of cylindrical samples before (*a*) and after (*b*) compressive testing

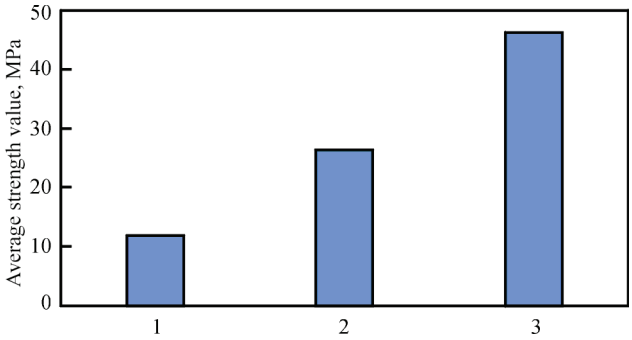

Figure 6. Results of mechanical compressive testing of cylindrical samples: *1* — foil of initial aluminium; *2* — Al+Ti bimetal; *3* — Al+Ti bimetal, produced using the net

in the material overlapping region by resistance welding method. Then, the thus formed samples were compressed with a controlled degree of upsetting to 50 % of the initial height. Figure 5 gives the sample appearance before and after compressive testing.

Obtained results showed that the strength of Al+Ti bimetal joints produced using the net is 3.8 times higher than that of the joints of pure aluminium (46.3 against 12.1 MPa), and is 1.7 higher than that of Al+Ti joints, produced without application of the net (46.3 against 26.5 MPa) (Figure 6).

It was further established that no foil delamination occurs on the bimetal samples produced using the net at compressive testing.

Conclusions

1. Welding of sheet Al+Ti bimetal materials is complicated because of the low deformability of the foil. Separate pores and cracks are observed in the joint zone.

2. Application of plastic deformation activators from refractory SiC and WC powders does not allow producing sound bimetal joints, first of all, due to introduction of hard particles into the material being welded, and formation of defects in the form of through-thickness holes.

3. Application of a steel net as plastic deformation activator on the foil contact surfaces allows an essential reduction of welding pressure and producing defectfree joints of titanium and aluminium, with higher strength levels, compared to layered Al+Ti joints, produced without the net application.

1. Petrushinets, L.V., Falchenko, Yu.V., Fedorchuk, V.E., Shinkarenko, V.S. (2018) Possibilities of manufacturing three-layer welded honeycomb panels from aluminium alloys. *The Paton Welding J.*, **7**, 25–29.
2. Bashurin, A.V., Mastikhin, E.Yu., Kolmykov, V.I. (2010) Diffusion welding of hollow bimetal panels. *Zagotovit*. *Proizvodstva v Mashinostroenii*, **1**, 13–15 [in Russian].
3. Kim, J.S., Park, J., Lee, K.S. et al. (2016) Correlation between bonding strength and mechanical properties in Mg/Al two-ply clad sheet. *Metals and Materials Int.*, **2** , 771–780.
4. Ma, M., Huo, P., Liu, W.C. et al. (2015) Microstructure and mechanical properties of Al/Ti/Al laminated composites prepared by roll bonding. *Mater. Sci. & Engin.: A*, **636**, 301–310.
5. Zhang, B., Kou, Y., Xia, Y.Y., Zhang, X. (2015) Modulation of strength and plasticity of multiscale Ni/Cu laminated composites. *Materials & Design*, **636**, 216–220.
6. Patselov, A., Greenberg, B., Gladkovskii et al. (2012) Layered metal-intermetallic composites in Ti–Al system: Strength under static and dynamic load. *AASRI Procedia*, **3**, 107–112.
7. Hailiang, Yu, Cheng, Lu, A. Kiet Tieu et al. (2016) Annealing effect on microstructure and mechanical properties of Al/Ti/Al laminate sheets. *Mater. Sci. & Engin. A*, **13**, 195–204.
8. Falchenko, Yu.V., Petrushynets, L.V., Polovetskii E.V. (2020) Peculiarities of producing layered metal composite materials on aluminium base. *The Paton Welding J.*, **4**, 9–18.
9. Lebedev, N.V., Agoltsov, A.Ya., Semochkin, A.N. (1980) Pressure welding of aluminium foil to copper one. *Voprosy Atomnoj Nauki i Tekhniki*, **1**, 163–166 [in Russian].
10. Karpachev, D.G., Doronkin, E.D., Tsukerman, S.A. et al. (2001) *Non-ferrous metals and alloys*: Refer. Book. Nizhni Novgorod, Venta-2 [in Russian].
11. Kozakov, N.F. (1968) *Vacuum diffusion welding*. Moscow, Mashinostroenie [in Russian].
12. Grigorenko, G.M., Polovetsky, E.V., Falchenko, Yu.V. et al. (2012) Influence of preheating temperature on structure of bimetal joints of AMg6 in solid state with VT6 using VDW method. *Sovrem. Elektrometall*., **4**, 37–41 [in Russian].

Received 07.07.2020

https://doi.org/10.37434/tpwj2020.08.05

IMPROVEMENT OF SERVICE PROPERTIES OF METAL STRUCTURES BY EXPLOSION TREATMENT

A.G. Bryzgalin, E.D. Pekar, P.A. Shlonskyi and **L.V. Tsarenko**
E.O. Paton Electric Welding Institute of the NAS of Ukraine
11 Kazymyr Malevych Str., 03150, Kyiv, Ukraine. E-mail: office@paton.kiev.ua

Explosion treatment of metals in the modern sense is represented by different technological processes based on application of the energy of explosion, and allowing improvement of certain service properties of the metals or welded structures. PWI developed technologies of explosion treatment to improve the corrosion resistance, dimensional stability, cyclic fatigue life of welded structures, lower the residual stresses, eliminate defects of tank shape, and increase the strength, ductility, and cold resistance of low-carbon steels. The above technologies have high mobility and responsiveness, and are independent of the external energy sources. Their disadvantage is limited applicability of explosion in settlements and long-term process of obtaining permits. However, there is extensive experience of application of explosion treatment under the conditions of operating industrial production. 15 Ref., 6 Figures.

Keywords: explosion treatment, welded structures, service properties, corrosion resistance, strength, ductility, fatigue life

The concept of «explosion treatment of metals» (ET) consists of a wide range of technological processes based on the specifics of pulsed impact of detonation products of explosives (Ex) on the treated material. The first patent, which describes the technology of joining pipes by high-velocity explosive deformation, was granted in Great Britain in 1898. The best known of the early publications was the report of a group of US researchers on the works on Ex effect on low-carbon steel, performed in 1919–1926. In 1940 the works by British researchers were published, which are devoted to different aspects of the problem of explosion treatment of metals. In 1951 N. McLeod claimed the first invention — explosive hardening of high-manganese steel. This method became applied in industry in the USA, Canada and the USSR. In 1966 the monograph by J.Reinhart and J.Pearson [1] was published that contained a review of investigation results obtained at that time on metal treatment by explosion.

The 1950s can be regarded as the beginning of systematic research and application of the method of pulsed treatment of metals, primarily due to the work of a group of scientists led by M.L. Lavrentiev, who discovered the phenomenon of welding and high-velocity oblique collision of metals, the focused study of which formed the base of explosion welding technology. Further investigations, conducted mainly by the USSR, USA and UK scientists, allowed development of a number of technologies, extensively used in industry [2].

Explosion welding became the most widely accepted of the pulsed technologies.

Unique capabilities of this welding method allow producing tight joints of metals differing by their properties that cannot be welded by any other methods, as well as composite materials of different composition.

High-manganese steels have the capability of an abrupt increase of surface hardness as a result of pulsed high-velocity impact. Surface hardening of steels by Ex is used to extend the service life of rapidly wearing parts of the railway, mining and ore processing machines and equipment. Unlike other known methods of surface hardening (roller rolling, shot-blasting, peening, etc.), which provide increase of hardness to the depth of up to 4 mm, ET allows achieving the hardened layer depth of up to 35 mm and more, that increases the product wear resistance not only due to hardness increase, but also due to a more favourable distribution of residual stresses (RS) induced in the near-surface layer by treatment.

The explosion stamping technology is applied in those cases, when it is impossible to use the traditional stamping methods, as the parts are thick, and it is necessary to lower the reverse plastic deformations to the maximum.

ET is widely used in the technologies of treatment of powder and composite materials [1]. The shock-wave effect at explosion loading allows modifying the properties and treating high-strength, hard, and hard-pressed powder materials; producing large-sized high-density billets and products of a complex shape that cannot be achieved by the traditional technologies.

A.G. Bryzgalin — https://orcid.ord/0000-0001-5886-3069, E.D. Pekar — https://orcid.ord/0000-0001-5025-4445

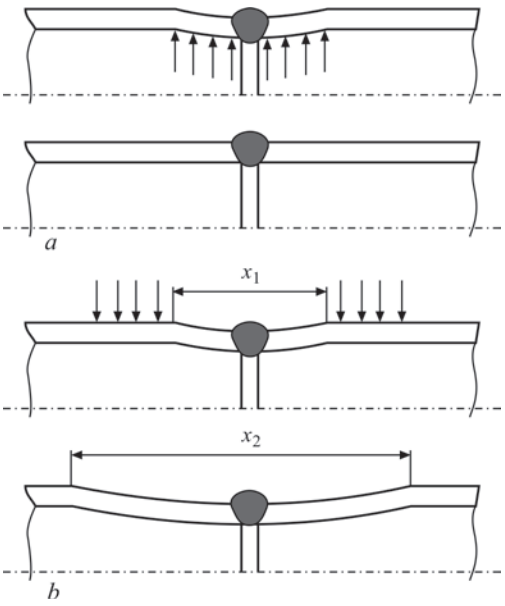

Figure 1. Principal diagrams of ET of girth welds of cylindrical structures: *a* — inner; *b* — external charge

Other kinds of ET, which are not as widely known, but also find application in industry, are new material synthesis, embossment, perforation, when the work tool force is applied due to explosion, riveting, tube-to-tubesheet welding, chips briquetting, etc.

In 1967 it was established at PWI that pulsed treatment [3] can significantly affect the service properties of metal structures.

It is possible to conditionally single out three main mechanisms of the effect of explosion treatment of metals on the change of structure service properties:

1. Change of metal structure, which is expressed in refinement and change of relative location of grains and nonmetallic inclusions, formation of twins and slip lines, significant increase of the number of dislocations, activating the mobility of which, for instance, by heating, leads to a positive change of service properties of the structure metal. This mechanism was used at development of the methods of increasing the wear resistance of cutting elements of mining equipment that is manufactured from high-strength manganese steel, making hardness standards, increasing the resistance of high-carbon steels to hydrogen embrittlement.

2. Changing or formation of new RS fields.

Two methods of realization of this mechanism can be singled out. One of them pertains to welded axisymmetric products, and the other — to flat welded sheets [4].

The first consists in the use of pipe wall throwing that leads to metal expansion in the zone of action of circumferential welding elastic tensile deformations, which is usually applied at ET of girth welds of predominantly large-sized shells, as well as pipelines with unrestricted access inside, or, contrarily, to swaging (upsetting) of the pipe wall in the zones of action of compressive plastic deformations. Figure 1 schematically shows «throwing» variants of ET of girth welds in structures of the type of cylindrical tanks and pipelines.

The parameters of external circular charges can be selected so that pipe radius in the zone of charge positioning after ET was smaller than that of the girth weld that will result in inducing compressive RS in the weld.

The second of the above-mentioned methods used at ET of sheet structures, consists in applying to the welded joint metal the normal pressure created by explosion, which leads to formation of plastic deformations in the treated metal plane — so-called stress-strain trace with biaxial compressive stresses. Their value can reach the metal yield limit, and it depends little on the initial stressed state of the welded joint [4]. Formation of such a «trace» in the metal leads to relaxation of the initial tensile stresses. Figure 2 gives the block diagrams of the location of Ex charges at treatment of flat welded joints.

Comparatively inexpensive and affordable detonation cords (DC) became widely accepted in ET practice. They are extensively used, in particular in the mining industry. Transverse dimensions of the «trace» depend on the quantity and arrangement of the cords on the surface being treated. Due to that the «trace» configuration is easily adjustable, and the «trace» depth can be considerable, reaching tens of millimeters. Thus, it becomes possible to effectively relieve RS in up to 50 mm thick joints. Figure 3 shows the yield bands that characterize the configuration and cross-sectional dimensions of the real «trace» of typ-

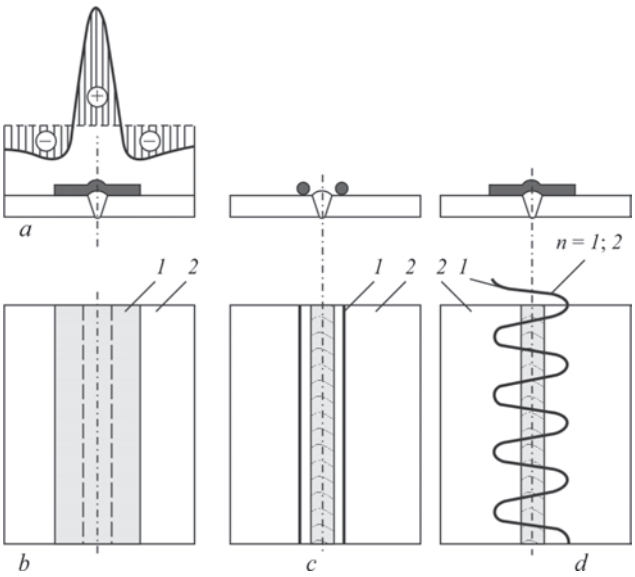

Figure 2. Principal diagrams of ET of welded joints on sheet structures: *a* — welding RS curve; *b* — linear scheme based on strip charge; *d* — «snake» scheme (*1* — Ex charge; *2* — welded joint)

ical size formed in low-carbon steel by detonation of DSh-A cord on its surface.

The majority of practically used ET technologies are based on application of exactly this mechanism that explains the need for a more flexible study of the processes proceeding in the metal at the moment of shock wave passage and interrelation between the loading parameters and the stress-strain state of welded structures.

3. Formation of macroplastic deformations in the structure body that allow regulating or changing its shape. Such tasks arise, as a rule, in case of the need to eliminate any defects in the form of large-sized sheet structures, for instance, so-called angularity of site joints of cylindrical tanks that are made by the method of deploying coiled blanks.

Further study of ET effect on the properties of metals and welded joints [5, 6] showed that ET allows solving a rather wide range of tasks, related to improvement of the quality and extension of welded structure service life. At present PWI has the priority in this direction of investigations, as here not only the mechanisms of explosion effect on the structure, stressed state and properties of welded joints have been studied, but various ET technologies have been developed and became rather widely accepted by industry [7, 8]. Let us give the most characteristic examples of ET application to improve the reliability and fatigue life of welded structures and give them new service properties.

1. Metal structures with a high level of working or residual stresses, susceptible to the hazard of a particular kind of spontaneous fracture of metal, known as stress corrosion cracking. It is manifested both in alkaline and acid environments. Proneness of metal structures to fracture in active working media is determined by three main conditions [6]: 1) metal properties; 2) stressed state; 3) environmental impact. Depending on specific conditions, different kinds of structure failure can occur: from mechanical fracture, when the role of the environment is insignificant, to kinds of fracture, when the role of stresses is insignificant, for instance, at general corrosion.

Presence of welded joints in the metal structure lowers its fatigue life under the impact of an aggressive medium. Specific features which determine the causes for, nature, kinetics and mechanism of welded joint destruction, depend mainly on thermophysical and chemico-metallurgical effect of welding, as it causes unfavourable changes of metal properties and stressed state that enhances the negative effect of the environment.

The stressed state affects the corrosion behaviour of metal as a result of the following phenomena [6]:

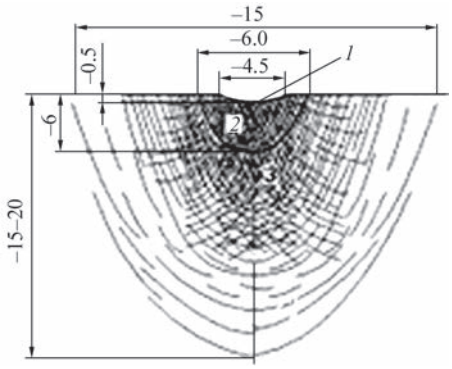

Figure 3. Chernov-Luders bands from DC explosion on the surface of St3 sample (band intensity corresponds to plastic deformation magnitude) [5]

- transfer of additional energy to the metal, causing reduction of its thermodynamic stability;
- violation under the impact of respective deformation, of the integrity and, hence, protective properties of oxide films that leads to graded distribution of surface potential;
- increase of the degree of nonuniformity related to appearance crystalline lattice defects under the impact of deformation and with formation of additional anode potentials.

On the whole, the danger of the impact of the stressed state on activation of the corrosion processes consists not only in increase of the general corrosion rate, but in the change of its nature, and its transformation from the uniform into the local one. Having a slight impact on general corrosion, the stresses intensify the local kinds of corrosion, the most dangerous of which is cracking.

It is established [6] that corrosion cracks are induced by tensile components of the stress tensor, irrespective of the loading method. For all the metals the time-to-fracture is continuously reduced with increase of stress magnitude. At the same time, in the majority of the cases, there is a stress threshold, below which cracking does not occur for a long time, or does not occur at all. The magnitude of threshold stresses depends on the specific conditions: metal properties, stressed state, and corrosion environment. Here, existence of threshold stresses is characteristic both for stresses caused by external loading, and for residual stresses.

The most dangerous are failures of welded structures in aggressive media. These are stresses related to metal hydrogenation during operation [9]. This fracture is characteristic for structural steels, particularly higher strength steels. The causes for predominant hydrogenation of the welded joints are structural heterogeneity of the welded joint and presence of RS of the first and second kind.

Lowering of RS in welded joints, operating in contact with the environment that hydrogenates the met-

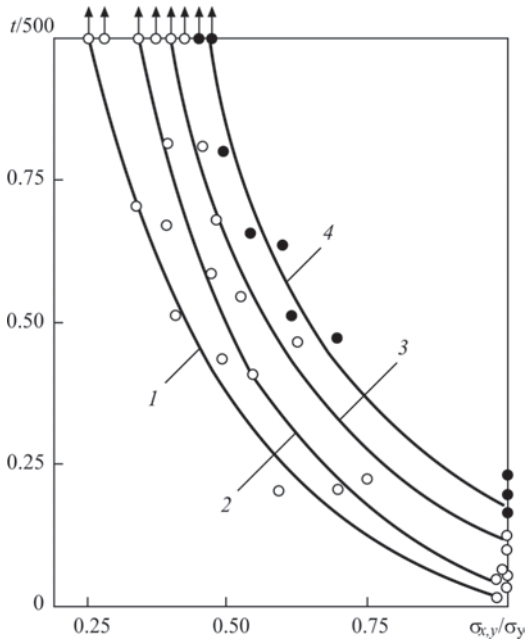

Figure 4. Dependence of fatigue life in boiling solutions of nitrates of butt welded joints of St3 steel on RS magnitude reduced to the yield limit: *1* — metal thickness of 6–8; *2* — 10–14; *3* — 16–22; *4* — 24–30 mm

al, is a necessary condition for increasing their fatigue life. In the majority of the cases, such a lowering is achieved by conducting heat treatment in high-temperature tempering mode. Heat treatment operation requires a lot of funds and time. ET application can be an alternative to heat treatment.

In alkaline environments ET enables ensuring «absolute» corrosion resistance [9] by lowering RS below the threshold values.

Figure 4 shows the fatigue life curves of welded butt joints of low-carbon steel in boiling solutions of nitrates [9].

One can see that RS lowering below the threshold level completely eliminates the possibility of corrosion cracking of the welded joint. It turned out that RS of threshold level depend on metal thickness. Prevention of stress corrosion cracking in alkaline environments is highly urgent, in particular, in aluminium

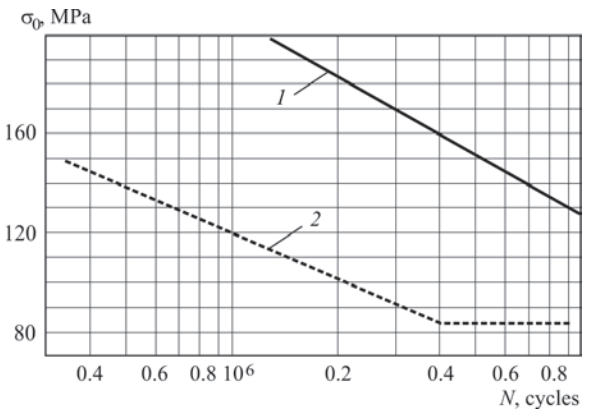

Figure 5. Fatigue life curves of samples with a transverse stiffener of AK type steel: *1* — after ET; *2* — initial state

industry in alumina production. The technology of ET of welded joints of tank equipment and process pipelines of decomposition sections was developed at PWI and became applied in the largest aluminium and alumina producing plants of the USSR and Yugoslavia [10].

2. Positive effect in the form of increase of fatigue life of welded joints at the stage of crack initiation in the high-cycle loading region is achieved at ET, firstly, due to relieving the tensile RS and, secondly, due to inducing compressive RS in the areas of stress concentration. PWI has accumulated extensive theoretical and experimental material, which is indicative of the high effectiveness of this kind of treatment [11]. It is found, in particular, that increase of fatigue resistance can be quite considerable, and it depends mainly on the scheme and intensity of explosion loading, as well as cycle characteristics.

Figure 5 gives the fatigue curves of samples from low-alloyed high-strength steel with a transverse stiffener, tested at a symmetrical loading cycle.

3. One of the important characteristics of strength of metals and welded joints exposed to variable loads is their ability to resist propagation of the already existing fatigue cracks. The significance of this characteristic consists in that the stage of crack propagation, determined by the number of cycles to fracture, can be equal to 70–90 % of the total fatigue life of the product. ET can be used to induce in the metal intensive «stress–strain traces» with preset distribution and magnitude of biaxial compressive stresses, which are a barrier to crack propagation and are capable of slowing down or totally preventing their propagation, as well as preventing their transition into brittle cracks [5].

4. The need to relieve RS arises also in those cases when their natural relaxation under the impact of variable loads can lead to inadmissible changes of the dimensions, geometry or relative position of the parts or sections of the structure, disturbance of the seats, etc. ET application in this case allows avoiding the appearance of warpage that affects the service properties of critical structures. Figure 6 illustrates the change of RS as a result of ET of the closing butt joint of a water conduit of approximately 6 m diameter in Tashlyk hydroelectric pumped storage power plant [5].

5. In practice characteristic form defects, so-called angularity, often develop in the area of closing vertical site welds in the large-sized tank facilities manufactured by the industrial method from coiled blanks and designed for petroleum product storage. In tank operation at their filling and emptying these defects have the role of stress raisers and cause wall damage as a result of low-cycle fatigue. Now the technology of ET of site butt joints of tanks of up to 10–50 thou m^3

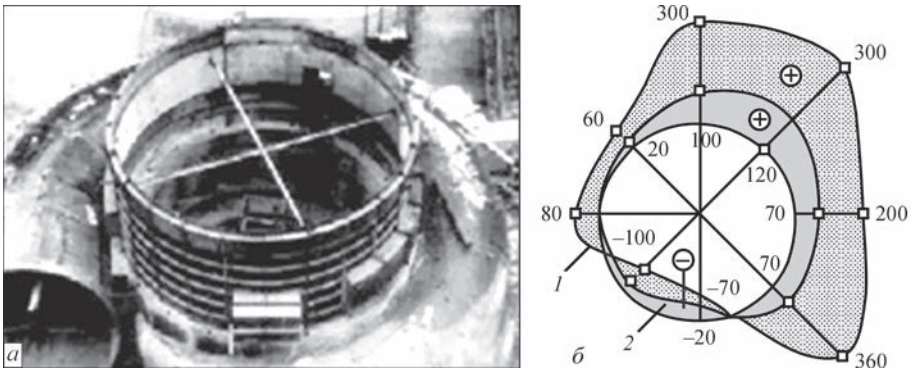

Figure 6. General view of a water conduit volute of the hydraulic unit of a pumped-storage plant (*a*) and curves of circumferential RS in the closing butt joint (*b*): *1* — in the initial state; *2* — after ET

volume has been developed and is used in production that allows extending the structure fatigue life 5 to 10 times [12]. The above-mentioned developments have already been brought to the stage of commercially applied technologies.

In 1980s PWI developed new technologies of combined explosion-thermit and preliminary ET of the edges to be welded, so-called explosion-welding treatment [13, 14]. The package of the proposed technologies enables improvement of the mechanical properties and structure of the metal by changing its fine structure as a result of intensive loading during explosion and further homogenizing of the structure during heat treatment or welding.

The majority of ET technologies that have become accepted in practice now, are based on the ability of this kind of postweld treatment to significantly lower and redistribute the RS. As was shown in [15], this effect can be achieved for a rather wide class of structures with up to 50 mm wall thickness.

Characterizing on the whole the considered effects, which are due to ET of welded joints, we will note that it enables achieving an improvement of a set of important properties of the welded joints up to the level matching the base metal that ensures the equivalent strength of welded structures operating under extreme conditions. The ET advantages and effectiveness are the base for its wide industrial application. Development of the technologies based on application of the studied treatment mechanisms should be performed for each specific case.

1. Rainhart, J.S., Pierson, J. (1966) *Explosive working of metals*. Moscow, Mir [in Russian].
2. Krupin, A.V., Soloviov, V.Ya., Popov, G.S. (1991) *Explosion treatment of metals*. Moscow, Metallurgiya [in Russian].
3. Mikheev, P.P., Trufyakov,V.I., Bushtedt, Yu.P. (1967) Application of pulsed treatment for improvement of reliability of welded joints. *Avtomatich. Svarka*, **10**, 63–64 [in Russian].
4. Dobrushin, L.D., Petushkov, V.G., Bryzgalin, A.G. et al. (2008) Explosion stress relieving in welded joints of metal structures. *Shock-Assisted Materials Synthesis and Processing. Science, Innovations and Industrial Implementation*. Moscow, Torus Press Ltd.
5. Petushkov, V.G. (2005) A*pplication of explosion in welding technology*. Kiev, Naukova Dumka [in Russian].
6. Steklov, O.I. (2005) *Strength of welded structures in aggressive media*. Moscow, Mashinostroenie [in Russian].
7. Lobanov, L.M., Dobrushin, L.D., Bryzgalin, A.G. et al. (2009) Widening of technological capabilities of explosion treatment for reducing residual stresses in welded joints on up to 5000 m^3 decomposers. *The Paton Welding J*., **11**, 46-48.
8. Petushkov, V.G., Bryzgalin, A.G. (1997) Improvement of service properties of welded structures by explosion treatment. *Welding and Surfacing Rev*., **8**, 167–175.
9. Kudinov, V.M., Petushkov, V.G. (1985) Resistance to corrosion cracking of welded joints treated by explosion. *Svarochn. Proizvodstvo*, **7**, 1–4 [in Russian].
10. Artemiev, V.I., Pashchin, A.N., Petushkov, V.G. et al. (1978) Application of explosion energy for improvement of corrosion resistance of welded joints of decomposers. *Tsvetnaya Metallurgiya*, **5**, 7–40 [in Russian].
11. Petushkov, V.G., Titov, V.A., Fadeenko, Yu.I. et al. (1988) *Method of explosion treatment of welded joints*. USSR author's cert. 1453762 [in Russian].
12. Petushkov, V.G., Pervoj, V.M., Titov, V.A. et al. (1991) *Method of reducing of angular residual deformations of welded joints*. USSR author's cert. 1700873 [in Russian].
13. Petushkov, V.G., Bryzgalin, A.G., Lokshina, E.Ya. et al. (1992) *Method of manufacture of welded metal structures*. USSR author's cert. 1760713 [in Russian].
14. Petushkov, V.G., Fadeenko, Yu.I., Smirnova, S.N. et al. (1988) Explosion treatment of low-carbon steel welded joints before their heat treatment. *Avtomatich. Svarka*, **7**, 68–69 [in Russian].
15. Petushkov, V.G., Titov, V.A., Bryzgalin, A.G. (2002) Limiting thickness of welded joints to be explosion treated. *The Paton Welding J*., **1**, 20–26.

Received 11.02.2020

https://doi.org/10.37434/tpwj2020.08.06

PEQULIARITIES OF FORMATION OF DISSIMILAR NICKEL-BASE ALLOY JOINTS IN FRICTION WELDING

I.V. Ziakhor, M.S. Zavertannyi, A.M. Levchuk and **L.M. Kapitanchuk**
E.O. Paton Electric Welding Institute of the NAS of Ukraine
11 Kazymyr Malevych Str., 03150, Kyiv, Ukraine. E-mail: office@paton.kiev.ua

When creating new designs of aircraft gas turbine engines, the urgent task is to replace the mechanical fasteners of structural elements from high-temperature nickel alloys with welded joints. The paper presents the results of research on the processes of heating, deformation and formation of the structure of joints during friction welding (FW) of dissimilar alloys — granular alloy EP741NP with wrought alloy EI698VD and casting alloy VZhL12U. The minimum values of pressure, at which upsetting is provided (deformation of billets in macrovolumes) are determined. The critical value of pressure, exceeding which leads to a change in the nature of the upsetting process in friction welding of EP741NP and VZhL12U alloys — from uniform shortening of the billets to stepwise. The range of changes in technological parameters of friction welding process, which ensures formation of defect-free welded joints, is determined. Microhardness studies have shown absence of areas with reduced microhardness in the zone of the joint of EP741NP and VZhL12U alloys. 22 Ref., 2 Tables, 11 Figures.

Keywords: friction welding, high-temperature nickel-base alloys, deformation, γ′-phase

High-temperature nickel alloys (HTNA): wrought, granular and casting, are widely used in manufacture of discs and blades of aviation gas turbine engines (GTE) [1–3]. Because of nonuniform heating and loading, turbine elements are made from dissimilar HTNA, which are connected by mechanical fasteners, that leads to greater weight of the turbine and engine as a whole. When new designs of aviation GTE are developed, replaced of mechanical fasteners by welded joints will allow reducing the engine weight at preservation of other service properties [4–8]. Therefore, application of welded assemblies from dissimilar HTNA in promising structures of aviation GTE is an extremely urgent problem.

Methods of fusion welding [9, 10], brazing [11, 12], and friction welding [13–18] are used to produce HTNA permanent joints. HTNA multicomponent alloying can result in formation of eutectic interlayers and chemical element segregation in brazing that adversely affects the characteristics of joint high-temperature resistance. Sound (defectfree) joints of HTNA are produced by fusion welding processes at the total content of aluminium and titanium (main elements forming the strengthening γ′-phase) in the alloy, which is not higher than 4 wt.%. At higher alloying of the alloys, the welds are prone to cracking [19].

Friction welding (FW) of different technological modifications — rotational FW and linear FW, is becoming ever wider applied abroad for producing permanent joints of high-alloyed HTNA, [13–15].

Producing sound joints of HTNA at FW is possible under the condition of providing a certain level of heat generation power during heating and pressure sufficient for metal deformation in the joint zone to a specified extent. Heat generation power value at FW is determined by a combination of relative rotation speed (or frequency and amplitude of relative vibration displacement at linear FW), pressure at heating and friction coefficient of specific alloys. It is known that sound joints cannot be produced without plastic deformation of metal macrovolumes in the zone of billet contact at FW [20]. Temperature range of deformation (TRD) of the high-temperature alloy depends on its chemical composition and is limited, on the one hand by the temperatures of recrystallization T_{recr} and complete dissolution of strengthening γ′-phase, T_{solvus}, and on the other hand — by the melting point — $T_{solidus}$.

With increase of the degree of HTNA alloying (Table 1) and volume fraction of γ′-phase, the alloy TRD becomes narrower — alloy melting point decreases, and the values of T_{recr} and T_{solvus} temperatures, rise. As producing a sound joint requires providing a certain extent of deformation of one or both of the billets, at which the oxides and the adsorbed films are pressed out beyond the cross-section limits [20], the value of billet upsetting is one of the parameters, controlled at

I.V. Ziakhor — https://orcid.org/0000-0001-7780-0688, M.S. Zavertannyi — https://orcid.org/0000-0002-8415-8555
A.M. Levchuk — A.M. https://orcid.org/0000-0002-0361-7394

Table 1. Chemical composition of studied alloys, wt.%

Alloy	Ni	Cr	Ti	Al	W	Mo	Nb	Co	V	Mn	Si	Hf	C
EI698VD	Base	14.4	2.74	1.69	0.05	2.98	2.04	–	0.05	0.08	0.20	–	0.05
VZhL12U	Same	9.7	4.5	5.4	1.4	3.1	0.8	14.0	0.8	0.01	0.03	–	0.18
EP741NP	»	9	1.9	5.1	5.6	3.8	2.6	15.8	–	0.5	0.5	0.3	0.04

Table 2 Some phase characteristics of studied alloys [21, 22]

Alloy	Total amount of γ′-phase, %	Solidus temperature, $T_{solidus}$	Temperature limit of γ′-phase dissolution, T_{solvus}, °C	Recrystallization temperature, $T_{recr.}$, °C	Deformation temperature		Hot plastic deformation ability
					Start	End	
EI698VD	25.0	1320	1030	1050–1100	1160	1000	Good
EP741NP	60.0	1270	1190	1150–1170	1140	1030	Very poor
VZhL12U	65.0	1273	1220	–	–	–	Same

FW. Sound joints can be formed only when a certain upsetting value has been reached [13, 17, 20].

Studying the thermal cycles and process of deformation (upsetting) of the billets at FW of dissimilar HTNA, in particular, disc (wrought and granular) and blade (casting) alloys, which are used in the design of turbines of local GTE developers and manufacturers, is of scientific interest and practical value.

The objective of the work is to establish the peculiarities of heating and deformation of dissimilar HTNA, formation of joint microstructure, depending on values of FW mode parameters, and on this base improve FW technology, which will ensure formation of sound welded joints.

Experimental procedure. Processes of heating and deformation at FW of dissimilar commercial alloys were studied: casting alloy VZh12U, granular alloy EP741NP, wrought alloy E1698VD, which are used in the designs of local developers and manufacturers of aviation GTE: SC «Ivchenko-Progress», JSC «Motor Sich». Specifically, as regards «disc–disc» welded assembly, FW of dissimilar nickel alloys — wrought E1698VD with granulated EP741NP, and for «disc–blade» assembly — granular EP741NP with casting VZhL12U, were studied.

Investigations were conducted on cylindrical samples of 12–15 mm diameter. Chemical composition and some characteristics of the studied alloys are given in Table 1 and Table 2.

Before welding, heat treatment of HTNA was performed by the following mode:

- for EI698VD alloy: first quenching at 1100 °C, soaking for 8 h; second quenching at 1000 °C, 4 h, ageing at 775 °C, 16 h;
- for EP741NP alloy: 1210 °C, soaking for 8 h, 870 °C, 32 h;
- for VZhL12U alloy: 1210 °C, soaking for 4 h; 950 °C, 16 h, and cooling in air in all the cases.

Test welding was conducted in laboratory unit ST120 with spindle rotation drive based on a dc motor with regulated rotation frequency in 40–300 rad/s range. Hydraulic drive ensures three-stage cyclogram of axial force application: rubbing-heating-forging in the range of 5–120 kN. ST120 unit allows realization of the technology of combined FW with regulated deceleration of rotation (Figure 1). During experiments on FW of EI698VD and EP741NP alloys, the process parameters were set in the following ranges: peripheral speed V = 1.0–1.5 m/s, heating pressure P_h = 50–440 MPa. In FW of EP741NP and VZhL12U alloys heating pressure was varied in the range of P_h = = 100–550 MPa, at peripheral speed V = 1 m/s.

Recording of welding mode parameters was performed by PC-based operational system using pressure sensor ADZ-SML-20.0-1, and upset control sensor SR 18-25-S «Megatron». During FW, recording of thermal cycles was performed, using chromel-alumel thermocouples of 0.5 mm diameter, welded to the billet surface at a certain distance from the contact zone. Measurement results were used to determine the distribution of sample heating temperature along the axis for different values of heating time t_h. Temperature values in the contact zone were found by interpolation of experimental data by the exponential law.

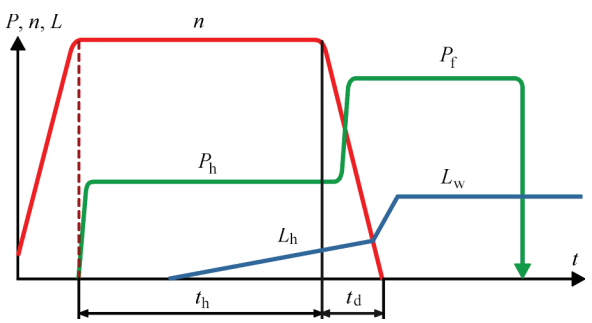

Figure 1. Cyclogram of combined FW with regulated deceleration of rotation: n — rotation frequency; P_h, P_f — pressure at heating and forging; L — upsetting; t_h — heating time; t_d — time of rotation deceleration

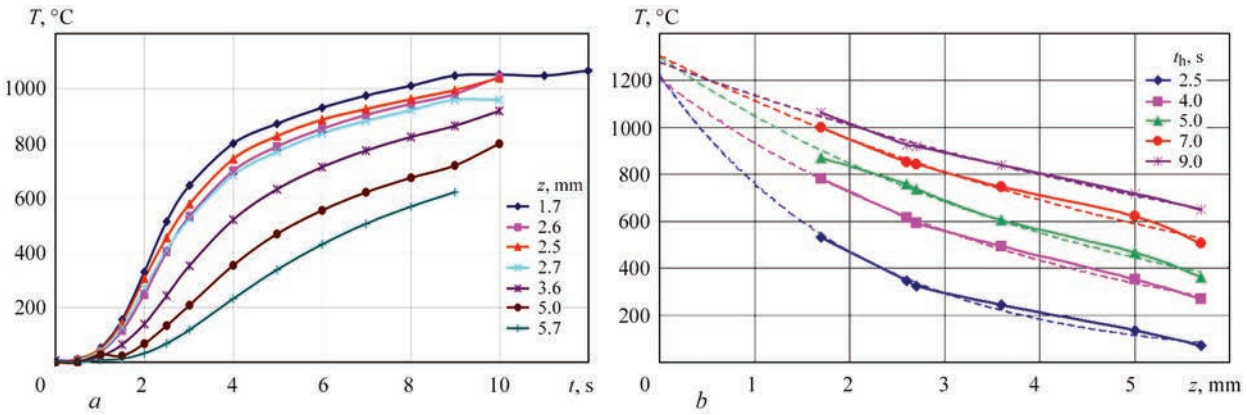

Figure 2. Change in time of temperature on the surface of a sample of EP741NP alloy at the distance from the contact surface z = 1.7; 2.6; 2.5; 2.7; 3.6; 5.0; 5.7 mm (*a*); temperature distribution at different values of heating time t_h = 2.5; 4.0; 5.0; 7.0; 9.0 s (*b*)

Tensile mechanical testing of standard samples of welded joints (GOST 1497–84) was conducted in TsDM-10 machine. Presence of surface defects (cracks, delamination) in the joint zone was detected at visual examination of the joint surface at x10 magnification, as well as using MMP4 microscope. Welded joint geometry and presence of defects were determined by metallographic examination of microsections prepared by a standard procedure.

Microstructure was studied in a light microscope Neophot-32, scanning electron microscope (SEM) JSM-35SA, Auger-microprobe JAMP-9500F, JEOL. Element distribution in the joint zone was determined using EDS-analyzer «INCA-450», Oxford Instruments Company, with approximately 1 μm diameter of the probe. Optical and electron microscopy was performed on microsections, prepared using chemical and electrolytic methods of structure detection. Measurements of metal microhardness in the HAZ across the joint line in 50 μm steps were conducted in microhardness meter M-400 (LECO) at 1.0–5.0 N load.

Experimental results. Results of studying the thermal cycles at different distance from the contact zone z at FW of EP174NP alloy to EI698VD alloy are given in Figure 2, *a* (peripheral speed V = 1.2 m/s, heating pressure P_h = 300 MPa). Obtained data were used to establish the temperature distribution from the side of EP741NP alloy for the moments of heating time t_h = 2.5; 4; 5; 7; 9 s (Figure 2, *b* — solid lines). Interpolation of experimental data to the contact plane (z = 0 mm) revealed that the temperature in the contact zone (Figure 2, *b* — dashed lines) is higher than melting temperature $T_{solidus}$ of EP741NP alloy.

Thermal cycles at different distance from contact zone z at FW of EP741NP alloy with VZhL12U alloy are given in Figure 3, *a* (V = m/s, P_h = 150 MPa), temperature distribution at different values of heating time t_h = 10, 15, 20, 25 s is shown in Figure 3, *b*).

It is established that the rate of metal heating in the contact zone at the initial stage of WF process reaches 1000 °C/s that in combination with exceeding the solidus temperature of EP741NP alloy can lead to partial melting of grain boundaries from the side of this alloy, and formation of a solid-liquid interlayer in the joint zone. Analysis of the temperature fields shows exceeding T_{solvus} and T_{recr} temperature in the contact zone for all the studied alloys. The width of the heating zone of high alloys EP741NP and VZhL12U up to the temperature higher than the values of temperatures of recrystallization and complete dissolution of strength-

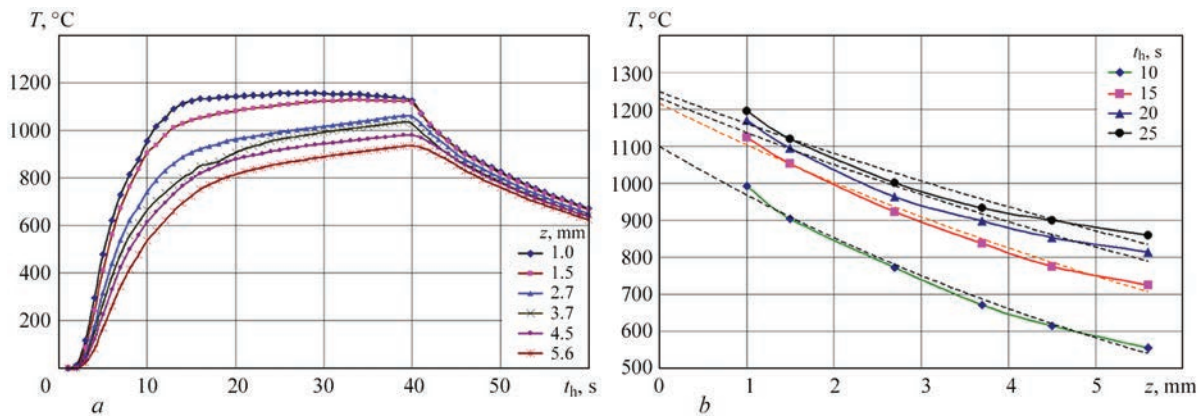

Figure 3. Change in time of temperature on the surface of a sample of VZhL12U alloy at FW with EP1741NP alloy at the distance from contact surface z = 1.0; 1.5; 2.7; 3.7; 4.5; 5.6 mm (*a*); temperature distribution from the side of VZhL12U alloy at different values of heating time t_h = 10; 15; 20; 25 s (*b*)

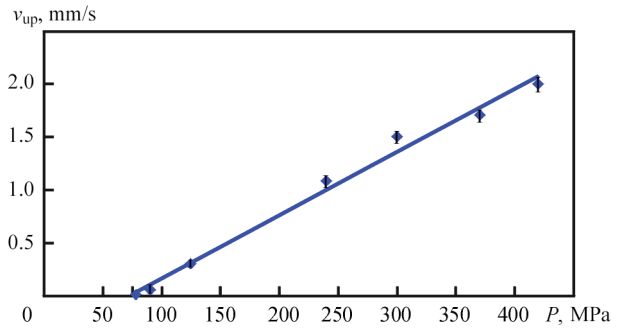

Figure 4. Dependence of upsetting speed on pressure at FW of EP1741NP alloy to EI698VD alloy (V = 1.0 m/s)

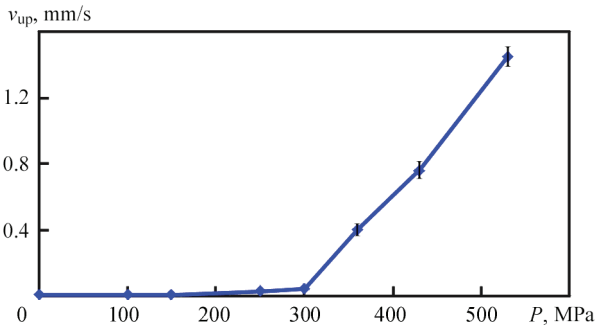

Figure 5. Dependence of upsetting speed on pressure at FW of EP1741NP and VZhL12U alloys (v = 1.0 m/s)

ening γ′-phase, is equal to less than 1 mm, that largely determines the conditions of billet deformation.

Deformation of billets (upsetting process) was studied at formation of welded joints of EI698VD alloy with EP741NP alloy and of VZhL12U alloy with EP741NP alloy. It is found that in the first case upsetting occurs predominantly due to wrought EI698VD alloy. Value of shortening of the billet from granular EP741NP alloy does not exceed 20 % of the total upset value at FW. Experimental results were used to plot the dependence of upsetting speed in FW of EI698VD alloy with EP741NP alloy on welding pressure (Figure 4). Dependence can be expressed by a linear function, in which upsetting speed rises in proportion to increase of welding pressure. As one can see from Figure 4, the process of billet upsetting begins, when pressure value $P_{h.min}$ = 80 MPa is exceeded.

Figure 5 gives the results of studying the upsetting process at FW of granular alloy EP741NP with casting alloy VZhL12U. It is established that at peripheral speed V = 1 m/s the process of billet upsetting at pressure value below $P_{h.min}$ = 300 MPa is practically not observed. Only after this value has been exceeded, the upsetting begins, which is accompanied by billet deformation in macrovolumes. In the range of pressure values of 300–530 MPa, the dependence of upsetting speed on pressure can be approximated by a linear function.

Thus, the process of upsetting (billet shortening) at FW starts only at a certain minimum value of pressure at heating $P_{h.min}$, which is different for a specific combination of alloys being welded. In welding of EI698VD and EP741NP alloys, welding starts in the case of exceeding pressure value $P_{h.min} > 80$ MPa and for a combination of VZhL12U and EP741NP alloys — at exceeding of pressure $P_{h.min}$ = 300 MPa. At smaller pressure values, metal heating in the contact zone up to solidus temperature of both or one of the alloys and formation of a thin metal interlayer in the solid-liquid state takes place. However, no upsetting of the billets, accompanied by ousting the oxides and adsorbed films beyond the billet cross-section limits, is observed. Under these conditions, sound welded joints cannot be formed.

Figure 6 gives the data on recording the parameters of the process of FW of EP741NP alloy with VZhL12U alloy. Anomalous step nature of the upsetting process at exceeding a certain critical value of pressure P_{crit} was found. Such a nature of the upsetting process is not characteristic for FW of other combinations of metals and alloys that were studied by the authors.

In particular, for peripheral speed of 1 m/s, P_{crit} value is equal to P_{crit} = 550 MPa. Billet deformation from the side of EP741NP alloy at P_h = 550 MPa is characterized by alternate change of the shortening rate: areas with a low upsetting speed v_{up} = 0.4–0.8 mm/s change to jumplike high-speed upsetting (v_{up} = 5 mm/s). Here, in areas with higher upsetting speed emissions of heated particles of metal, which probably was in the solid-liquid state, from the contact zone, were observed.

Obtained data were the base for determination of the change of technological parameters of FW process of dissimilar HTNA, namely granular alloy EP741NP with wrought disc alloy EI698VD and casting blade alloy VZhL12U. Technology of combined FW was improved. It ensures absence of anomalous phenomena in the upsetting process and formation of sound joints at FW of dissimilar high HTNA.

A photo of macrosection of the joint of VZhL12U and EP741NP alloys, produced by the improved technology of combined FW, is given in Figure 7, *a*. In the

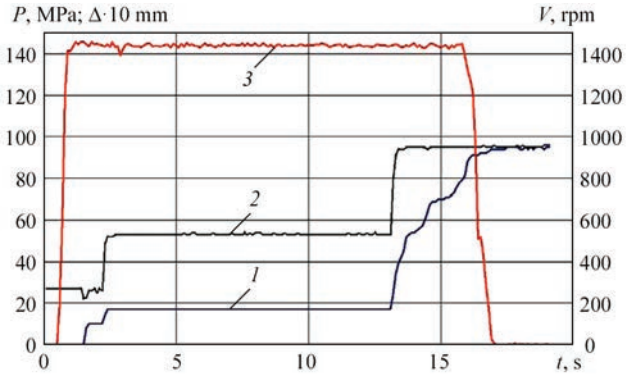

Figure 6. Results of recording the parameters of FW of VZhL12U and EP1741NP alloys: *1* — welding pressure P; *2* — upsetting (shortening) of the billet Δ; *3* — rotation frequency n

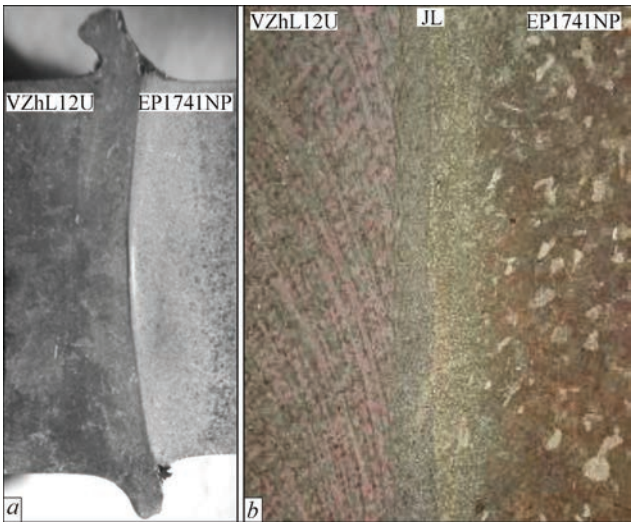

Figure 7. Macrosection (×100) (*a*) and microstructure (*b*) of the joint of VZhL12U and EP1741NP alloys

joint zone, formation of a reinforcement characteristic for FW from the side of VZhL12U alloy and its absence from the side of EP741NP alloy, are observed. Any defects, in particular, cracks and undercuts in the peripheral part of the billet cross-section are absent in the joint zone (Figure 7, *b*).

Microstructure (Figure 8) of the welded joint from the side of both the alloys is characterized by presence of typical for FW areas, located on both sides from the joint line (JL): zones of dynamic recrystallization (ZDR1 and ZDR2); zones of thermomechanical impact

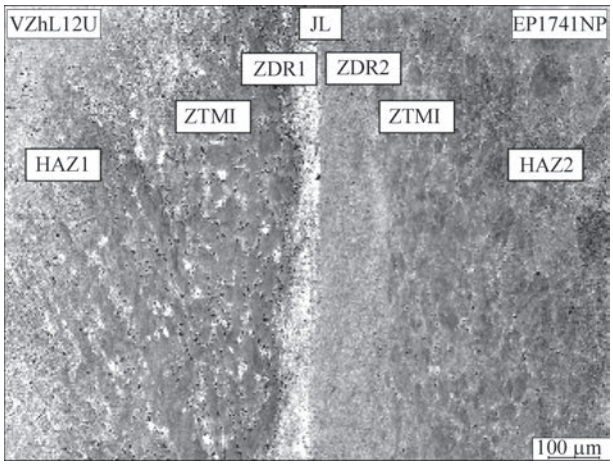

Figure 8. SEM image of the zone of VZhL12U and EP1741NP alloys joint

(ZTMI1 and ZTMI2), and heat-affected zones (HAZ1 and HAZ2), respectively, for VZhL12U and EP741NP. ZTMI1 structure from the side of VZhL12U alloy is characterized by the change of orientation of base metal dendrites in the radial direction that is indicative of plastic deformation of this alloy in the macrovolumes.

Figure 9 gives the microstructure of metal on the line of the joint of VZhL12U and EP741NP alloys. In different parts of billet cross-section (central, peripheral) similarity of metal microstructure along the JL is observed. Average grain size in the zone of dynamic recrystallization of the alloys is equal to 3–4 μm from the side of EP741NP alloy and is close to 2 μm from the side of

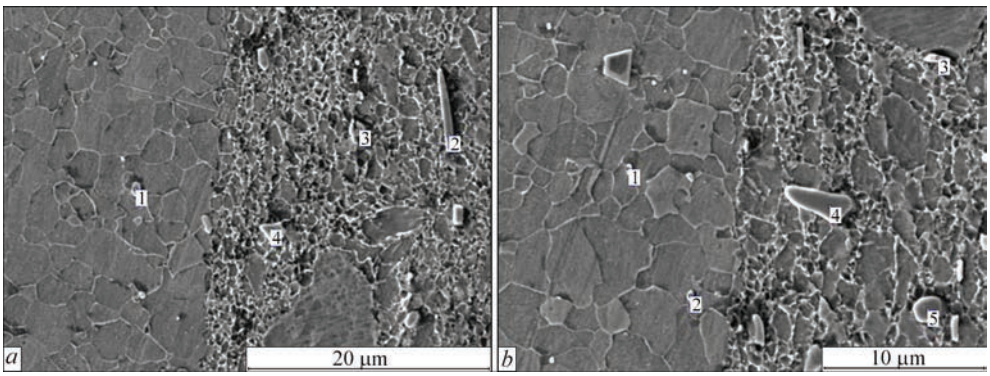

Figure 9. SEM image of microstructure of the zone of VZhL12U and EP1741NP alloys joint in the central (*a*) and peripheral (*b*) parts of billet cross-section

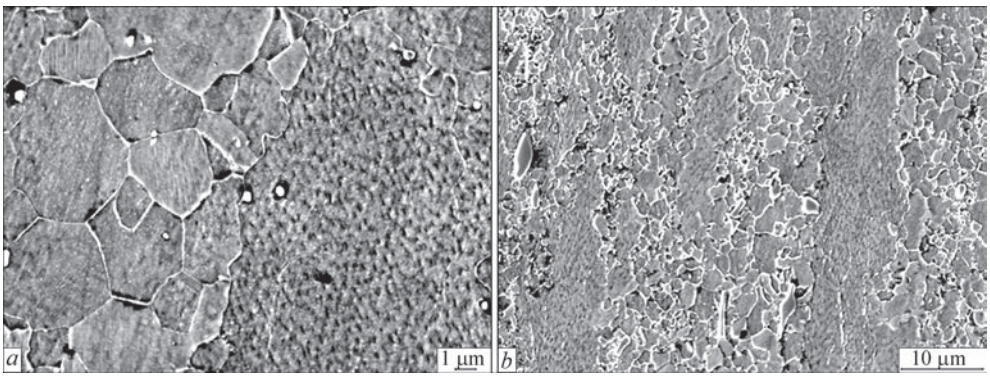

Figure 10. SEM image of the boundary between ZDR and ZTMI of EP1741NP (*a*), and VZhL12U (*b*) alloys

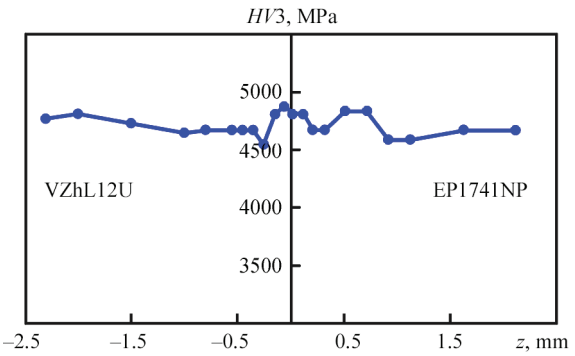

Figure 11. Microhardness distribution in the zone of VZhL12U and EP1741NP alloys joint

VZhL12U alloy. Metal microstructure along JL is indicative of solid-phase nature of joint formation, both in the central, and in the peripheral parts of billet cross-section.

When studying metal microstructure in ZTMI (Figure 10, *a*), a clear-cut boundary between ZDR and ZTMI is observed from the side of EP741NP — fine dynamically recrystallized ZDR grains, where during FW strengthening γ′-phase was completely dissolved (on the left), and partially deformed grain in ZTMI with partially dissolved γ′-phase (on the right). Microstructure of ZMTI of VZhL12U alloy is characterized by presence of base metal grains deformed during FW (Figure 10, *b*), in which strengthening γ′-phase is partially dissolved, and of dynamically recrystallized grains of up to 3 μm size, where γ′-phase is completely dissolved.

Figure 11 gives microhardness distribution in the zone of welded joint of EP741NP and VZhL12U alloys. Absence of areas with lower microhardness values was established. Microhardness increase near the joint line was detected, which, most probably, is related to grain refinement in the dynamic recrystallization zone.

Conclusions

1. Investigations of thermal cycles in friction welding of dissimilar high-temperature nickel alloys EP741NP and EI698VD, as well as EP741NP and VZhL12U alloys showed the possibility of achieving in the contact zone the solidus temperature of one of the alloys and formation of an interlayer in the solid-liquid state.

2. Investigations of the process of deformation of EP741NP with EI698VD, and VZhL12U alloys at FW with peripheral speed V = 1.0–1.2 m/s allowed establishing minimum values of pressure $P_{h.min}$, at which upsetting (deformation in macrovolumes) of the billets is ensured: $P_{h.min}$ = 80 MPa for a combination of EP741NP with EI698VD and $P_{h.min}$ = 300 MPa for a combination of EP741NP and VZhL12U.

3. Anomalous step nature of upsetting at FW of EP741NP and VZhL12U alloys at exceeding a certain critical value of pressure P_{crit} was detected. In particular, for peripheral speed V = 1 m/s this value is P_{crit} = 550 MPa. An optimum range of the change of technological parameters of FW process of dissimilar HTNA was determined, namely granular alloy EP741NP with wrought disc alloy EI698VD and casting blade alloy VZhL12U.

4. Technology of combined FW was improved, which provides absence of anomalous phenomena in upsetting process and formation of sound joints at FW of dissimilar high HTNA. Investigations of microhardness distribution in the joint zone of EP741NP and VZhL12U alloys showed absence of areas with lowered microhardness values.

1. Furrer, D., Fecht, H. (1999) Ni-based superalloys for turbine discs. *JOM*, **1**, 14–17.
2. Das, N. (2010) Advances in nickel-based cast superalloys. *Transact. of the Indian Institute of Metals,* 63(**2–3**), 265–274.
3. Romanov, V.V., Koval, V.A. (2020) Application of new materials in conversion of ship and aviation GTE into stationary GTI. *Eastern-European J. of Enterprise Technologies*, **3**, 4–7 [in Russian].
4. Maslenkov, S.B. (2001) *Technology of producing of permanent joint in manufacture of gas turbine engines.* Moscow, Nauka i Tekhnologii [in Russian].
5. Ospennikova, O.G., Lukin, V.I., Afanasiev-Khodykin, A.N., Galushka, I.A. (2018) Manufacture of «blisk» type structure of dissimilar material combination (Review). *Trudy VIAM,* **10**, 10–16. DOI: 10.18577/2307-6046-2018-0-10-10-16 [in Russian].
6. Magerramova, L.A. (2011) Application of bimetal blisks, manufactured by HIP method from granulated and cast nickel superalloys to improve reliability and service life of gas turbines. *Vestnik UGATU*, 15(**4**), 44, 33–38 [in Russian].
7. Ospennikova, O.G. (2012) Strategy of development of heat-resistant alloys and steels of special purpose, protective and thermal-barrier coatings. *Aviats. Materialy i Tekhnologii*, **5**, 19–36 [in Russian].
8. Shmotin, Yu.N., Starkov, R.Yu., Danilov, D.V. et al. (2012) New materials for advanced engine of PJSC NPO Saturn. *Ibid*., **2**, 6–8 [in Russian].
9. Lukin, V.I., Kovalchuk, V.G., Golev, E.V. et al. (2016) Electron beam welding of high-strength cast nickel alloy VZh172L. *Svarochn. Proizvodstvo*, **5**, 44–49 [in Russian].
10. Yushchenko, K.A., Zadery, V.A., Zvyagintseva, A.V. et al. (2008) Sensitivity to cracking and structural changes in EBW of single crystals of heat-resistant nickel alloys. *The Paton Welding J.*, **2**, 6–13.
11. Rylnikov, V.S., Afanasiev-Khodykin, A.N., Timofeeva, O.B. (2013) Features of technology of diffusion brazing of heat-resistant alloy EP975 and cast single-crystal intermetallic alloy VKNA-4U for blisk structure. *Svarochn. Proizvodstvo*, **7**, 19–25 [in Russian].
12. Rylnikov, V.S., Afanasiev-Khodykin, A.N., Galushka, I.A. (2013) Technology of brazing of «blisk» type structure from dissimilar alloys. *Trudy VIAM*, **10**. URL: http://viam-works.ru/plugins/content/journal/uploads/articles/pdf/251.pdf [in Russian].
13. Li, W., Vairis, A., Preuss, M., Ma, T. (2016) Linear and rotary friction welding review. *Int. Materials Reviews*, 61(**2**), 71–100. DOI: 10.1080/09506608.2015.1109214.
14. Senkov, O.N., Mahaffey, D.W., Semiatin, S.L., Woodward, C. (2014) Inertia friction welding of dissimilar superalloys Mar-M247 and LSHR. *Metallurgical and Materials Transact. A*, **45A**, 5545–5561. DOI: 10.1007/s11661-014-2512-x.

15. Ola, O.T., Ojo, O.A., Wanjara, P., Chaturvedi, M.C. (2011) Analysis of microstructural changes induced by linear friction welding in a nickel-base superalloy. *Ib d.*, **2** , 3761–3777. DOI: 10.1007/s11661-011-0774-0.
16. Lukin, V.I., Samorukov, M.L. (2017) Peculiarities of formation of structure of heat-resistant wrought alloy VZh175 welded joints, produced by rotary friction welding. *Sva och Proizvodstvo*, **6**, 25–33 [in Russian].
17. Bychkov, V.M., Selivanov, A.S., Medvedev, A.Yu. et al. (2012) Investigation of weldability of heat-resistant nickel alloy EP742 by linear friction welding method. *Vestn k UGATU*, 16(**7**), 52, 112–116 [in Russian].
18. Lukin, V.I., Kovalchuk, V.G., Samorukov, M.L. et al. (2010) Peculiarities of friction welding technology of joints from VKNA-25 and EP975 alloys. *Sva och Proizvodstvo*, **5**, 28–33 [in Russian].
19. Sorokin, L.I. (2005) Formation of hot cracks in welding of heat-resistant nickel alloys (Review). *Ibid.*, **7**, 29–33 [in Russian].
20. Lebedev, V.K., Chernenko, I.A., Villya, V.I. (1987) *Friction weldig* : Refer. Book. Leningrad, Mashinostroenie [in Russian].
21. Vaulin, D.D., Eremenko, V.I., Vlasova, O.N. et al. (2006) Technological features of the manufacture of stamped semi-finished products from heat-resistant nickel alloys. In: *Persp ctive techl ogies for ligh d sp cil l loys*. Moscow, FIZMATLIT, 294–301 [in Russian].
22. Bondarev, B.I., Fatkullin, O.Kh., Eremenko, V.N. et al. (1999) Development of heat-resistant nickel alloys for gas turbine discs. *Tekhl ogiyL yogkikhSp u ov*, **3**, 49–53 [in Russian].

Received 13.07.2020

https://doi.org/10.37434/tpwj2020.08.07

APPLICATION OF MAGNETIC-PULSE WELDING TO JOIN PLATES FROM SIMILAR AND DISSIMILAR ALLOYS

M.A. Polieshchuk, I.V. Matveiev, V.O. Bovkun, L.I. Adeeva and **A.Yu. Tunik**
E.O. Paton Electric Welding Institute of the NAS of Ukraine
11 Kazymyr Malevych Str., 03150, Kyiv, Ukraine. E-mail: office@paton.kiev.ua

The paper provides analysis of the state-of-the-art and confirmation of the relevance of studying the process of magnetic-pulse welding (MPW) of flat parts from similar and dissimilar metals. Results are presented of studying the possibility of performance of magnetic-pulse welding of flat samples in a modified batch-produced N-126A unit, using an experimental flat rectangular inductor. Process scheme is given. Technology is described for producing joints of flat metal parts 1.0–1.5 mm thick of similar materials of A5N and AMG2 alloys, as well as dissimilar materials – copper, A5N alloy and ANG2 alloy to 12Kh18N10T stainless steel (cold-worked). Conducted metallographic studies showed that a common feature for MPW of similar and dissimilar metals is specific bonding of welded plates in the zones (regions) equidistant from the center of the inductor flat turn. Thickness of mobile plates becomes smaller, and microhardness in the welding zones becomes higher. Sound welding was found within the two-zone joint shape. Welded joint quality was assessed by the results of mechanical strength testing. 10 Ref., 1 Table, 9 Figures.

Keywords: magnetic-pulse welding, cold welding, solid-state welding, microstructure, microhardness

The objective of the work is to study the current tendencies in development of the technology of magnetic-pulse welding (MPW), investigation of the possibility of high-quality MPW of flat samples from similar and dissimilar metals and alloys produced locally, and metallographic examination of welded joint formation.

MPW (magnetic-pulse welding) is a relatively new technology, compared to the traditional welding methods. It is a process of solid-state cold welding of conductive metals, in which the impact of pulsed inductor magnetic field is used. At interaction of inductor current with induced current repulsion forces arise between the inductor and part. As a result, the part, gaining a high movement speed, moves towards the stationary part. Collision of the surfaces leads to considerable plastic deformations, which ensure the welded joint formation. Collision velocity is higher than 300 m/s, and pressure in the contact zone is up to 10^2–10^4 MPa [1].

Today there are already enough examples of industrial application of MPW in manufacture of hull structures of vehicles, in aerospace sector, nuclear power engineering, defense industry complex, etc. [2].

This technology is of special interest in manufacture of hull structures of vehicles, primarily due to the possibility of joining dissimilar metals. Here, the following advantages of the technology are pointed out: welding of similar and dissimilar materials to each other, complete absence of thermal deformation, high welding speed (pulse duration ~ 30 μs), high welding quality and repeatability of the results, low power consumption (~ 10 times less than in MIG welding), possibility of process automation, and of making rectilinear welded joints of up to 3 m length. At MPW there is no need for the operation of part scraping, for consumable materials (welding wire, gases) or local exhaust ventilation, due to the absence of harmful emissions.

Specialists say that deep introduction of MPW allows developing lighter weight frames and other elements of car structures from dissimilar metals that will lead to lowering of their weight to 70 %, as well as reduction of fuel consumption by 10 %. It will promote reduction of harmful emissions into the environment, also in car manufacturing («green technology») [3]. Experts also claim that MPW potential is very high, and real mass deployment is anticipated in the next few years [4]. At present, starting from the moment of invention of this technology, the majority of works have been related to MPW of the bodies of revolution. The process of MPW of flat parts was proposed relatively recently, and the number of publications on this subject over the last years has increased, but very slowly. In our opinion, researchers are not in a hurry to disclose the technicalities of the process.

This, however, does not diminish the relevance of the topic. This is indicated by creation within the EU framework of a major JOIN'EM project [5], aimed at studying the processes of welding dissimilar metals (predominantly copper-aluminium, including flat

M.A. Polieshchuk — https://orcid.org/0000-0002-5992-4641, I.V. Matveiev — https://orcid.org/0000-0003-0683-0761,
V.O. Bovkun — https://orcid.org/0000-0001-7019-8671, A.Yu. Tunik — https://orcid.org/0000-0001-6801-6461

Figure 1. N-126A unit

items) by MPW. This project was founded in 2017, and operates within the EU Horizon 2020 Research and Innovation Programme [6]. That is, for the first time in modern welding history, a decision was taken on the European interstate level to support studies of MPW as a technology, which the most completely meets tomorrow's challenges.

Reduction of structure weight is one of the ways to achieve this correspondence. Successive replacement of traditional iron-based alloys by light and special alloys, as well as their combinations with the traditional materials is one of the main trends of modern industry. Technologically, this raises the problems of joining dissimilar metals, which cannot be done by the traditional fusion welding methods. Another significant factor that fuels the interest to technologies of dissimilar metal welding now is the problem of replacement of parts and products from copper and copper alloys by hybrid copper-aluminium products [7], which are joined by welding in the cold state. In this case, none of the fusion welding processes can guarantee a sound joint.

The relevance of this topic is due to copper being a more expensive metal, compared to, for instance, aluminium (approximately 2 to 4 times). Its cost is rising continuously because of a rapid growth of the demand for it practically in all the sectors of economy, particularly, in electric engineering, electronic and power generation industry. At the same time, aluminium is very close to copper in terms of heat conductivity and electric conductivity (~ 60 %), at much lower specific density (~ 30 %) and cost.

Research work performed at PWI resulted in development of MPW techniques for flat metal parts and producing samples, using this process. Realization of MPW process on locally produced metals and alloys is also relevant, their composition and properties often differing from their foreign analogs.

In order to conduct the experiments, batch-produced unit N-126A (Figure 1), manufactured by PWI Pilot Plant of Welding Equipment, was upgraded for MPW of cylindrical parts. In particular, changes were made in the electric diagram, design of high-voltage current conduits and arc discharger.

Experiments were conducted at charge voltage of 10–18 kV, at maximum current of 200–500 kA. Current was switched using controlled arc discharger of «trigatron» type. Total capacitance of the capacitors was equal to 115 μF. Width of inductor working turn was 5 mm. Current was measured, using super high-speed USB oscilloscope DATAMAN 570 and respective software for processing and post-processing of the obtained data.

General scheme of the process of MPW of flat parts from one side with application of single-turn E-shaped inductor is given in Figure 2, and the scheme of movement of the part being welded is shown in Figure 3.

Flat samples of metal alloys 1.0–1.5 mm thick were used in the work. Qualitative approach was applied for evaluation of the results.

Appearance of some samples joined by MPW, is shown in Figure 4.

Plates of aluminium alloys A5N and ANG2, copper of grade M1 and cold-worked stainless steel 12Kh18N9T were used to produce joints of similar and dissimilar metals by MPW method.

A5N is a ductile, corrosion-resistant alloy, with minimum content of additives. Alloy composition is

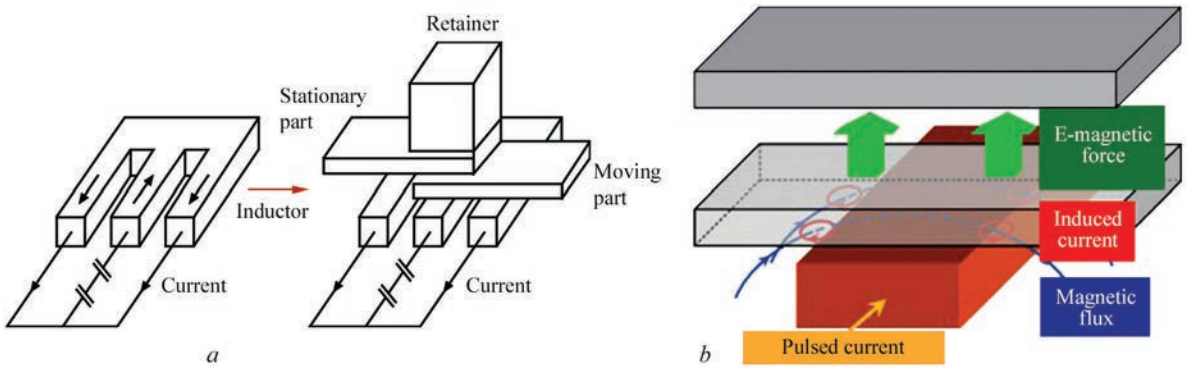

Figure 2. General scheme of the process of MPW of flat parts

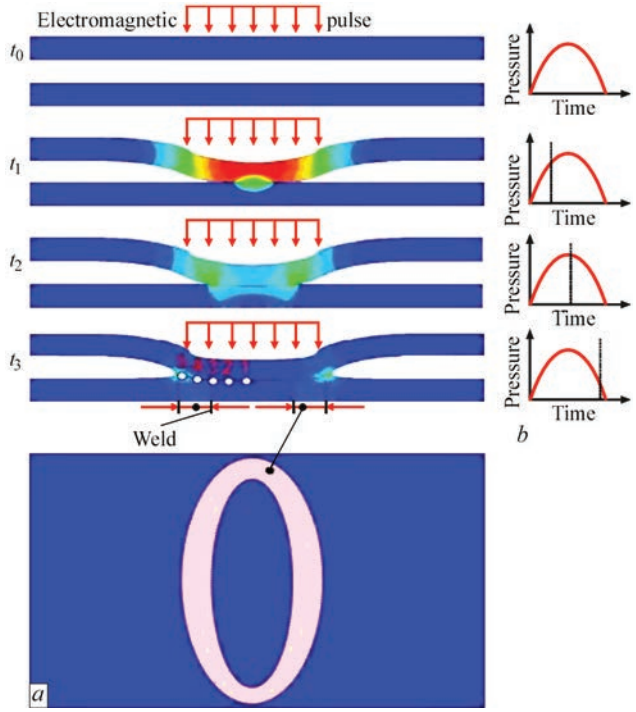

Figure 3. Scheme of movement of the part being welded (*a*) and welded zone shape (*b*)

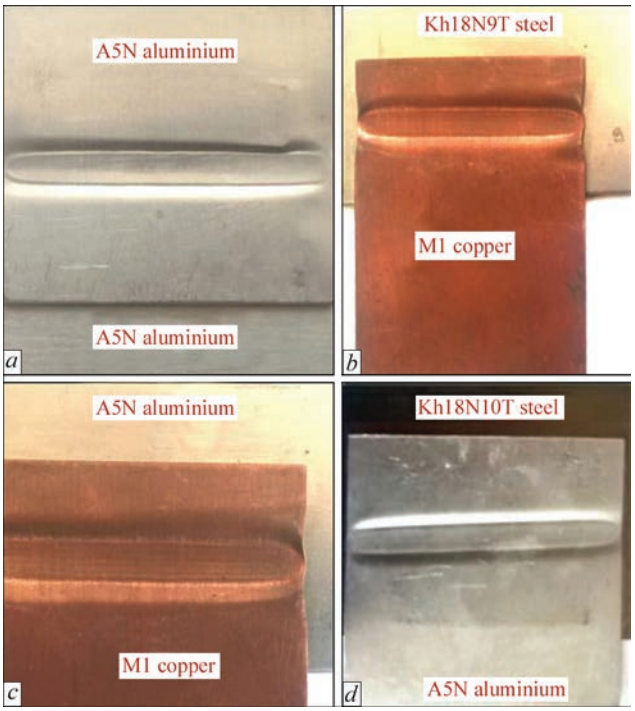

Figure 4. Appearance of flat samples, bonded by MPW: *a* — similar; *b–d* — dissimilar metals

as follows, wt.%: > 99.5 Al; < 0.3 Fe; < 0.25 Si and other additives (Ti, Mn, Cu, Mg, Zn, Ga). «N» means the cold-worked state, i.e. owing to additional treatment the sheets acquire higher rigidity, but have lower elasticity. Alloy microhardness is equal to 465 MPa. AMG2 is a wrought aluminium alloy. It composition is as follows, wt.%: > 95.7–98.2 Al; 1.7–2.4 Mg and other additives (Fe, Ti, Mn, Cu, Cr, Zn), 0.15 all together. Alloy microhardness is equal to 605 MPa. M1 is oxygenfree copper, which contains, wt.%: 99.95 Cu; 0.003 O_2, 0.002 P. Copper microhardness is equal to 890 MPa. Cold-worked 12Kh18N9T is stainless steel, which is corrosion- and heat-resistant, containing the following alloying elements and additives, wt.%: ≤ 0.12 C; 17.0–19.0 Cr; 8.0–9.5 Ni; 0.80 Ti; ≤ 0.8 Si; ≤ 2.0 Mn; ≤ 0.020 S; ≤0 .035 P. Steel microhardness is equal to 4630 MPa.

Investigations were conducted with application of a procedure, including metallography — NEOPHOT-32 optical microscope, durometric analysis — hardness meter M-400 of LECO at 0.098 and 0.249 N load. Chemical etching of metallographic sections was conducted using the following reagents: 50 % aqueous solution of HNO_3 (detection of copper struc-

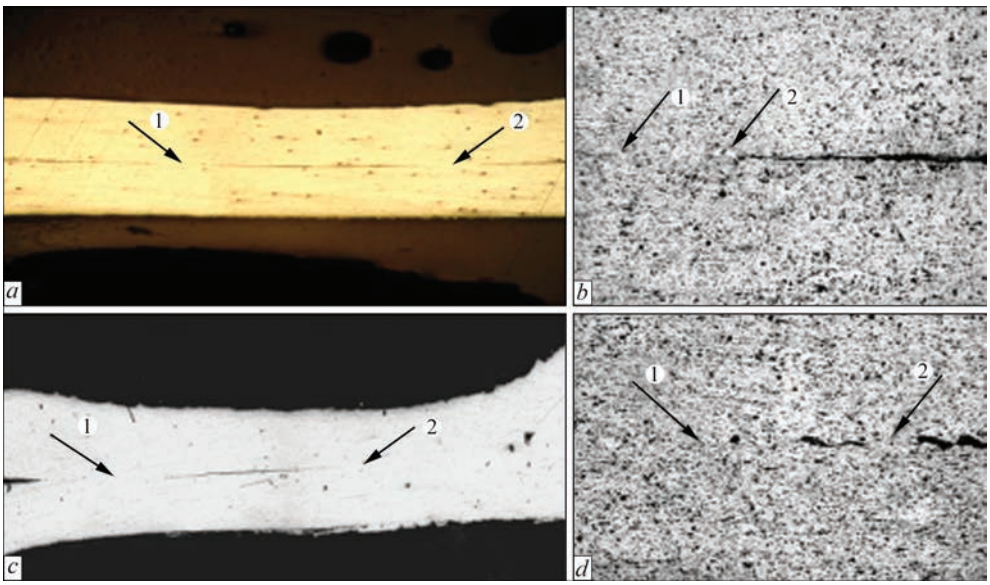

Figure 5. Microstructure of joints of similar plates from A5N alloy, produced by MPW at voltage of 16 kV (*a*, *b*) and 18 kV (*c*, *d*): *a, c* — ×25; *b, d* — ×400 (etched)

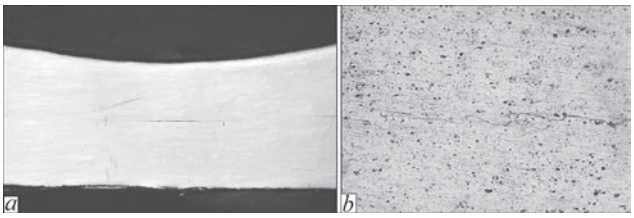

Figure 6. Microstructure of joints of similar plates of AMG2 alloy at voltage of 18 kV: *a* — ×25; *b* —×400 (etched)

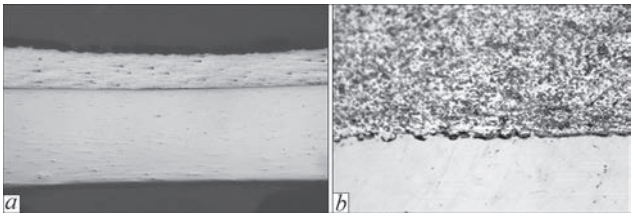

Figure 7. Microstructure of a joint of dissimilar plates of alloy AMG2 and stainless steel Kh18N10T, produced by MPW at 18 kV voltage: *a* — ×25; *b* —×400 (etched)

ture); HNO_3:HCl:H_2O in the ratio of 3:1:1 (detection of aluminium alloy structure).

A common feature for MPW of plates of similar and dissimilar metals is specific bonding of welded plates (Figure 3, *b*; Figure 5, zones 1, 2) in two zones (regions), equidistant from the center of inductor flat turn [8–10].

In welding plates of aluminium alloy A5N at 16 kV voltage, bonding occurred in two regions of 0.52 mm length, located at 1.02 mm distance from the center of inductor flat turn. Plate thickness in these regions was reduced for the upper and lower plates by 20 and 24 %, respectively, compared to initial thickness (1.0 mm). Microhardness of the moving and stationary plates increased by not more than 3 %, compared to initial state of the alloy (*HV*0.1 – 465 MPa, see Table). At MPW higher voltage (18 kV), the length of bonding regions increases up to 1.72 and 2.32 mm. Thickness of both the plates is reduced by 30 %, hardness increases up to 9 % (Figure 5, see Table).

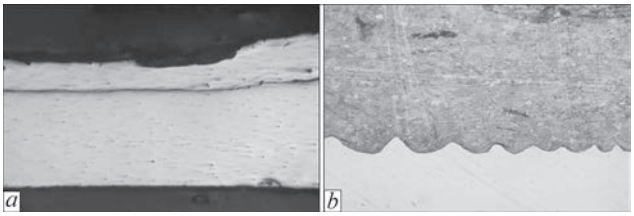

Figure 8. Microstructure of a joint of dissimilar plates of copper M1 and stainless steel Kh18N10T, produced by MPW at the voltage of 18 kV; *a* — ×25; *b* — ×400 (etched)

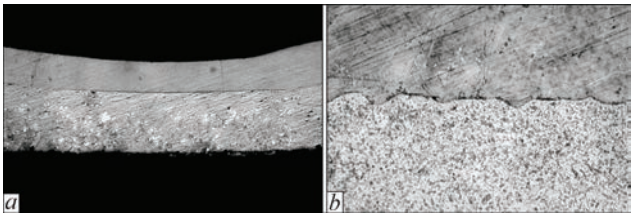

Figure 9. Microstructure of a joint of copper (M1) and aluminium alloy A5N

In welding AMG2 alloy, having a higher hardness (607 MPa) than that of A5N alloy, two bonding areas of the length of 1.28 and 1.04 mm at 1.06 mm distance from the center of pulse impact are found. Compared with the initial state, thickness in the bonding zones decreased by 20 %, and microhardness increased to 32 % (Figure 6, see Table).

In welding dissimilar metals — aluminium alloy AMG2 to stainless steel 12Kh18N10T, two wavelike bonding regions of 1.4 and 1.0 mm length were observed at 1 mm distance from the center of discharge initiation. Microhardness of moving plate of AMG2 somewhat increases (3 %), and that of stainless steel remains practically unchanged. Thickness of moving plate decreases by 38 %, and that of stationary plate does not change (Figure 7, see Table).

At MPW of plates from copper of grade M1 (moving) and stainless steel 12Kh18N10T (stationary), bonding is observed in two regions of 0.5 and 0.4 mm

Characteristics of MPW joints

Joined materials (grade)	*U*, kV	Gap between the plates, mm	Plate thickness, mm		Distance from the center, mm	Joint regions, mm		*HV*01 BM, MPa	*HV*01, in joint regions, MPa
			Before MPW	After MPW		I	II		
Al / Al — A5N / A5N	16	0.8	1 / 1	0.80 / 0.72	1.02	0.52	0.52	465	(I) 478 (II) 468
Al / Al — A5H / A5H	18	0.8	1 / 1	0.44 / 0.44	1.00	1.72	2.32	462	(I) 502 (II) 478
Al / Al — AMG2 / AMG2	18	1.0	1 / 1	0.80 / 0.88	1.06	1.28	1.04	607	(I) 804 (II) 736
Al / Steel — (AMG2) / (12Kh18N9T)	18	1.0	1.0 / 1.5	0.62 / 1.50	1.00	1.40	1.00	515 / 4630	(I) 530 (II) 496
Cu / Steel — (M1) / (12Kh18N9T)	18	0.8	0.8 / 1.5	0.46 / 1.50	1.20	0.50	0.4	891 / 4630	(I) 1078 (II) 1200
Cu / Al — (M1) / (A5N)	18	0.8	0.8 / 1.2	0.45 / 0.90	1.70	0.57	0.57	768 / 376	(I) 1216 (II) 1188

length, at the distance of 0.1 and 0.2 mm from the center of discharge initiation. Bonding region is of wave-like shape. Thickness of moving copper plate was reduced by 43 %, and its microhardness in bonding zones increased by 22 %. Thickness and microhardness of the stationary plate did not change (Figure 8, see Table).

If the moving plate metal is copper, and that of the stationary plate is aluminium alloy A5N, two wavy regions of metal bonding 0.57 mm long are observed, at 1.7 mm distance from the center of discharge initiation. Thickness of moving copper plate was reduced by 44, and that of the stationary aluminium plate — by 25 %. Copper microhardness in the bonding regions increased by 50 %, and that of aluminium — by ~ 13 % (Figure 9, Table 1).

Welded joint quality was evaluated by the results of mechanical strength tests. Evaluation of the joints was conducted with separation of the moving plate from the stationary one (base). Samples which demonstrate an acceptable quality of the joint broke through the moving plate metal, usually softer and less strong, than that of the base.

Conclusions

1. MPW of flat samples of similar and dissimilar metals and alloys produced locally was performed at PWI in upgraded N-126A unit.

2. Metallographic examination showed that bonding of parallel metal plates occurs in two regions located at the same distance from the center of the inductor flat turn.

3. Formation of a sound welded joint within the mentioned regions was detected. Samples broke through moving plate metal, which was usually softer than that of the base.

4. Relevant tendencies in development of technologies and investigations in MPW field allow us making the following statements:

- MPW is an effective technology, with high scientific-practical potential and it requires performance of further research on the technique and technology of welding similar and dissimilar metals;
- Objects of investigation and development will be MPW technological aspects for improvement of weldability of both existing and new materials; reduction of the process power consumption; and experimental-design developments for improvement of the tools (special kinds of inductors, etc.).

1. https://app.aws.org/wj/supplement/WJ_2015_08_s257.pdf
2. Miranda, R.M., Tomás, B., Santos, T.G., Fernandes, N. *Magnetic-pulse welding on the cutting edge of industrial applications.* http://www.scielo.br/pdf/si/v19n1/a09v19n1.pdf
3. *Dana: Magnetic-pulse welding.* November 06, 2000. https://europe.autonews.com/articl
4. The next wave in manufacturing. Solid state cold welding. *Automotive industries*. October, 2007. http://www.ai-online.com/Adv/Previous/show_issue.php?id=1982
5. André Cereja et al. *The JOIN'EM Project: How to join dissimilar metals with electromagnetic welding*. https://www.machinedesign.com/mechanical/join-em-project-how-join-dissimilar-metals-electromagnetic-welding, http://join-em.eu/
6. *Program Horizon 2020.* https://ec.europa.eu/programmes/horizon2020/en
7. Zhang, Y., L'Eplattenier, P., Daehn, G.S., Babu, S. (2009) Numerical simulation and experimental study for magnetic-pulse welding process on AA6061-T6 and Cu101 sheet. *ASM International*, 715–720.
8. Aizawa T., Okogawa K., Yoshizawa M., Henmi N. (2001) Impulse magnetic pressure seam welding of aluminium sheets. *Impact Eng. Appl.*, 827–32.
9. Aizawa, T. (2004) Methods for electromagnetic pressure seam welding of Al/Fe sheets. *Weld. Int.*, 18(**11**), 868–72.
10. Kore, S.D., Date, P.P., Kulkarni, S.V. (2007) Effect of process parameters on electromagnetic impact welding of aluminum sheets. *International J. of Impact Engineering*, **34**, 1327–1341.

Received 07.05.2020

https://doi.org/10.37434/tpwj2020.08.08

EXPLOSION WELDING OF COPPER-ALUMINIUM PIPES BY THE «REVERSE SCHEME»

P.S. Shlyonskyi
E.O. Paton Electric Welding Institute of the NAS of Ukraine
11 Kazymyr Malevych Str., 03150, Kyiv, Ukraine. E-mail: office@paton.kiev.ua

Explosion welding by the «reverse scheme» of pipe billets from copper and aluminium with 36 mm outer diameter and 200 mm length was studied. For welding by this scheme, a steel rod of smaller diameter than that of inner (copper) pipe was used as the filler-support for this pipe, and the gap was filled by a low-melting Wood's alloy. 6 Ref., 4 Figures.

Keywords: explosion welding, «reverse scheme», bimetal pipes, copper, aluminium

Current-conducting copper-aluminium elements, made by explosion welding (EW) by the parallel scheme cannot be applied for joining multiconductor (flexible) electric cables from dissimilar materials (copper-aluminium) [1].

Manufacture of bimetal products by explosion welding is widely demanded in the global industry. EW can be used to manufacture products of both plane and cylindrical shape [2]. Problems of producing copper-aluminium bimetal by the parallel schematic are quite well studied [3, 4], while the features of producing bimetal copper-aluminium pipes are practically not described in publications.

The objective of this work was experimental study of the possibility of producing copper-aluminium pipe billets by the method of explosion welding by the «reverse scheme», in particular, for manufacturing the transition pieces for joining copper and aluminium cables.

Tubes from AD1 aluminium with 6 mm wall thickness were used as the cladding layer, and tubes from M2 copper of 19×1.5 mm size were the base.

It is obvious that in the case of external cladding of a thin-walled copper tube by a thick-walled aluminium tube, the filler (material inside the copper tube), which acts as a support for the latter, has an important role.

Known is the application of metal shot as the support for cladding curvilinear surfaces of turbine blades [5], and metal shot with liquid to obtain two-layer pipe billets with an inner corrosion-resistant layer from 08Kh18N10T stainless steel [6]. Filling the space between the shots by liquid allows lowering the shot pressure in the zone of its contact with the product that reduces the depth of shot imprints on the pipe inner surface.

Considering that copper is quite ductile, and presence of dents on the inner surface of the copper pipe will reduce the area of contact with the cable, it will adversely affect the product serviceability on the

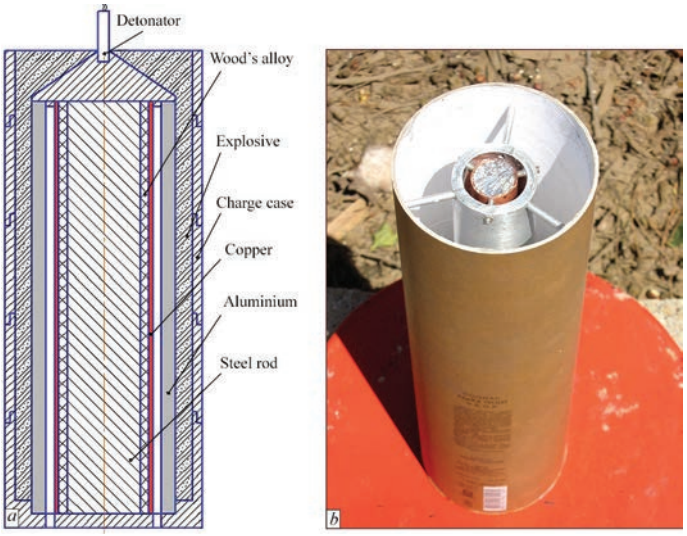

Figure 1. Scheme of assembly for explosion welding in order to produce a bimetal pipe billet (*a*) and billet for explosion welding with a steel rod, covered by Wood's alloy inside the copper tube (*b*)

P.S. Shlyonskyi — http://orcid.org/0000-0002-3566-1752

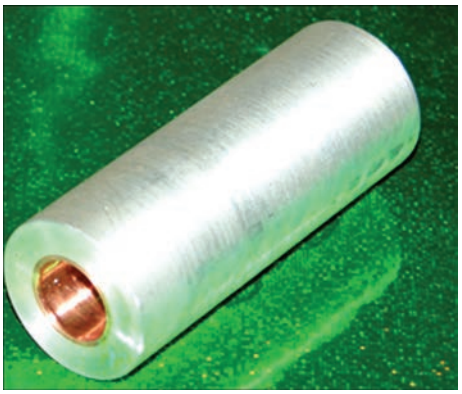

Figure 2. Sample of a bimetal pipe billet (AD1 — outer layer, M2 — inner)

whole, and, therefore, application of filler from metal shot is inacceptable for this material.

After conducting experimental work, it was determined that the optimum scheme of external cladding for pipe billets from ductile materials, in order to prevent their deformation under the impact of explosion and to obtain smooth inner surface, is the scheme (Figure 1, *a*) with application of a steel rod, which was inserted with a 1 mm gap into the copper tube, prefilled by molten Wood's alloy (Figure 1, *b*).

Thus, it eliminates the gap between the tube and the rod, and after explosion welding it enables easily removing the rod by heating up to approximately 70 °C.

Test bimetal copper-aluminium billets with an inner copper layer from 1.5 mm copper were produced by the results of optimizing the modes (Figure 2).

Metallographic investigations were conducted using MMO-1600NA microscope after microsection etching by aluminium in sodium hydroxyde solution. Figure 3 presents the microstructure of the joint produced in the optimum mode.

Figure 3 shows a weak wave profile that for the case of welding copper to aluminium is indicative of the fact that the energy is enough, and a clearly defined zone of the joint with a small amount of intermetallic inclusions.

As the standard procedures for assessment of tearing strength of layers of a bimetal ring cut out of the pipe billet, are absent, qualitative evaluation of the adhesion strength of the layers was performed using the known procedure of flattening testing of a bimetal ring (Figure 4), and the ring was cut out of a bimetal pipe billet. Testing was conducted with the purpose of revealing cracks and delaminations in the joint zone under the impact of the load.

Figure 4 shows that no delamination occurred in the joint zone after compression of the bimetal ring.

As a result of the conducted studies, it was shown that in order to lower the deformation of the welded bil-

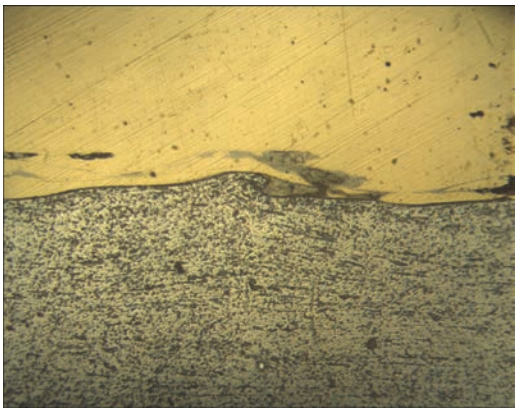

Figure 3. Microstructure (×100) of the joint produced in the optimum mode

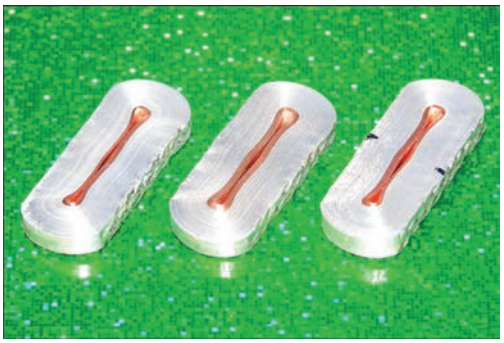

Figure 4. Samples of rings cut out of a bimetal pipe billet after flattening

lets under the impact of explosion and to obtain a smooth inner surface of the thin-walled pipe, on which another pipe is applied, in explosion welding by the «reverse scheme» it is rational to use a metal rod of a smaller diameter with gap filling by Wood's alloy.

1. Chugunov, E.A., Kuzmin, S.V., Lysak, V.I. et al. (2001) Energy saving composite elements of current-conducting assemblies of electrical power circuits. *Energetik*, **9**, 13–15 [in Russian].
2. Lysak, V.I., Kuzmin, S.V. (2005) *Explosion welding*. Moscow, Mashinostroenie [in Russian].
3. Chuvichilov, V.A. (2005) *Investigation and development of technology of explosion welding manufacture of electrotechnical purpose composites with two-sided symmetrical cladding*: Syn. of Thesis for Cand. of Techn. Sci. Degree. Volgograd [in Russian].
4. Peev, A.P. (2001) *Development of technological processes of explosion welding manufacture of copper-aluminium elements of current-conducting assemblies for power engineering and electrometallurgy enterprises*: Syn. of Thesis for Cand. of Techn. Sci. Degree. Volgograd [in Russian].
5. Konon, Yu.A., Pervukhin, L.B., Chudnovsky, A.A. (1987) *Explosion welding*. Moscow, Mashinostroenie [in Russian].
6. Malakhov, A.Yu., Sajkov, I.V., Pervukhin, L.B. (2016) Peculiarities of explosion welding of pipes by «reverse scheme». *Vestnik Tambov. Un-ta. Ser: Estestvennye i Tekhnicheskie Nauki*, 21(**3**), 1139–1141 [in Russian].

Received 19.06.2020

AUNP-002 PLANT

AUNP-002 plant was developed by «SP «VISP» Company (Kyiv) and is designed for automatic surfacing of outer surface of parts of rolling mill LPTs-1700, namely clutches, bearing bodies (pads), spindles, by a technological metal layer, using solid wire in shielding gas atmosphere, as well as flux-cored wire. The plant is designed for operation at ambient temperature from 0 up to +30 °C.

Plant is an equipment complex, allowing surfacing of flat and cylindrical parts by a technological metal layer. The plant base are the assembled left and right columns with rail guides, along which moves the gantry, carrying the process equipment.

Rail guides, along which the carriage moves, are mounted in the upper part of the gantry. The carriage platform can accommodate exhaust gas filtering system, drums with flux-cored wire or solid wire, as well as a vertical carriage, which provides vertical movement of the torch.

The design allows torch adjustment by height and width, as well as regulation of the angle of inclination. Plant operation is controlled from a remote panel and main display.

Specification

No	Parameter description	Data
1	Dimensions (max) of surfaced parts, mm length width height	 3000 1200 1500
2	Surfacing process	MIG/MAG FCAW-G
3	Surfacing wire diameter, mm	1.6; 2.0; 2.4; 2.8; 3.2
4	Length of gantry horizontal movement, mm	3970
5	Length of horizontal movement of gantry carriage, mm	2500
6	Length of vertical movement of torch carriage, mm	1300
7	Speed of horizontal movement of gantry carriage, mm/min	3–6000
8	Speed of horizontal movement of gantry carriage, mm/min	3–6000
9	Speed of vertical movement of torch carriage, mm/min	3–6000
10	Maximum consumed power of control cabinet, kW	4
11	Maximum consumed power of aspiration system, kW	3
12	Maximum consumed power of welding source, kW	70
13	Maximum consumed power of the plant, kW	77
14	Mains parameters	3N~/50 Hz 380 V
15	Overall dimensions, mm length width height	 5300 5200 4300
16	Weight without welding equipment, kg	5200

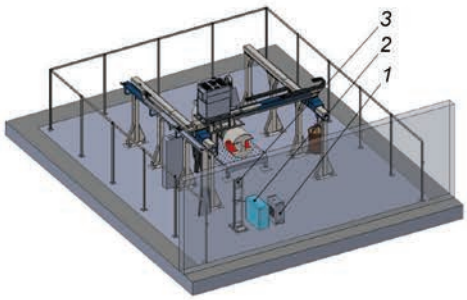

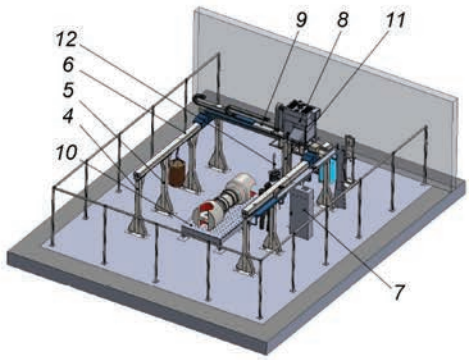

1. Autonomous cooling unit
2. Power unit
3. Ramp
4. Side rack
5. Middle rack
6. Guide beam
7. Electric cabinet
8. Exhaust gas filtering system
9. Gantry
10. Welding table
11. Vertical carriage
12. Control panel